General Disclaimer

One or more of the Following Statements may affect this Document

- This document has been reproduced from the best copy furnished by the organizational source. It is being released in the interest of making available as much information as possible.

- This document may contain data, which exceeds the sheet parameters. It was furnished in this condition by the organizational source and is the best copy available.

- This document may contain tone-on-tone or color graphs, charts and/or pictures, which have been reproduced in black and white.

- This document is paginated as submitted by the original source.

- Portions of this document are not fully legible due to the historical nature of some of the material. However, it is the best reproduction available from the original submission.

Produced by the NASA Center for Aerospace Information (CASI)

UNITED TECHNOLOGIES
HAMILTON STANDARD

Addendum
SVHSER 7236
Revision A
October 1984

CR-171823
C.1

ADDENDUM

DEVELOPMENT OF A PREPROTOTYPE

TIMES

WASTEWATER RECOVERY SUBSYSTEM

BY

GERARD F. DEHNER

PREPARED UNDER CONTRACT NO. NAS 9-15471

BY

HAMILTON STANDARD

DIVISION OF UNITED TECHNOLOGIES CORPORATION

WINDSOR LOCKS, CONNECTICUT

FOR

NATIONAL AERONAUTICS AND SPACE ADMINISTRATION

LYNDON B. JOHNSON SPACE CENTER

HOUSTON, TEXAS

JULY, 1984

(NASA-CR-171823) DEVELOPMENT OF A PREPROTOTYPE TIMES WASTEWATER RECOVERY SUBSYSTEM, ADDENDUM Final Report, Feb. 1982 - Jul. 1984 (United Technologies Corp.) 116 p HC A06/MF A01 CSCL 06K G3/54

N85-16468

Unclas
13031

UNITED TECHNOLOGIES
HAMILTON STANDARD

Addendum
SVHSER 7236
Revision A
October 1984

ADDENDUM

DEVELOPMENT OF A PREPROTOTYPE

TIMES

WASTEWATER RECOVERY SUBSYSTEM

BY

GERARD F. DEHNER

PREPARED UNDER CONTRACT NO. NAS 9-15471

BY

HAMILTON STANDARD

DIVISION OF UNITED TECHNOLOGIES CORPORATION

WINDSOR LOCKS, CONNECTICUT

FOR

NATIONAL AERONAUTICS AND SPACE ADMINISTRATION

LYNDON B. JOHNSON SPACE CENTER

HOUSTON, TEXAS

JULY, 1984

Table of Contents

Title	Page Number
SECOND GENERATION OPERATIONAL IMPROVEMENTS AND TEST VERIFICATION	
SUMMARY	1
IMPROVED TEMPERATURE CONTROL	1
Objective	1
Background	1
Results	4
Discussion	4
Cold Side Recirculation Testing-Fan Cooled Heat Exchanger	4
Constant Presure Flash Cooling Testing	5
WATER QUALITY IMPROVEMENTS	9
Objective	9
Background	9
Results	9
Discussion	9
SUBSYSTEM OPERATIONAL IMPROVEMENTS	17
Objective	17
Background	17
Results	17
Discussion	18
Recycle Loop Modifications	18
HFM Flow Headers	18
Recycle Tank Removal	21
Condensate Component Modifications	24
Condensate Pump Bypass Loop	24
Accumulator Vacuum Break	24
Accumulator Production Rate Calculation	26
SOLIDS HANDLING IMPROVEMENTS	27
Objective	27
Background	27
Results	27
Discussion	27
Recycle Solids Concentrating Calculation	28
Recycle Loop Dump	28
Batch Processing	29
WASTEWATER PRETREATMENT OPTIMIZATION	33
Objective	33
Background	33
Results	33
Discussion	33
Chromic/Sulfuric Acid Pretreatment	33
Oxone	34
MEMBRANE REJUVENATION CONCEPTS	39
Objective	39
Background	39
Results	39
Discussion	39
Syringe Cleaning	40
Water Purge Cleaning	40
Detergent Cleaning	40
Sulfuric Acid Cleaning	41
Sodium Hydroxide Flush	42
Nitric Acid Rejuvenation	42

Table of Contents (Continued)

Title	Page Number
TIMES II STUDY EFFORT	43
SUMMARY	43
THERMOELECTRIC REGENERATOR IMPROVEMENT	43
Objective	43
Background	43
Results	44
Discussion	44
Gas Separator Testing	44
TIMES I TER Power Requirements	46
Sizing For Low Specific Energy Operation	57
Thermoelectric Module Comparison	61
TIMES II TER	74
Proposed Gas-Liquid Separator Operation	74
TIMES II Main Condenser And Aftercooler Preliminary Design	80
RECYCLE LOOP pH OPERATIONAL CRITERIA	85
Objective	85
Background	85
Results	85
Discussion	85
Urine Feed	85
Wash Water Considerations	86
RECYCLE LOOP COMPONENT OPTIMIZATION	87
Objective	87
Background	87
Results	87
Discussion	88
Recycle Loop Volume	88
Recycle Pump Motor	90
HOLLOW FIBER MEMBRANE EVAPORATOR IMPROVEMENT	98
Objective	98
Background	98
Results	98
Discussion	100
TIMES I Evaporator	100
Preliminary Sizing For TIMES II Evaporator	104
Evaporator Layout And Package Integration	104
TER/HFM Assembly	107
Evaporator Header Manifolds	107

List of Tables

Table Number	Title	Page Number
29	TIMES Second Generation Water Analysis Comparison	10
30	TIMES Second Generation Water Analysis Report	12
31	Ion Exchange Resin Results	15
32	Hollow Fiber Membrane Pressure Drop	20
33	Oxone/Materials Corrosion Testing (130°F)	35
34	EMU Separator Test	47
35	Nominal Power Requirements	56
36	Total Equivalent Weight	59
37	Wastewater Concentrating Cycle Comparison	91
38	Motor Manufacturers	97
39	Increased Length Membrane Pressure Drop	101

List of Figures

Figure Number	Title	Page Number
79	TIMES Second Generation Operation Improvements Testing	2
80	Second Generation TIMES Schematic	3
81	Gas Generation Test Schematics	6
82	Process Temperature Rise For Reduced Recycle Loop Volume	8
83	Second Generation Testing Water Quality Parameters	16
84	HFM Flow Distribution Headers	19
85	Solute Concentrating Run	22
86	Recycle Concentrating Run Comparison	23
87	Accumulator Vacuum Break Schematic	25
88	Batch Flow Schematic	30
89	Continuous Flow Normalized Specific Energy	31
90	Batch/Continuous Flow Specific Energy Comparison	32
91	Urine/Oxone 53% Run	36
92	Urine/Wash Water Testing Oxone Pretreat	37
93	Gas/Liquid Separator/TIMES Schematic	45
94	Water Production vs. Solids Concentration 26.5 VDC	48
95	Water Production Rate vs. Water Production 26.5 VDC	49
96	Power vs. Water Production 26.5 VDC	50
97	Specific Energy vs. Water Production 26.5 VDC	51
98	Water Production vs. Solids Concentration 29 VDC	52
99	Water Production Rate vs. Water Production 29 VDC	53
100	Power vs. Water Production 29 VDC	54
101	Specific Energy vs. Water Production 29 VDC	55
102	TIMES II Preliminary Sizing	58
103	TIMES I Thermoelectric Module Characteristics	60
104	Thermoelectric Module Comparison	62
105	Thermoelectric Module Comparison	63
106	Cambion Thermoelectric Performance	64
107	Cambion Thermoelectric Performance	65
108	Melcor Thermoelectrics Performance	66
109	Melcor Thermoelectrics Performance	67
110	Melcor Thermoelectrics Performance	68
111	Zero Heat Load Maximum Delta-T vs. Hot Side Temperature	70
112	Maximum Voltage Per Thermoelectric Couple vs. Hot Side Temperature	71
113	Maximum Q /N vs. Hot Side Temperature	72
114	Normalized Design/Performance Chart	73
115	Cambion Module 801-1010 Performance	75
116	Cambion Module 801-1010 Electrical Characteristics	76
117	Water Separator Geometry	78
118	Water Separator Performance Characteristics	79
119	TIMES II Condenser Circuit Schematic	81
120	TIMES II Aftercooler	84
121	Duty Cycle vs. Subsystem Volume	89
122	Globe Brush DC Motor #100A 108-9 Performance Curves	93
123	Aeroflex Brushless DC Motor #BM15C-1 Performance Curves	94
124	Singer AC Motor #E2161-17 Performance Curves	96
125	Redesigned TIMES I HFM Evaporator	99
126	Subsystem Membrane Performance	105
127	7.5 Ft. Membrane Bundle Flow Characteristics	106
128	TER/HFM Layout	108
129	TIMES II Package Layout	109

SUMMARY

The contents of this addendum to the TIMES Wastewater Recovery Subsystem Final Report cover the period from February 1982 through July 1984. Included are the results of Second Generation Operational Improvements and TIMES II Study work.

Second Generation Operational Improvements included six work tasks, the goals of which were to improve the overall performance capabilities of the original TIMES preprototype. The six tasks were:

- Improved Temperature Control
- Water Quality Improvements
- Subsystem Operational Improvements
- Solid Handling Improvements
- Wastewater Pretreatment Optimization
- Membrane Rejuvenation Concepts

Work performed for these tasks included hardware modifications to the subsystem, and over 1800 hours of wastewater processing testing to evaluate the implemented modifications.

The TIMES II Study included four work tasks that addressed new design concepts for a new, advanced preprototype TIMES. The four tasks were:

- Thermoelectric Regenerator Improvement
- Recycle Loop pH Operational Criteria
- Recycle Loop Component Optimization
- Hollow Fiber Membrane Evaporator Improvement

Work performed for these tasks resulted in preliminary design concepts for an integrated Thermoelectric Regenerator/HFM Evaporator. Included in the design concepts were preliminary specifications for improved processing components.

SECOND GENERATION OPERATIONAL IMPROVEMENTS AND TEST VERIFICATION

SUMMARY

Six tasks are described in this section reflecting subsystem hardware and software modifications and test evaluation. The overall results are illustrated in Figure 79 which shows the water production rate, the specific energy corrected to 26.5 VDC, and the product water conductivity at various points in the testing. This figure can be used as a guide to accompany the discussion of test results in the following sections.

The subsystem configuration determined by the consideration of the results of the completed work tasks is shown in Figure 80. The changes were integrated into the existing subsystem hardware as specified by the Statement of Work (SOW).

IMPROVED TEMPERATURE CONTROL

Objective

A number of alternative temperature control options were studied and described under Design and Performance Improvements. Of these, two appeared to offer the most successful approach towards simplifying the control scheme and reducing the associated power requirements. The objective of this task is to fabricate, install, and test hardware in order to determine the better operational design.

Background

Of the eight different temperature control options studied under Design and Performance Improvement tasks, only Option 2, Figure 72, cold side recirculation with fan assist, and Option 8, Figure 78, fixed condensate pressure, were chosen for test evaluation. An effort was made to ensure that an alternative option would not only perform satisfactorily in its primary role as a temperature control scheme, but also that a quantitative advantage over the present design could be demonstrated. Ideally, the chosen approach would reduce the number of components, simplify overall subsystem operation, and be capable of operating reliably over the range of operating conditions encountered during a wastewater concentration run. An operating hot side temperature range of 57-66°C (135-150°F) is desirable, since below that range the membrane permeation rate decreases, while above that range the urea decomposition rate increases significantly. To maintain this hot side temperature range, the cold side must be cooled in some manner, since the TER establishes a hot to cold side differential temperature dependent on the operating point.

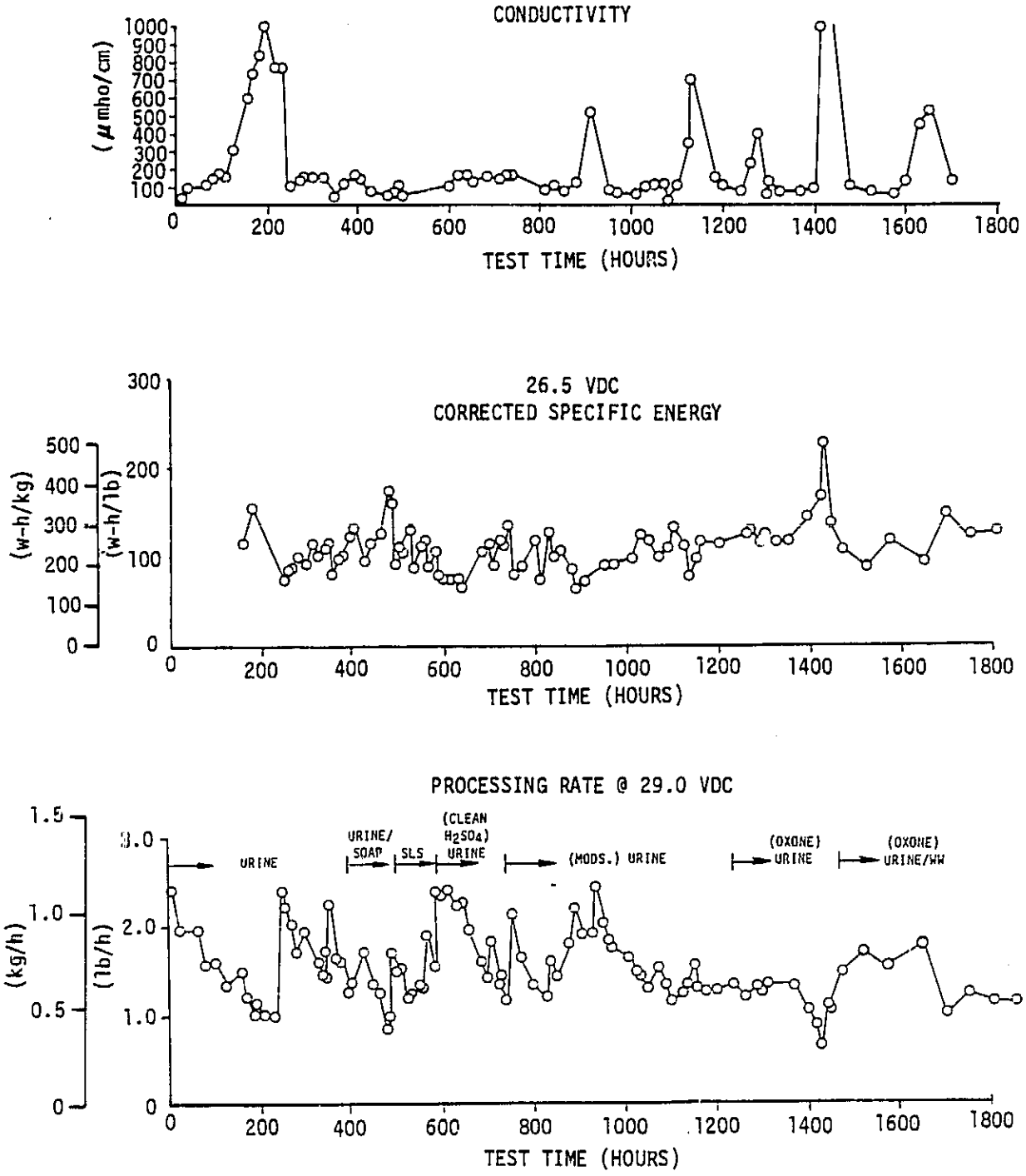

FIGURE 79

TIMES SECOND GENERATION
OPERATION IMPROVEMENTS TESTING

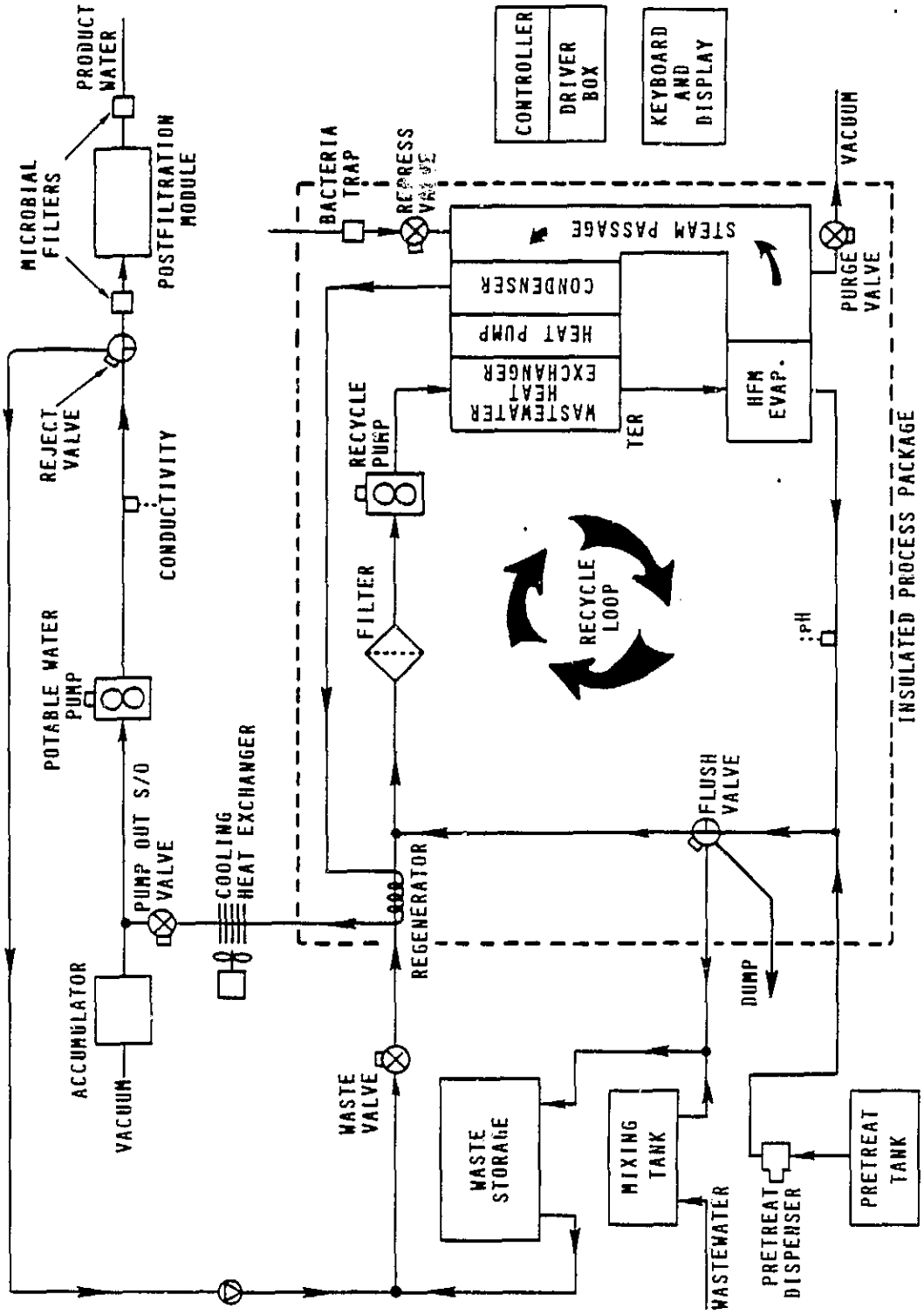

FIGURE 80
SECOND GENERATION TIMES SCHEMATIC

Results

Both cooling schemes as tested on the subsystem successfully maintained temperature control. Option 8, fixed condensate pressure, was chosed as the most desirable technique because it reduces the number of components involved, and simplifies subsystem operation. In place of a large convection heat exchanger and recirculation pump, a simple small, finned-tube heat exchanger with an integral axial fan is employed. There is no control logic associated with the cooling process in that the operating conditions are preset by the accumulator reference spring selection. A new accumulator spring was installed that is expected to establish a 57-59°C (135-138°F) operating temperature at the HFM inlet, with an unconcentrated wastewater feed.

Discussion

As discussed in the Design and Performance Improvements Section, temperature control Option 2, Figure 72, utilizes a fan cooled, liquid recirculating heat exchanger. A portion of the total condensate load is recirculated in a loop that includes the heat exchanger and TER cold side heat exchanger, thereby cooling the recirculate and the TER cold junctions. In this way, the TER hot side heat exchanger inlet temperature is controlled at the operating temperature of 66°C (150°F).

In contrast, Option 8, Figure 78, utilizes a fan cooled heat exchanger, but in this case there is no condensate recirculation. The condensate line downstream of the TER and heat exchanger is subjected to a reference pressure through the use of a spring-loaded accumulator. This quasi-constant pressure is sensed at the TER in the area of the porous plates. If the condensing saturation temperature (hence pressure) is higher than the accumulator reference pressure, condensate flashing will occur and this will immediately cool the TER cold side, forcing down the hot side temperature as well. The actual operating temperature is dependent on the accumulator spring reference pressure chosen.

Cold Side Recirculation Testing - Fan Cooled Heat Exchanger

In order to test Option 2, the previously employed convection heat exchanger (Item 211) was modified with duct work and fitted with a shrouded 28 VDC fan. Otherwise the subsystem schematic was the same as pictured in Figure 41. The assembly was mounted horizontally directly below the processing package, and the previously used condensate recirculation pump was connected into the loop.

The subsystem was started on 2/16/82 with a pretreated urine feed and allowed to reach operating conditions. After a week of non-continuous operation, the dissolved solids level reached approximately 20%, and a failure shutdown due to recycle tank overtemperature occurred. Within another week of operation, two more shutdowns were experienced due to recycle tank overtemperature. The cause was air/vapor locking in the condensate recirculation pump, resulting in the loss of cooling for the subsystem. At 139 hours it was decided to reduce the speed of the coolant pump (hence suction head) by decreasing the operating voltage from 28 to 10 VDC. This technique prevented the pump from cavitating, and stable temperature control was achieved. The subsystem was operated for nearly two months in this configuration without any further loss of temperature control.

Constant Pressure Flash Cooling Testing

At 488 hours, the subsystem wastewater feed was switched from pretreated urine to a detergent and water mix. Having demonstrated successful operation on recirculation cooling, it was decided to modify the cooling technique to the Option 8 configuration, Figure 78. To accomplish this, the recirculation loop was removed from the subsystem, one end of the heat exchanger was connected directly to a tap at the TER bottom condensate header, and the other end connected to the accumulator. At 504 hours, the subsystem was started up using recirculation and allowed to reach and maintain the 66°C (150°F) operating temperature for several hours. At that point, the recirculation loop was disconnected (the capillary temporarily left in place) and constant reference pressure cooling was initiated. Within two hours, a failure shutdown due to recycle tank overtemperature occurred. The subsystem was connected to a vacuum flash (in place of the accumulator) at a pressure of 7.6 kPa (1.1 psia). The evaporator inlet temperature stabilized at 66°C (150°F) after two hours. Apparently the accumulator suction pressure was not low enough with the capillary restrictor in the line to allow flashing at the porous plates to occur. It was then decided to remove the capillary from the condensate line, downstream of the TER, in order to ensure that all the flashing occurred in the porous plate cold side heat exchanger interfacial area as originally called for in the Option 8 investigation. With this change, the evaporator temperature decreased to 64°C (147°F) and remained there overnight. At 552 hours the TER tap connection was changed so that condensate was drawn from the TER top condensate header. The evaporator temperature again stabilized at 64.5°C (148°F) and remained there all day.

Returning to an unconcentrated pretreated urine feed at 583 hours and reconnecting the accumulator in place of the vacuum flask, the evaporator temperature stabilized at 66.5°C (148°F). The water production rate at this time was 1.0 kg/h (2.2 lb/h). By 684 hours the dissolved solids level in the recycle loop reached 24 percent and the evaporator inlet temperature had risen to 68°C (154°F) as expected. At 750 hours, the subsystem was shutdown and the large ducted heat exchanger was removed and replaced with a small liquid-cooled, tube in tube, coiled heat exchanger, mounted vertically. The subsystem was started up with a water feed, and by the next day, temperature control was lost, so the vertical coil was replaced with a flat stainless steel coil, tube in tube heat exchanger. The evaporator temperature again stabilized at 60°C (150°F). At 830 hours we attempted to gauge the effect of the different cooling techniques on gas bubble generation in the condensate line. The test setups are shown in Figure 81. The first test involved running the subsystem with a constant 18 percent urine solids concentration in the recycle loop, using the flashing condenser cooling scheme. The quantity of gas collected averaged 85 cc/min (3.0×10^{-5} ft^3/min) at 8.3 kPa (1.2 psia) steam pressure. The water production rate at that point was 0.76 kg/h (1.67 lb/h).

The test was repeated using liquid recirculation as the cooling scheme. The quantity of gas collected averaged 78 cc/min (2.8×10^{-5} ft^3/min) at 11.9 kPa (1.73 psia). The water production rate was 0.70 kg/h (1.54 lb/h). The test was repeated a third time using liquid recirculation, but here the regenerative heat exchanger was bypassed. The quantity of gas collected averaged 84 cc/min (3.0×10^{-5} ft^3/min) at 15.2 kPa (2.2 psia), with a water production rate of 0.86 kg/h (1.90 lb/h).

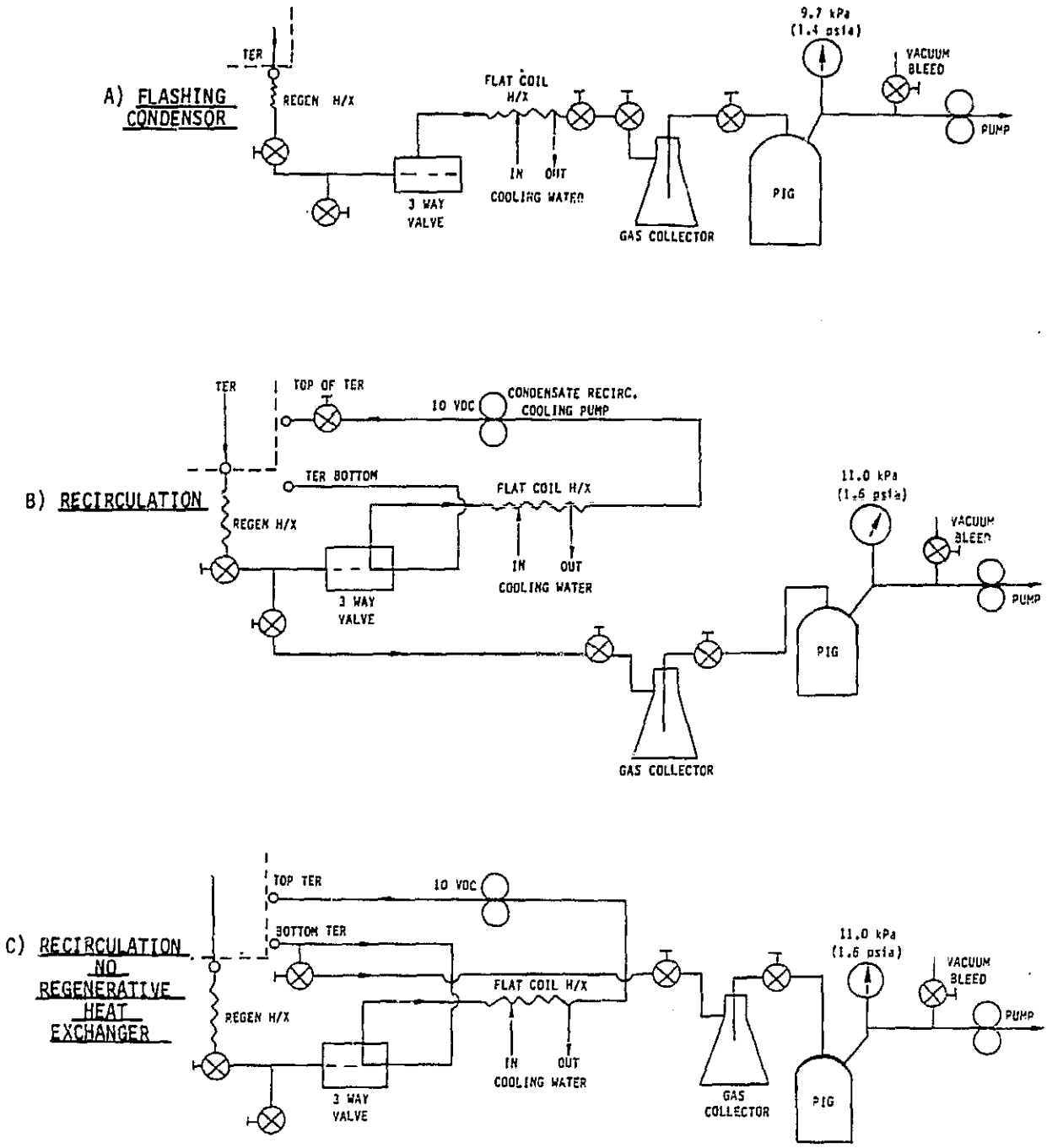

FIGURE 81

GAS GENERATION TEST SCHEMATICS

At 932 hours the TER porous plates were replaced with the original smaller pore size plates modified by the addition of a 200 X 200 mesh stainless steel screen tack welded to the surface adjacent to the pin fin heat exchanger. The former was done in order to reduce the quantity of gas that was being transported into the condensate flow, and the latter to provide more ΔT (hence ΔP) for water transport through the plates. At 1,072 hours the 10 liter (0.35 ft^3) recycle tank was removed leaving only the one liter (0.035 ft^3) filter tank as the major volume element in the loop. As seen in Figure 82, with the smaller recycle loop volume, concentrating runs took less time, and HFM temperature swings became more uniform. With 40 percent solids in the loop, the nominal HFM temperature reached 70°C (158°F) from an initial point of 60°C (140°F). The TER cold side temperature, at the 50 percent level in the accumulator, was 55°C (131°F). This was higher than desired so the accumulator was lowered by 0.25 m (0.83 ft) to create a lower pressure at the TER, created by the head of water. Testing continued and the process temperature range remained essentially the same.

It was decided to replace the accumulator spring with a new spring that would provide a lower suction pressure. After this was done, the TER cold side temperature decreased to 52°C (125°F). The HFM inlet temperature equilibriated 64°C (140°F) with a tap water feed, but it was felt that the membranes were fouled, resulting in a low water production rate. With new membranes the expected operating temperature would be in the 57-59°C (135-138°F) range.

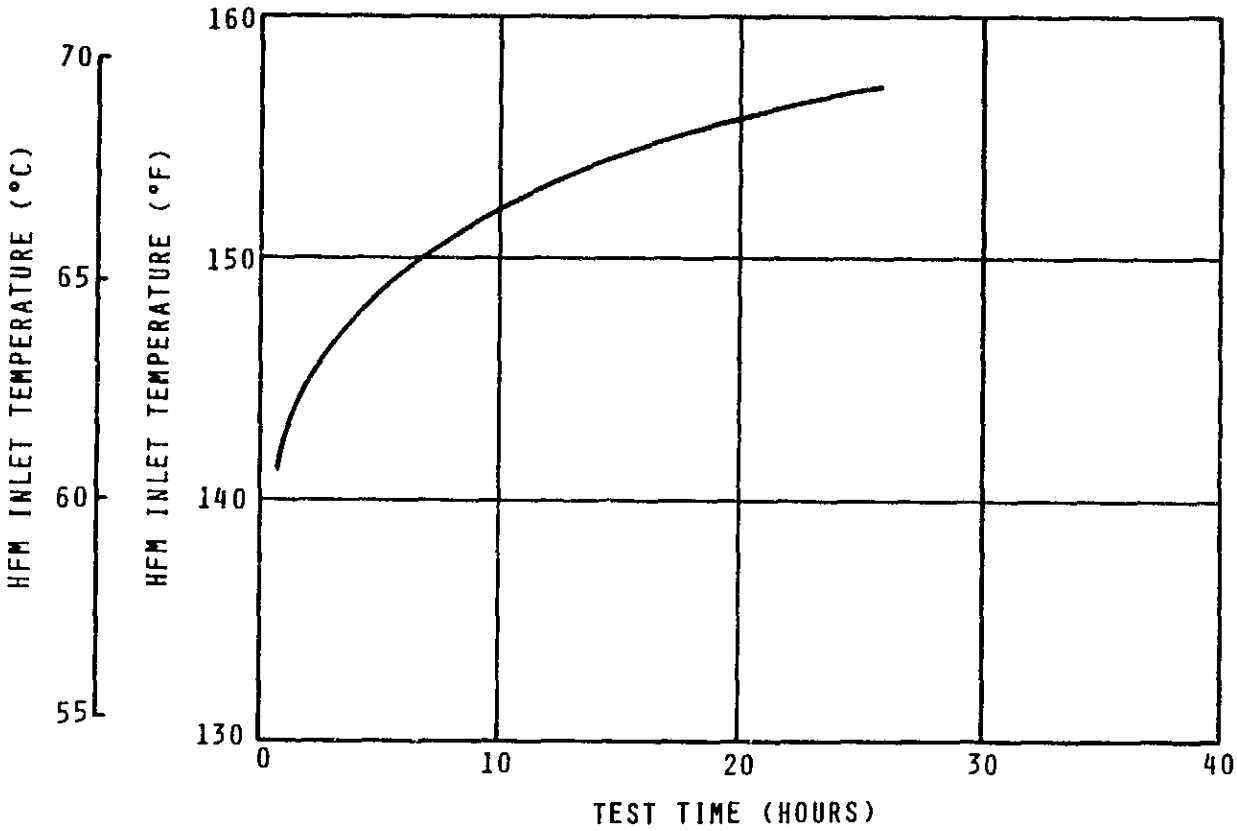

FIGURE 82

PROCESS TEMPERATURE RISE
FOR REDUCED RECYCLE LOOP VOLUME

WATER QUALITY IMPROVEMENT

Objective

A number of alternative approaches to reducing ammonia levels in the product water were previously investigated. Of these, the most satisfactory approach was determined to be ammonium ion removal via a new strong acid ion exchange resin.

The objective of this task is to replace the presently employed ion exchange resin located in the posttreatment multifilter, with the new resin previously demonstrated to be a more efficient ammonium ion scrubber.

Background

It was previously found that a strong acid cation exchange resin could be substituted for the weak acid exchanger employed in the multifiltration canister, in order to reduce ammonium ion levels in the product water. To evaluate this effect, the old resin was removed from the canister and it was refilled with a quantity of new resin required for 90 days of operation.

Results

The replacement of the weak acid ion exchange resin (used during the TIMES Acceptance Testing), by a strong acid resin in the posttreatment canister resulted in the complete removal of ammonium and other ions from the product water as seen in Table 29. The removal process did, however, lower the water pH because hydrogen ions were exchanged with the ammonium ions. A weak base anion exchange resin added to the posttreatment line downstream of the canister neutralized a portion of the acidity, but it appears that a strong base exchanger would be required for complete neutralization. Additional testing using a strong base exchanger is recommended.

Discussion

Upon disasembly of the multifilter assembly, it was discovered that the Ionac CC weak acid ion exchange resin had become highly compacted and was contaminated with charcoal fines. Since very little room for wet expansion was allowed when the bed was initially packed, compaction of both the resin beads and charcoal granules along their common bed interface occurred.

Table 29

TIMES
SECOND GENERATION WATER ANALYSIS COMPARISON

	Verification Test, 21% Solids		Improved Posttreatment, 26% Solids	
	Non-Posttreated	Posttreated	Non-Posttreated	Posttreated
pH	3.5	4.3	3.3	3.9
Conductivity, μmho/cm	197.6	146.5	154.3	38.1
Ammonia As N, ppb	770	1125	3650	<10
Organic Carbon, ppm	56	20	71	15
Chromium, ppb	<10	180	45	<10
Iron, ppb	<10	180	45	<10
Nickel, ppb	<10	<10	10	<10

The strong acid ion exchange resin, IR-118H swells 20 percent when wet, so only 100 cc (6.1 in^3) of wet resin was able to be loaded into the multifilter canister. This gives a total removal capacity of 140 milliequivalents. Assuming an average level of 3 ppm of NH_4^+ in the product water, this amount of resin would be sufficient for 90 days of water processing. Urine testing was initiated on 2/19/82 using the chromic/sulfuric acid pretreatment. Water samples were taken periodically from the raw and posttreated product water taps. The results of the water analysis tests are reported in Table 30. It can be seen that the IR-118H resin was extremely effective in eliminating NH_4^+ ions from the raw product water since the level was reduced to <10 ppb from as high as 133,000 ppb. In addition, conductivity was reduced to approximately 50 mho/cm. Several water quality parameters are plotted in Figure 83 for various recycle fluid pH levels. It should be noted that above pH = 4.5 in the recycle fluid, raw water quality, in terms of NH_4^+ and conductivity, degraded rapidly. The reason for the rise in the recycle pH is due to the time/temperature dependence of the urea decomposition reaction. The time for concentrating the dissolved solids from 3.5-40 percent was about 200 hours, which allows the NH_3 production to exceed the neutralization capacity of the incoming pretreated urine.

As more NH_4^+ is removed from the raw water by ion exchange with hydrogen ions, the product water pH declines proportionately. This free mineral acidity could be absorbed by a weak base anion exchange resin. Any remaining acidity due to weak acids (either organic or inorganic) would require a different approach such as the use of a strong base anion exchange resin, with an upstream weak base exchanger to protect it from organic fouling. As a partial test, two weak base exchangers were fabricated using Ionac AFP-329 a macroporous styrene divinyl-benzene based tertiary amine resin, and Ionac A-260, a granular aliphatic amine resin. The results are shown in Table 31. It can be seen that the pH has been raised using the AFP-329 bed, but that complete neutralization was not achieved. The A-260 bed was able to neutralize the product water to a greater degree than the AFP-329.

Before the anion resin beds were tested, the plumbing arrangement of the ion exchange and charcoal beds was changed. The charcoal which had previously been upstream of the ion exchanger was now situated downstream. No significant effect was noted.

Table 30

T I M E S

SECOND GENERATION WATER ANALYSIS REPORT

DETERMINATION	3/15/82 0800 40.5% Solids 482-22 (PT)	3/26/82 1000 15% Solids 482-23 (non-PT)	3/26/82 1200 15% Solids 482-24 (PT)	4/2/82 1030 26.5% Solids 482-25 (Non-PT)	4/2/82 1430 26.5% Solids 482-26 (PT)
pH	2.8	3.5	3.6	3.6	4.0
Total Solids, ppm	179.5	2.9	18.2	9.2	15.5
Organic Carbon, ppm	45	54	14	54	15
Inorganic Carbon, ppm	12	71	50	44	69
Chromium as Cr, ppb	16	10	< 10	10	< 10
Iron as Fe, ppb	< 10	80	< 10	45	< 10
Manganese as Mn, ppb	< 10	< 10	< 10	< 10	< 10
Nickel as Ni, ppb	< 10	< 10	< 10	< 10	< 10
Ammonia as N, ppb	< 10	590	< 10	4350	< 10
Sulfate as SO_4^{-2}, ppb	135,000	< 500	5150	< 500	< 500
Chloride as Cl^-, ppb	18,835	210	1950	190	680
Cond, μmhos/Cm	506.0	115.5	96.4	122.1	38.6
Urea, ppm	1.85	1.00	1.60	< 0.5	1.50
Titanium	100	< 100	< 100	< 100	< 100

Table 30 (Continued)

T I M E S

SECOND GENERATION WATER ANALYSIS REPORT

DETERMINATION	2/19/82 0900 10% Solids 482-17 (Non-PT)	2/19/82 1030 10% Solids 482-18 (PT)	3/2/82 0900 27.5% Solids 482-19 (Non-PT)	3/2/82 1100 27.5% Solids 482-20 (PT)	3/5/82 0800 40.5% Solids 482-21 (Non-PT)
pH	4.4	4.7	6.7	3.1	6.6
Total Solids, ppm	3.7	16.9	5.5	87.4	8.6
Organic Carbon, ppm	30	6	50	22	84
Inorganic Carbon, ppm	19	9	69	15	85
Chromium as Cr, ppb	< 10	< 10	< 10	< 10	12
Iron as Fe, ppb	8.5	< 10	24	< 10	22
Manganese as Mn, ppb	< 10	< 10	< 10	< 10	< 10
Nickel as Ni, ppb	< 10	10	< 10	10	12
Ammonia as N, ppb	1310	< 10	100,000	< 10	133,000
Sulfate as SO_4^{-2}, ppb	< 500	< 500	< 500	28,750	< 500
Chloride as Cl^-, ppb	< 50	620	< 50	13,735	50
Cond, μmhos/Cm	82.5	11.4	365.2	309.1	464.2
Urea, ppm	< 0.5	< 0.5	< 0.5	0.6	3.25
Titanium	< 100	< 100	< 100	< 100	< 100

Table 30 (Continued)

T I M E S

SECOND GENERATION WATER ANALYSIS REPORT

DETERMINATION	5/18/82 26% Solids 582-57 (Non-PT)	5/18/82 26% Solids 582-58 (PT)
pH	3.3	3.9
Total Solids, ppm	2.4	4.0
Organic Carbon, ppm	71	15
Inorganic Carbon, ppm	52	17
Chromium as Cr, ppb	12	< 10
Iron as Fe, ppb	45	< 10
Manganese as Mn, ppb	< 10	< 10
Nickel as Ni, ppb	10	< 10
Ammonia as N, ppb	3650	< 10
Sulfate as SO_4^{-2}, ppb	---	---
Chloride as Cl^-, ppb	1153	190
Cond, μmhos/Cm	154.3	38.1
Urea, ppm	---	---
Titanium	<100	<100

Table 31

ION EXCHANGE RESIN RESULTS

Ionac A-260 & A-329 Weak Base Resins

	Water pH	Conductivity (μmho/cm)	Recycle pH	Solids %
Sample #1				
Non-Posttreated	5.45	280	4.85	37.5
Posttreated	4.00	55	---	---
Post A-329	4.50	40	---	---
Sample #2				
Non-Posttreated	6.45	165	4.40	18.4
Posttreated	3.90	66	---	---
Post A-329	4.55	45	---	---
Sample #3				
Non-Posttreated	7.05	195	4.75	20.7
Posttreated	---	---	---	---
Post A-329	4.75	38	---	---
Sample #4				
Non-Posttreated	7.05	195	---	---
Posttreated	---	---	---	---
Post A-260	6.25	48	---	---

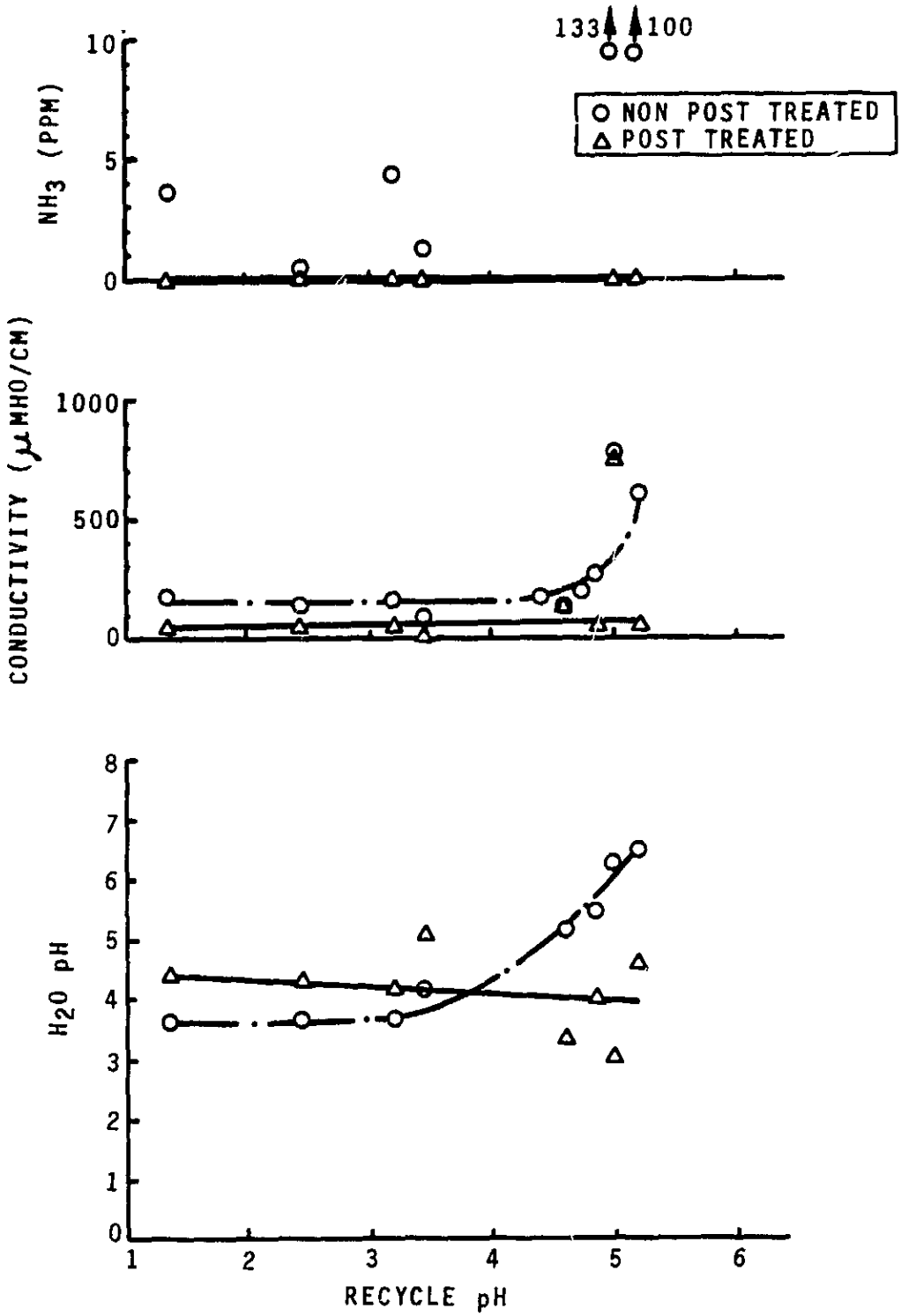

FIGURE 83

SECOND GENERATION TESTING
WATER QUALITY PARAMETERS

SUBSYSTEM OPERATIONAL IMPROVEMENTS

Objective

A revised procedure for startup and shutdown of the subsystem is desirable to enable an operator to easily change the operating mode depending on test conditions. The objective of this task is to implement hardware and software modifications to generally provide improved operational capabilities, and specifically to provide automatic isolation of fluid lines where needed during a failure shutdown. The goal is to maintain separation of wastewater and product water, as well as to allow immediate restart upon correction of the failure condition.

Background

While the TIMES was designed to provide hands-off operation over the full range of conditions encountered during normal wastewater processing, testing to date has indicated that during startup from cold conditions, and after a failure shutdown, some operator manipulation was necessary. Because of the membrane tube header seal design, fluid migration, while small, was evident in the steam shell during transient modes. Upon restart, this accumulated fluid occasionally migrated to the condensate line, thereby contaminating the product water. By providing automatic fluid line isolation, it was felt measurable fluid migration would virtually be halted. In addition, during normal or failure shutdowns, the subsystem vacuum is broken with an inrush of ambient air. Upon restart, some of this air is not pumped out by normal purge procedures; it becomes trapped in the condensate plumbing, and results in near or total air binding of the accumulator and condensate pump. These and other potential operating shortcomings can be overcome by making changes in controller based operating conditions, and through hardware additions and modifications.

Results

Improvements were realized relative to startup and shutdown procedures as well as to overall operating capabilities, through hardware modifications to the recycle and condensate loops.

Flow distribution headers were installed in the HFM to increase fluid velocities through the membrane bundles, thereby reducing the potential for clogging of the tubes with locally precipitated material. The large recycle tank was removed from the unit to reduce the urine concentrating cycle time. This shorter cycle resulted in better recycle fluid pH control and higher quality water. In addition, cold startup time intervals were reduced significantly.

The condensate pump was fitted with a bypass loop to enable it to keep primed during episodes of high gas loading. The most significant improvement in the startup procedure was gained through the addition of a vacuum-break solenoid valve in the line to the accumulator. This configuration enabled the subsystem to startup even with a large gas load such as would occur after a failure shutdown.

The water production rate calculation was modified so that readings from the waste storage tank quantity sensor were used instead of the number of accumulator cycles, eliminating the error introduced if gases are present in the accumulator.

Discussion

The implementation of subsystem hardware modifications and the associated controller logic, occurred in the two main areas of fluid management, namely the recycle and condensate loops. While changes to the recycle fluid components and logic mainly improve the performance capability of the subsystem, modifications to the condensate loop impact the actual operation of the evaporation/condensation/product delivery process.

Recycle Loop Modifications

At the end of 1,600 hours of wastewater processing it became obvious that material occlusion of the membrane tubes was occuring, principally due to a chromium based precipitate. Chromium is used in the pretreatment mix along with sulfuric acid. Several times the tubes had to be cleaned by water soaking, as well as by syringe purging each individual tube.

It was decided to improve the situation by 1) increasing the fluid velocity through the tubes, and 2) removing the 10 liter (0.35 ft^3) recycle tank.

HFM Flow Headers:

While the 25 micron recycle filter will remove particulates entrained in the recycle fluid, some localized precipitation can occur in flow stagnation areas where very low fluid velocities occur. This material will not reenter the bulk fluid stream, and hence will not be removed by the filter. With time, a clot can build up, shutting down flow even more, resulting in clogged tubes.

The chances of a precipitate material agglomerating to such an extent as to clog the HFM tubes are reduced by increasing the bulk fluid velocity. In the HFM this was done by adding a plate over each end of the tube headers. The plates distribute the flow into several passes in contrast to parallel flow through the tube bundles. The arrangement is shown in Figure 84 and the details are described more fully below.

The TIMES membrane evaporator is composed of 18 membrane bundles with 92 membranes per bundle. Initially the recycle urine flowed through all these bundles in parallel. To alleviate any flow maldistribution, the design was changed to increase the pressure drop along the flow path by increasing the flow velocity within the tubes. This resulted in a new header design in which the flow path through the 18 tube bundles was modified to 4 passes of 3 bundles each followed by 3 passes of 2 bundles each. The results of this modification are shown in Table 32 in which the new predicted pressure drop is 21.1 kPa (3.1 psid).

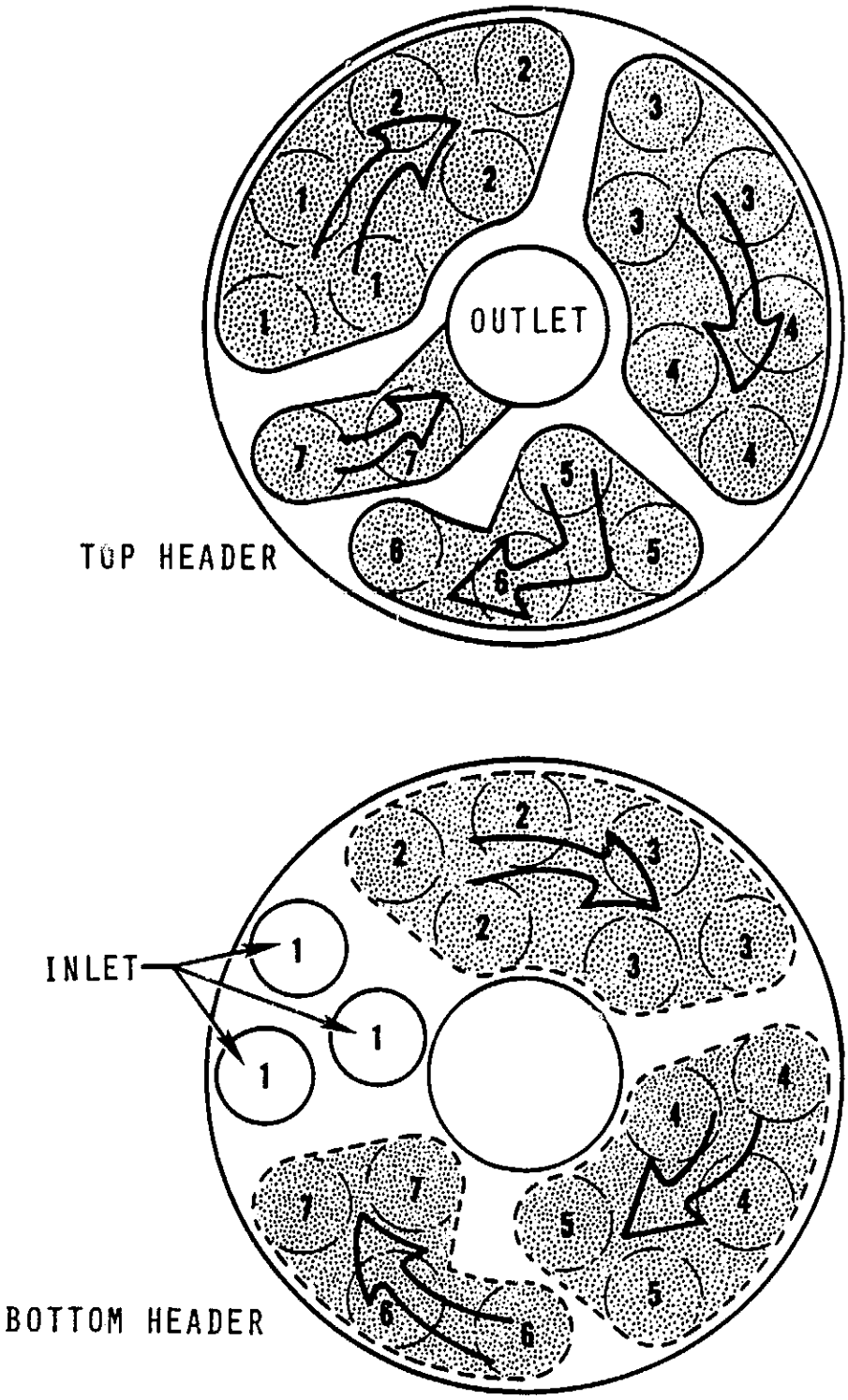

FIGURE 84

HFM FLOW DISTRIBUTION HEADERS

Table 32

HOLLOW FIBER MEMBRANE PRESSURE DROP

	Initial Design (One Pass Design)	Header Redesign	
		Passes 1,2,3,4	Passes 5,6,7
Tubes per pass	1656	276	184
Flow per tube kg/h (lb/h)	0.11 (0.24)	0.66 (1.45)	0.98 (2.17)
Velocity m/sec (ft/sec)	0.03 (0.10)	0.19 (0.62)	0.28 (0.93)
Reynolds No.	35	213	319
Pressure drop per pass kPa (psid)	0.41 (0.06)	2.48 (0.36)	3.72 (0.54)
Total pressure drop kPa (psid)	0.41 (0.06)	21.1 (3.06)	

As shown, in the initial design the average velocity through the tubes was 0.030 m/sec (0.10 ft/sec) with a pressure drop through the tubes of 0.41 kPa (0.06 psid). Experience in heat exchanger and packed bed design indicates that in a liquid system the pressure drop should be approximately 3.4 kPa (0.5 psid) to prevent maldistribution. Using this as a basic criteria, the TIMES evaporator was redesigned for a multipass approach. To maintain reasonable pressure drops [<34.5 kPa (<5 psid)], as well as to maintain an adequate margin on that number, the specified 3 bundle/2 bundle arrangement was established. The first 4 passes are 3 bundles per pass with an average velocity of 0.19 m/sec (0.62 ft/sec) through each tube and a pressure drop across each pass of 2.5 kPa (0.36 psid). The last 3 passes comprise 2 bundles per pass with an average velocity of 0.28 m/sec (0.93 ft/sec) and a pressure drop per pass of 3.7 kPa (0.54 psid). The higher velocities and pressure drops were intentionally incorporated in the downstream passes since this is where the solids concentration will be higher and more scrubbing action will be required.

The tube physical properties were as follows: tube OD = 1.27 cm (0.50 in); wall thickness = 0.013 cm (0.005 in); tube ID = 0.10 cm (0.040 in); tube length = 38.1 cm (15 in). The physical properties of the urine were as follows: solids concentration = 40%; density = 1184 kg/m^3 (73.9 lb/ft^3); viscosity = 1.08 centipoise (2.6 lb/h-ft); total flow = 182 kg/h (400 lb/h). The properties of urine were extracted from references based on 21°C (70°F) and since the TIMES operates at 66°C (150°F) it was necessary to scale the viscosity data. Several techniques are known for establishing the viscosity of mixtures. In each one of these correlations the mixture viscosity is directly proportional to the viscosity of the pure liquid. Thus, the viscosity of concentrated urine at 66°C (150°F) was established by multiplying its viscosity at 21°C (70°F) by the ratio of the viscosity of pure water at both temperatures.

Recycle Tank Removal:

A typical solute concentrating run is shown in Figure 85. As can be seen, the total time required is approximately 240 hours. As previously demonstrated in the Design and Performance Improvements section, urea decomposition is time and temperature dependent. As the amount of ammonia from urea decomposition increases, the pH level also increases due to the neutralization of the available pretreatment acid. Since the amount of chromium precipitated is pH and time dependent, a condition exists where this long cycle time contributes not only to a large degree of ammonia formation, but to chromium precipitate as well.

As the volume of the recycle loop is reduced, cycle time is decreased provided the same water production rate versus solids concentration profile is maintained. As seen in Figure 86, by removing the TIMES recycle tank, the total recycle loop volume and the associated concentrating cycle time is reduced by 85 percent. This means a concentrating run can be accomplished in approximately 40 hours, significantly reducing the chances for significant precipitate accumulation.

Once the main tank is removed the recycle loop consists of the 1.0 liter (0.035 ft^3) filter tank, the HFM, TER, and the interconnecting plumbing for a total volume of 1.2 liters (0.042 ft^3).

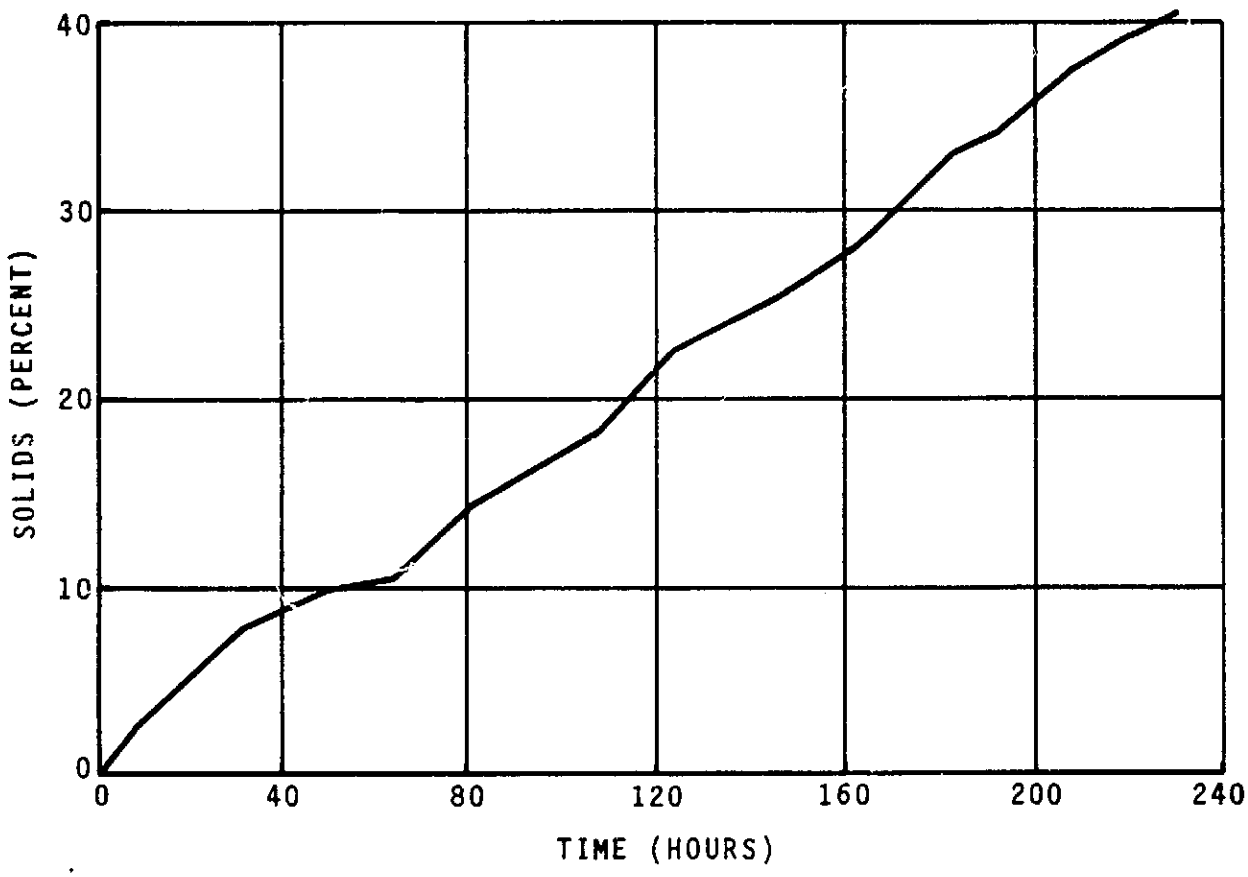

FIGURE 85

SOLUTE CONCENTRATING RUN

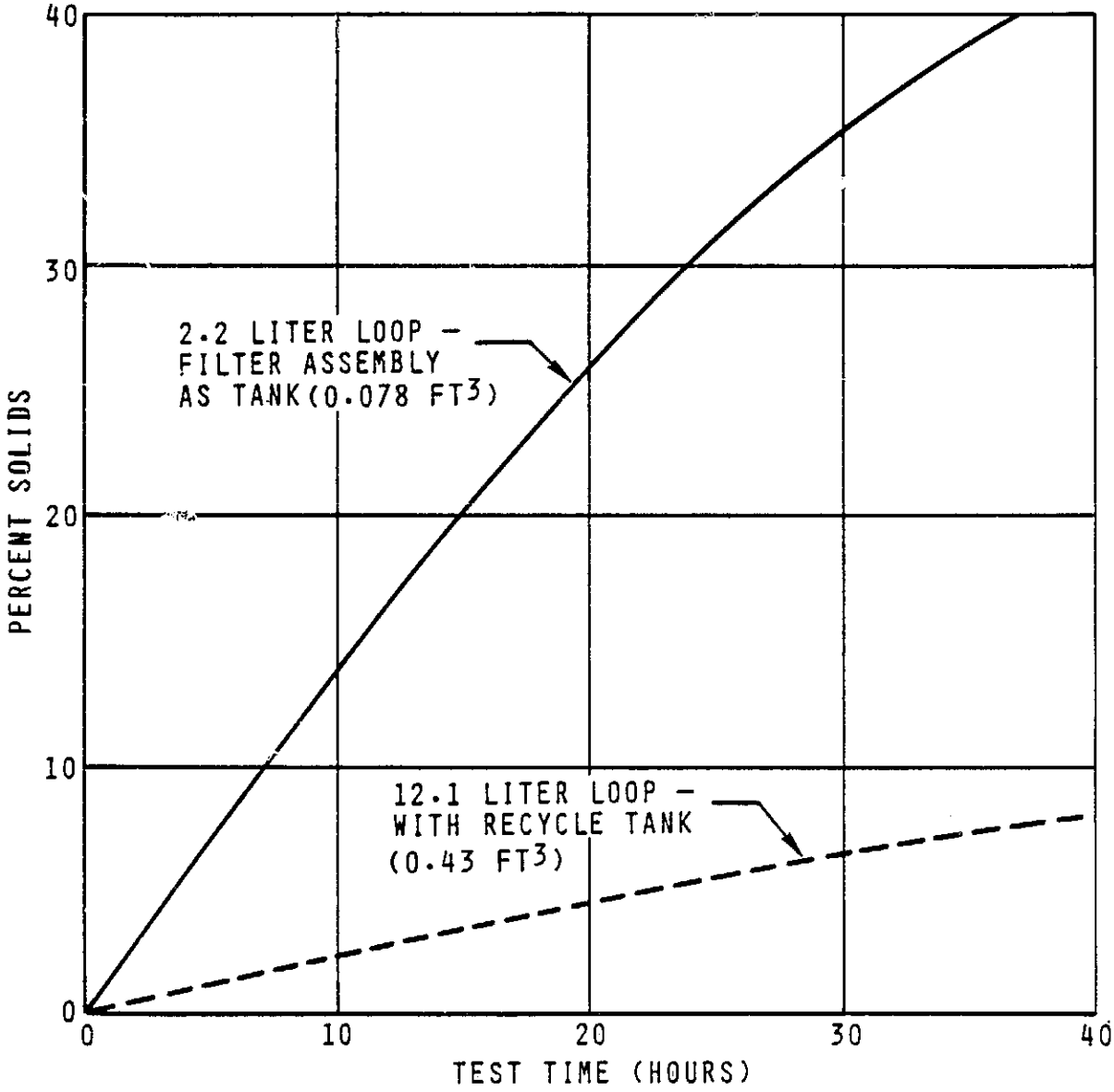

FIGURE 86

RECYCLE CONCENTRATING
RUN COMPARISON

Condensate Component Modifications

The porous plate, accumulator, and condensate pump combination were designed to provide product water free of non-condensible gas on a batch basis. While the Teflon gear pump is capable of pumping a small amount of non-condensible gas, a larger transient load (such as occurs during startup and after a failure shutdown) supplied by the accumulator causes the pump to effectively become gas bound, and thereby unable to pump any liquid. When this happens, the accumulator does not empty, and eventually the evaporation/condensation process is throttled.

Two relatively simple fixes that were implemented included the addition of both a condensate pump bypass loop, and a vacuum breaking solenoid valve to the accumulator. These approaches are discussed in the following paragraphs.

Condensate Pump Bypass Loop:

The idea of adding a bypass loop to the pump was to allow a quantity of non-condensible gas delivered from the accumulator to become trapped between pockets of liquid in such a way that the gears of the pump were always wetted and therefore primed. The loop consists of a 0.953 cm (.375 in) X 61 cm (24 in) long tube which has a volume greater than the largest expected gas bubble arriving from the accumulator. As long as the gears of the pump are kept wetted, some of the gas will be pumped out with liquid, so that eventually the total two phase flow will be handled. A manual needle valve was also added to control the amount of bypass.

Accumulator Vacuum Break:

By far the most effective means of ensuring accumulator dumping during a gas-bound pump condition is to relieve the vacuum on the reference side of the accumulator. The increased pressure pushes the rolling diaphragm towards the low end stop, forcing the two-phase fluid through to the pump inlet. Thus assisted, the pump is able to keep primed and can then discharge the accumulator. The schematic is shown in Figure 87.

As seen in the schematic, the vacuum break solenoid valve installed into the subsystem is electrically interconnected to Item 119, the condensate line isolation solenoid valve. The isolation valve shuts off the condensate line to the accumulator when the condensate pump is energized. Simultaneously, the vacuum break solenoid switches from the vacuum source, to a filtered ambient air source, which is restricted with a needle valve to control the rate of air bleeding into the accumulator. The air flow is kept low enough to minimize what would be considered cabin air loss, and fast enough to allow accumulator discharge in a maximum of roughly a one minute interval. When the accumulator reaches its low limit of 25 percent quantity, the vacuum break solenoid is deenergized allowing the valve to switch from the ambient air source back to the vacuum source. Since a finite amount of time (10-20 sec) is required to purge the air charge and reach full vacuum in the accumulator, the condensate isolation valve deenergization is delayed by 20 sec using a timer delay. This prevents condensate from backflowing into the TER under reverse pressure conditions present during the reestablishment of the reference vacuum.

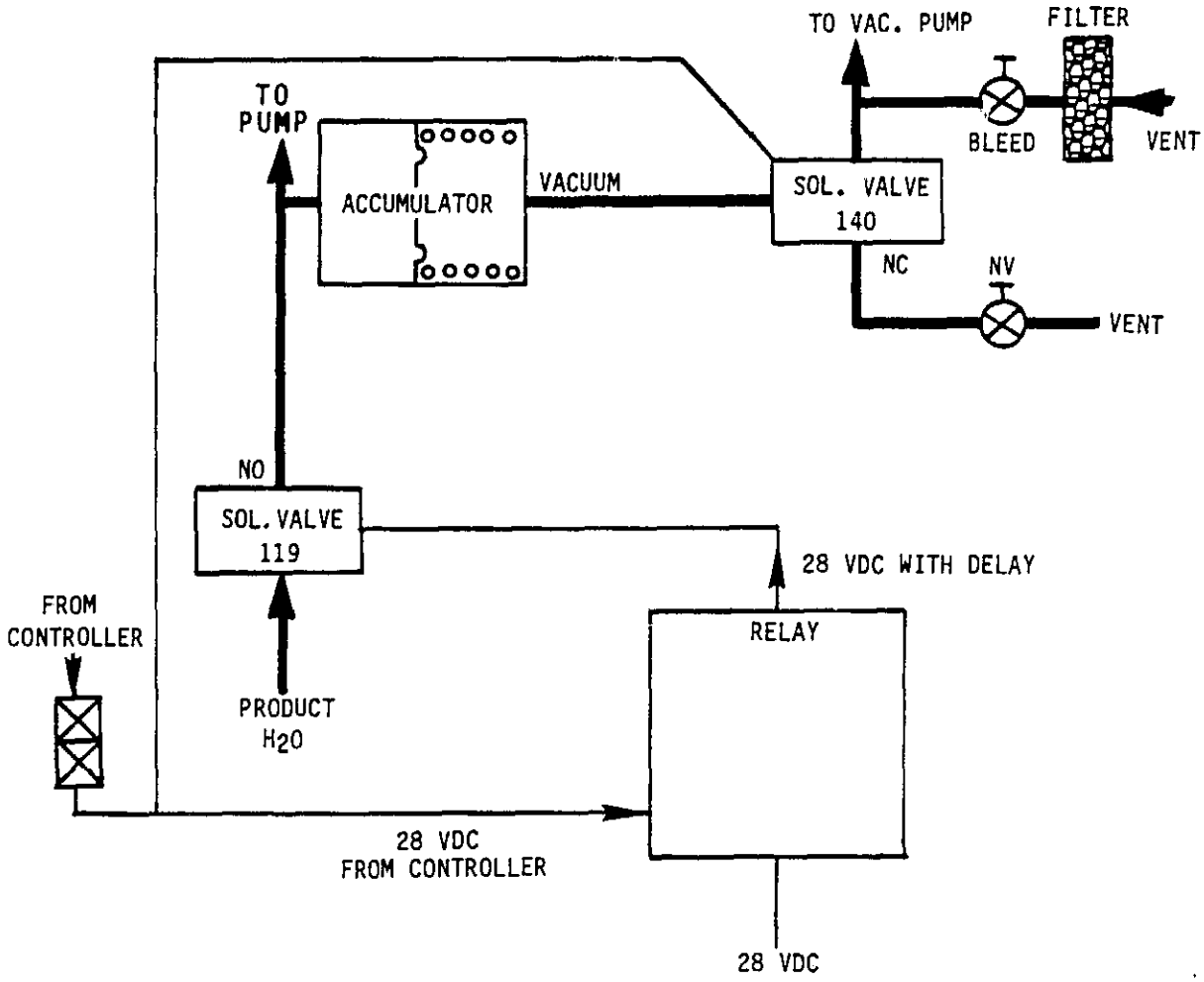

FIGURE 87

ACCUMULATOR VACUUM BREAK SCHEMATIC

Accumulator Production Rate Calculation

The controller logic used to calculate the water production rate was based on the number of accumulator dump cycles occurring in a given period of time. This calculation presumed that only water was collected and discharged from the known volume of the accumulator. Once non-condensible gas appeared in the condensate line, it collected in the accumulator, and the delivered volume of liquid was reduced proportionately. This led to errors in the calculated water production rate.

In order to circumvent this problem, another technique had to be employed. With the batch delivery approach employed on TIMES connecting a flowmeter into the delivery line was not deemed practical. Another direct means of calculating product water was to employ the quantity sensor located in the waste storage tank. Since the recycle loop is constant volume, the volume of product water delivered must equal the volume of waste fluid introduced. To calculate a mass balance on the water input and output requires only that the feed solute concentration be known.

The controller logic was modified so that the deliverable volume of waste fluid from the waste storage tank (when corrected for fill cycles) yielded the approximate mass of water produced. In practice no effort was made to track the input solute concentration since no suitable on-line sensor was available for that purpose. The quantity sensor was constructed of a float and 40 magnetically driven switches that provided a discrete set of outputs as the liquid level changed, in contrast to a more desirable infinite resolution sensor. The result was that the calculations performed were based on discrete data, and an averaging technique had to be employed to smooth out the resulting output readings.

SOLIDS HANDLING IMPROVEMENTS

Objective

Presently employed procedures for determining solids concentration, as well as changing out the recycle tank on the basis of that information, while effective, are somewhat cumbersome and time consuming.

The objectives of this task are to determine a method for calculating and displaying the solids concentration, and to evaluate a means by which the recycle fluid may be purged from the subsystem without removing the recycle tank.

Background

The subsystem had employed a colormeter/turbidometer in order to determine the approximate dissolved solids concentration in the recycle fluid. Due to the fact that some colloidially suspended particles existed despite the filter, changes in color density, expected to be proportional to dissolved solids, were not proportional in practice. As a result, the dissolved solids had to be monitored by taking fluid samples and employing various drying techniques that took up to two days before results could be obtained. When the dissolved solids level was determined to be elevated, the subsystem was shutdown and the recycle tank changed out. While providing for spill proof fluid purging, the tank changeout procedure was cumbersome and resulted in a 3-4 hour interval before a startup temperature could be reached.

Results

A relationship for determining recycle solids at any point in time based on the total water produced, was added to the controller logic. This allows an operator to more accurately determine the point at which the subsystem should be shutdown.

A motor driven valve was substituted for the manual recycle drain valve so that an automatic recycle fluid dump is initiated at the end of a concentrating cycle. This allows the operator to maintain hands-off operation of the subsystem from startup to shutdown.

A batch processing mode was reevaluated for its impact on the specific energy requirement. While some possible improvement was indicatd through the use of this procedure, it is not being recommended since it requires more hardware, primarily for fluid storage.

Discussion

The overall solids handling procedure could potentially be improved by, 1) programming the controller to calculate the dissolved solids based on total water produced, 2) enabling the recycle loop to be flushed out in place using interface connections already available, and 3) concentrating the waste fluid in stages.

Recycle Solids Concentrating Calculation

A relationship expressing the dissolved solids concentration based on the total volume of water produced, can be determined. If factors for the initial solids level present in the loop, as well as the input feed solids are included, the equation is as follows:

$$\% \text{ dissolved solids} = 50\sqrt{4.34 + 1.729\, X_{in}\, W_T} - 104 + X_i$$

where X_{in} = solute weight fraction in feed
X_i = solute weight fraction initially in loop
W_T = pounds of product water

It is based on the solute weight fraction, X, relationship with urine density as follows:

$$\text{density} = 0.4775\, X + 0.99325$$

The solids equation becomes a useful tool for determining when the concentrating cycle should be terminated, since the goal of the cycle is to obtain a certain water recovery. Figure 21 in the Subsystem Analysis section illustrates the relationship of these parameters.

Recycle Loop Dump

Once the large recycle tank was removed from the system, the remaining loop volume totaled 2.2 liters (0.077 ft^3). The filter tank which now acts as the only removable recycle component represents 1.2 liters (0.042 ft^3) or 54 percent of the total. While it is still possible to remove the tank when the final desired solids concentration is reached, it is not as efficient to do so as before, since only 54 percent of the concentrated solids will be removed.

With the addition of a manual three-way drain valve, the subsystem now has the capability of dumping the concentrated waste fluid out of the recycle loop, while simultaneously refilling with fresh, pretreated wastewater. Since there are a number of components such as the filter that create areas of turbulent flow, and therefore, mixing of the high and low density streams, the dump procedure had to be tested to determine the optimum dump time. Too little flush time meant not enough fresh feed replaced the volume of waste fluid in the loop, resulting in a higher than expected residual solids concentration. Too much flush time meant more fresh feed than needed was used in a volume replacement basis, resulting in an inefficient process. Dump cycles on the order of 45 sec. yielded a dump volume of 2.5 liters (0.088 ft^3), or slightly greater than the recycle loop volume. Residual solids concentration level decreased to 7 percent from a pre-dump level of 32 percent.

It was decided to keep the recycle dump volume at 2.5 liters (0.088 ft^3) to minimize fresh waste fluid loss. Having a higher than usual initial solids concentration was acceptable as long as the level was known for the solids calculation. A 5-way electrically actuated valve was installed in place of Item 104, a 3-way valve, although only two of the positions (flush and recycle) were made active. The dump position will be utilized when the associated controller software is implemented at a future date.

Batch Processing

In previous studies, comparisons were made for operating the TIMES in the continuously concentrating mode versus adding another holding tank and concentrating solids in stages. The latter option allowed for less operation at higher concentration, therefore, lowering the average system specific energy. The results, with the system as conceived then, was a savings of 11.4 W-h/kg (5.2 W-h/lb) or 4.7 percent.

An updated analysis has reviewed this mode of operation with the present design having a recycle loop volume of 2.2 liters (0.078 ft^3). It was assumed that the concentration cycle was from 8 to 44% solids.

Figure 88 shows the TIMES simplified flow loop schematic. In the present subsystem, pretreated urine, having a nominal 3% solids concentration is fed into the loop continuously, at a volumetric rate equal to the volumetric water production rate. When the loop reaches a 44% measured solids concentration the system is flushed with 2.5 liters (0.088 ft^3) of unconcentrated urine. The end result is a loop with a solids concentration of approximately 8 percent. From here the concentration process is repeated.

In the modified operation, the process would be as follows:

Step 1: The loop, containing urine with approximately 8% solids is run until solids concentration builds to 25%. The loop is then flushed into the variable displacement tank using fresh urine from the waste tank until the variable displacement tank (VDT) is filled. Taking into account the mixing that would occur, the VDT solids concentration would be approximately 20% and the loop would be left with approximately 8.7% solids.

Step 2: The loop is run until the solids concentration reaches 20%. The waste tank is then shut off.

Step 3: Using the 20% solids in the VDT as feed, the loop is concentrated from 20 to 44% solids. The entire system is then flushed, and steps 1-3 repeated.

It is anticipated that, by processing a greater percentage of the urine at lower solids concentrations, the subsystem can be made to operate more energy efficiently. Figure 89 shows subsystem specific energy, normalized to pure water 176 W-h/kg (80 W-h/lb) versus solids concentration.

Figure 90 is a graphical representation of the energy that can be saved during the concentration cycle if the three step process is used. Using straight line integration, this process saves an average of approximately 16.0 W-h/kg (7.25 W-h/lb) over the continuous process. This is an average of approximately 6.15% energy savings.

The above predictions assume that, for the modified subsystem, no heat leak from the VDT would occur which would add to make-up heat input. Any required additional heating would subtract from the predicted advantage.

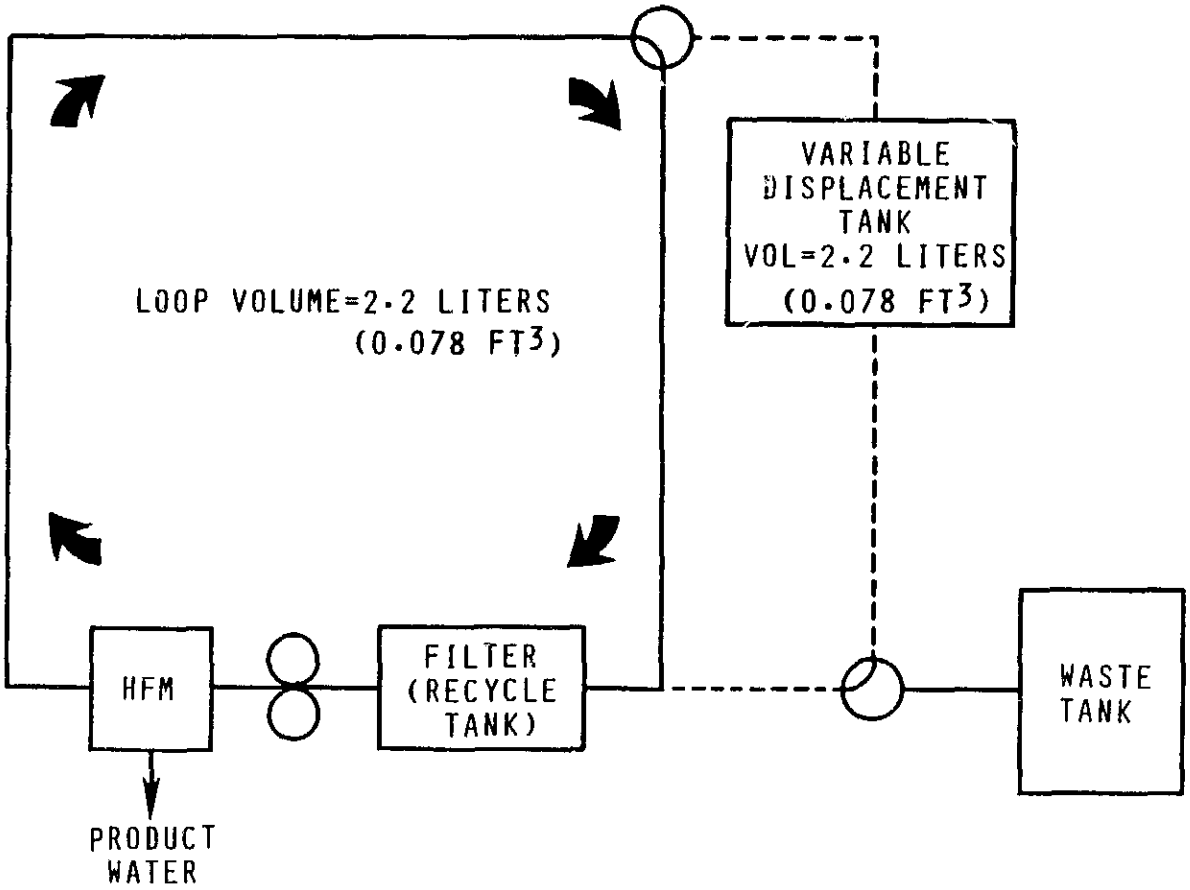

FIGURE 88

BATCH FLOW SCHEMATIC

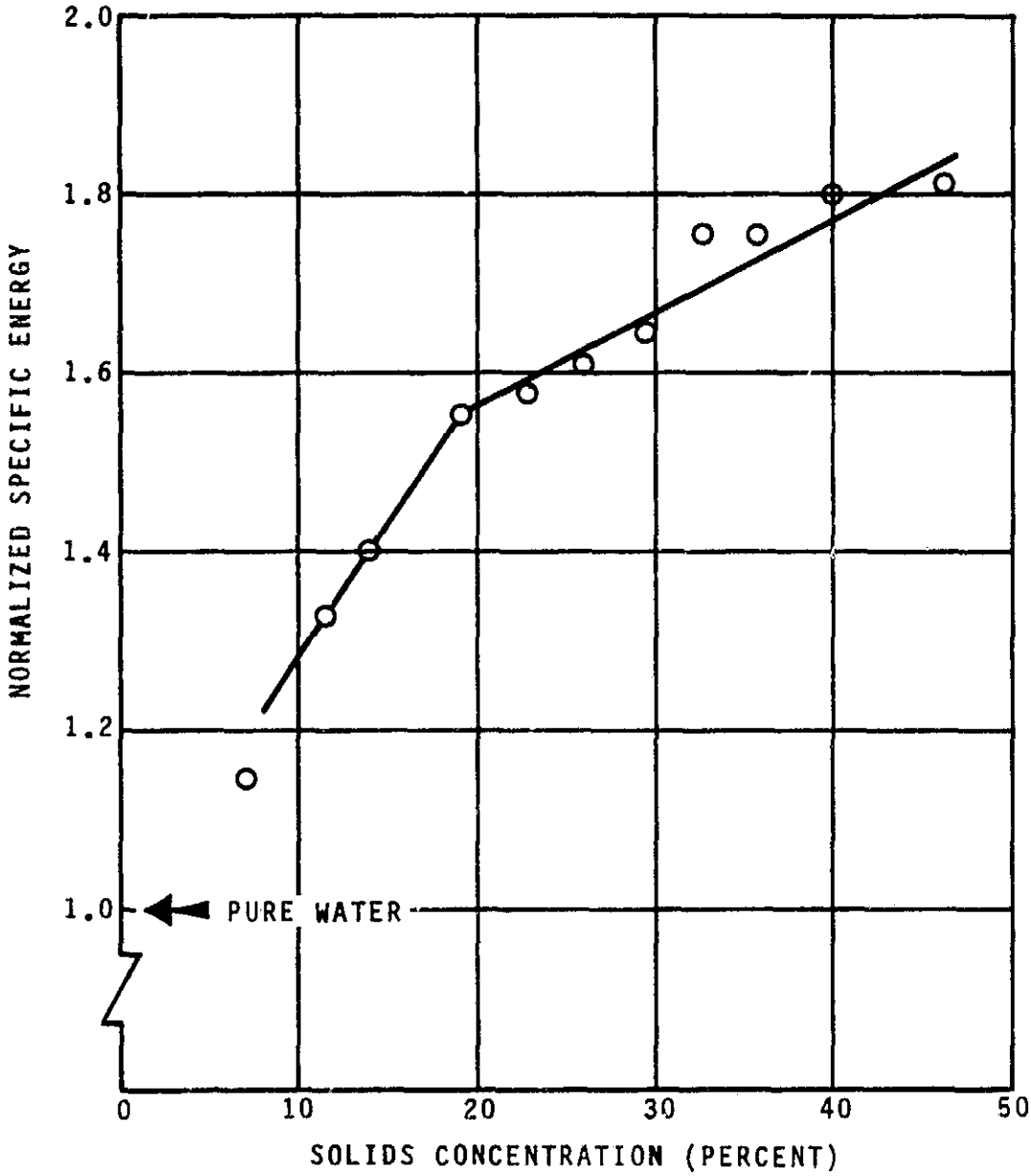

FIGURE 89

NORMALIZED SPECIFIC ENERGY

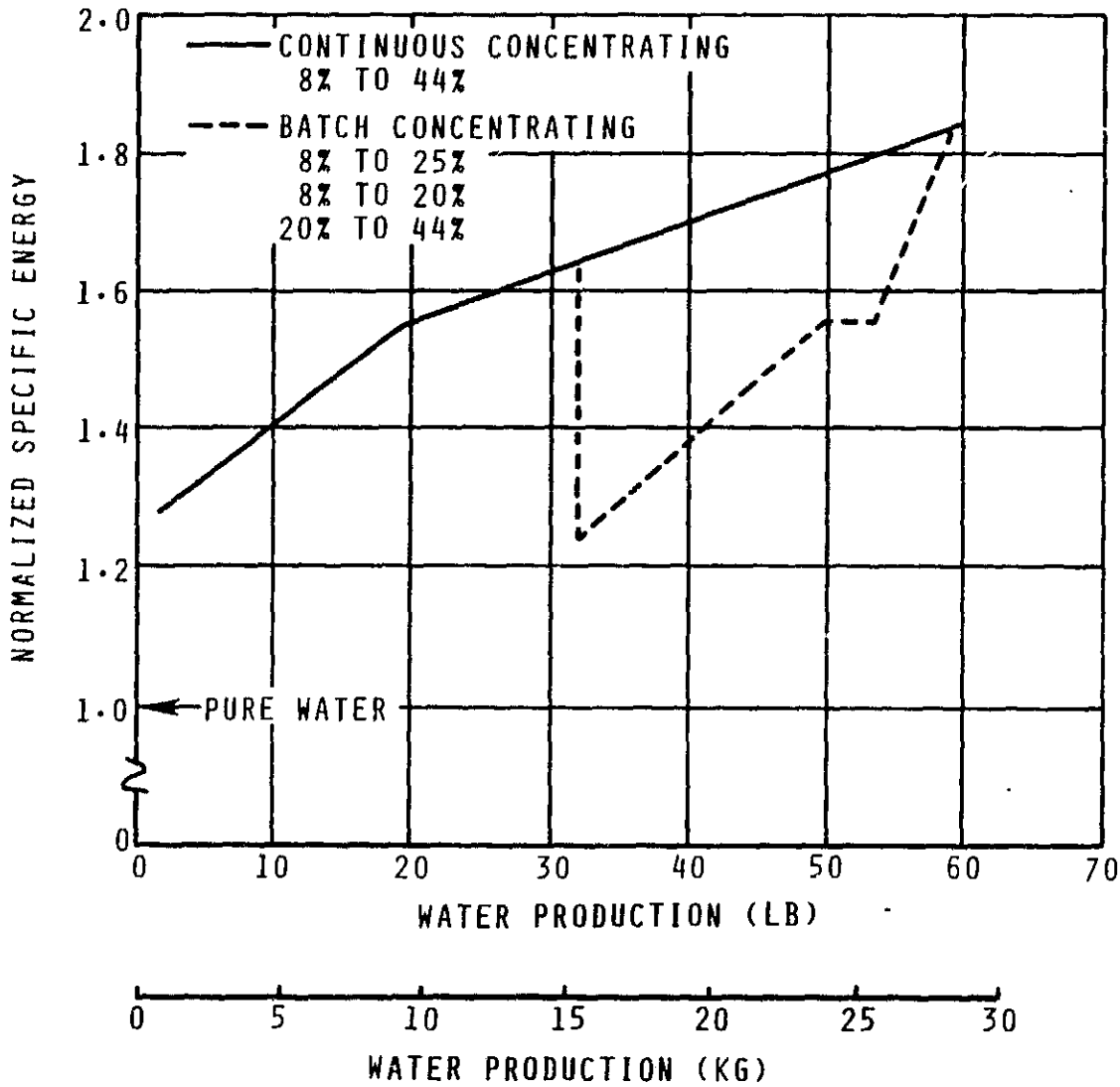

FIGURE 90

BATCH/CONTINUOUS FLOW
SPECIFIC ENERGY COMPARISON

WASTEWATER PRETREATMENT OPTIMIZATION

Objective

The acid pretreatment mix presently used in the subsystem is effective as a biocide and as a pH control agent. Nevertheless, it was felt that it would be valuable to investigate and compare other pretreatments in the subsystem. The objective of this task is to evaluate another pretreatment, Oxone powder/ sulfuric acid, for use with urine and wash water, and to compare the results with those obtained with the chromic/sulfuric acid mix.

Background

Previous subsystem testing has employed a chromic/sulfuric acid pretreatment mix added to incoming urine and wash water feed prior to introduction into the recycle loop. Transients in recycle loop pH towards less acidic conditions have occurred during the long cycle time associated with concentrating the dissolved solids in the loop, resulting in the need to add extra pretreat into the loop periodically or, at the least, increasing the initial dosage. Recycle loop pH control may better be implemented by injecting the pretreatment, or acid portion only, directly into the loop on demand, especially if a non-liquid biocide is employed to initially pretreat the urine. In this way, sulfuric acid, for example, would be used as an additive after the initial pretreatment.

Results

The chromic/sulfuric acid pretreatment mix in the original strength of 0.4% by weight was not able to prevent loss of pH control. Doubling the dosage resulted in excessive chromium precipitation leading to HFM tube clogging. Leaving the chromium concentration as originally specified, and doubling the sulfuric content eliminated clogging problems, but tube coating was still observed.

The Oxone powder/sulfuric acid pretreatment did not result in any precipitate problems, and actually seemed to clean the chromium coated membranes. pH control was maintained throughout the test period and overall subsystem performance was enhanced. This pretreatment is recommended for use for urine and wash water processing over the chromium-based mix.

Discussion

Chromic/Sulfuric Acid Pretreatment

The chromic/sulfuric acid pretreatment recommended to fix free ammonia and kill microorganisms contained the following component proportions:

Chromium Trioxide	= 11.0% (by weight)
Sulfuric Acid	= 44.7
Water	= 44.3

The pretreat was designed to be added into the mixing tank in the weight proportion of 0.4% as raw urine was introduced into the subsystem. However, for all of the testing to date, the urine and pretreatment were actually mixed outside of the subsystem, because of the nature of the collection logistics, i.e., it was not feasible to interface the subsystem with donors in a non-laboratory environment. At the beginning of the urine testing, it became obvious that a single dose was not sufficient to keep pH levels in the 3-3.5 range very long. This result was also noted by the associated rise in product water conductivity (see Figure 79). Thereafter, the dosage was doubled and pH control was then maintained. Initial pH averaged 2.2 with this new dosage. As noted in the previous section, this increased amount of chromium led to more frequent tube clogging by chromium based precipitates. So it was decided to double only the sulfuric acid proportion and reduce the chromium level back to the original value. pH levels now initially were 2.4 when 0.4% of pretreat and an additional 0.075% of H_2SO_4 was used. The HFM was inspected after this dosage was used, and although gross tube clogging was not noted, tube coating was still present.

Oxone:

Oxone was recommended as an alternate pretreatment chemical by NASA/JSC. Oxone is a DuPont product, available in powder form. In a 1% solution, it is acidic, yielding a pH level of 2-3. It is used in laundry bleaches and scouring powders, and is a very strong oxidant. It also has the capability to convert chloride ions to more biocidal oxidized forms including hypochlorite ions.

Used for TIMES, the pretreatment procedure consisted of the addition of the oxone powder and sulfuric acid to a tank of urine in the following proportions:

Oxone	= 4.0 mg/cc
H_2SO_4	= 2.5
H_2O	= 5.0

The resulting nominal pH was 2.3. When used with wash water, the urine was pretreated as usual, and then was diluted with wash water to make a 10% urine/90% wash water mix. No additional pretreat was added.

A material corrosion test was initiated to evaluate the effect of the oxone pretreated urine on the subsystem construction materials. The results are given in Table 33. No effects were noted on any of the materials tested.

The results of urine processing using the oxone pretreatment are included in Figure 79. Included in that test period is a concentrating run to 53%, a milestone that was not reached with the chromium-based pretreatment. This run is shown in Figure 91. Note that the rise in the HFM inlet temperature reached 14°C (25°F).

The first urine/wash water run using the oxone pretreatment is shown in Figure 92. The rise in HFM inlet operating temperature is less than that for urine alone, due to the lower solids concentration at the end point.

Table 33

OXONE/MATERIALS CORROSION TESTING (130°F)

Solution	Item	Days	Remarks
Oxone/Urine (pH = 2.0 - 8.5)	Stainless Steel Tubing	55	No Change
	Viton-GF Plug	45	No Change
	Hypalon Plug	45	No Change
	Viton-A O-Ring	55	No Change
	Nafion Membrane	45	No Change
Oxone/Urine/Soap (pH = 3.0 - 7.0)	Viton-GF Molded Plug	30	No Change

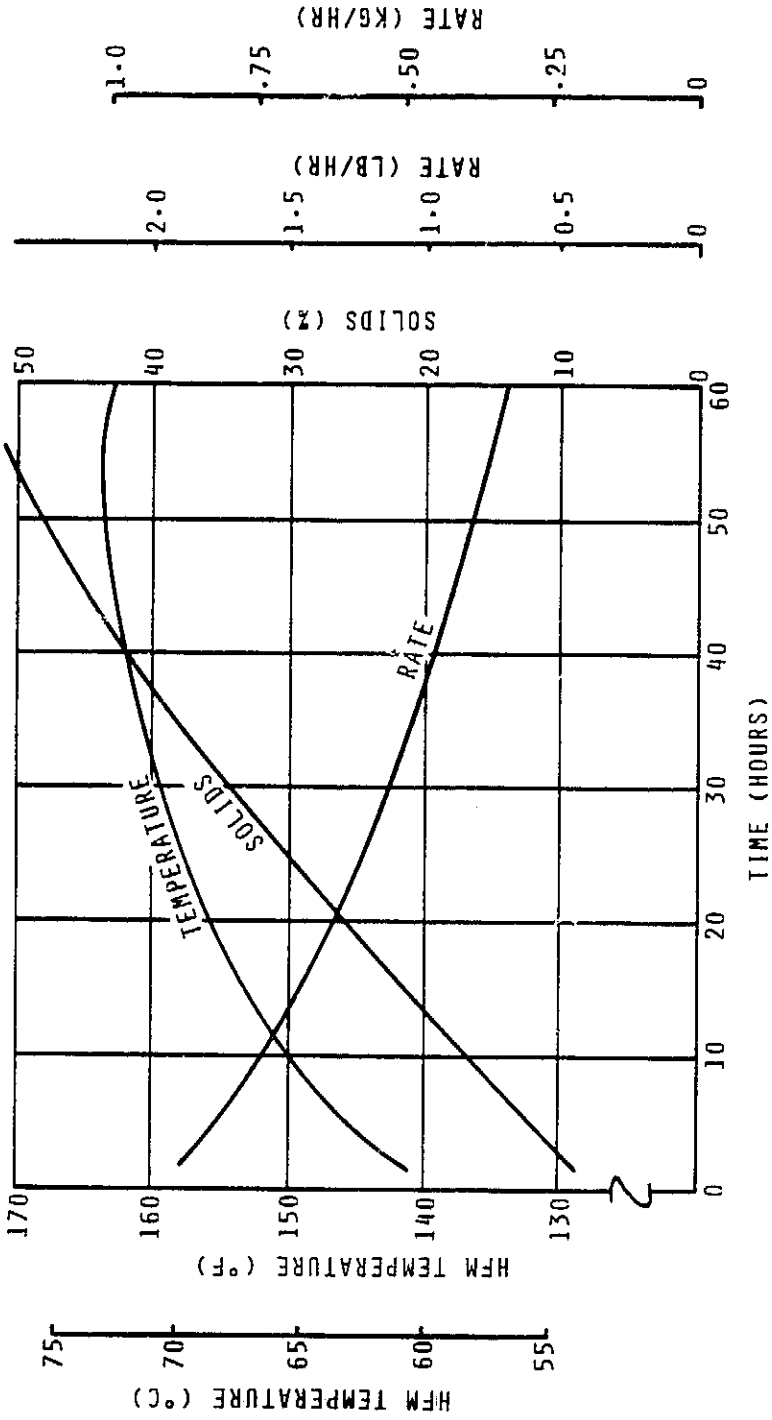

FIGURE 91

URINE/OXONE TESTING
53% RUN

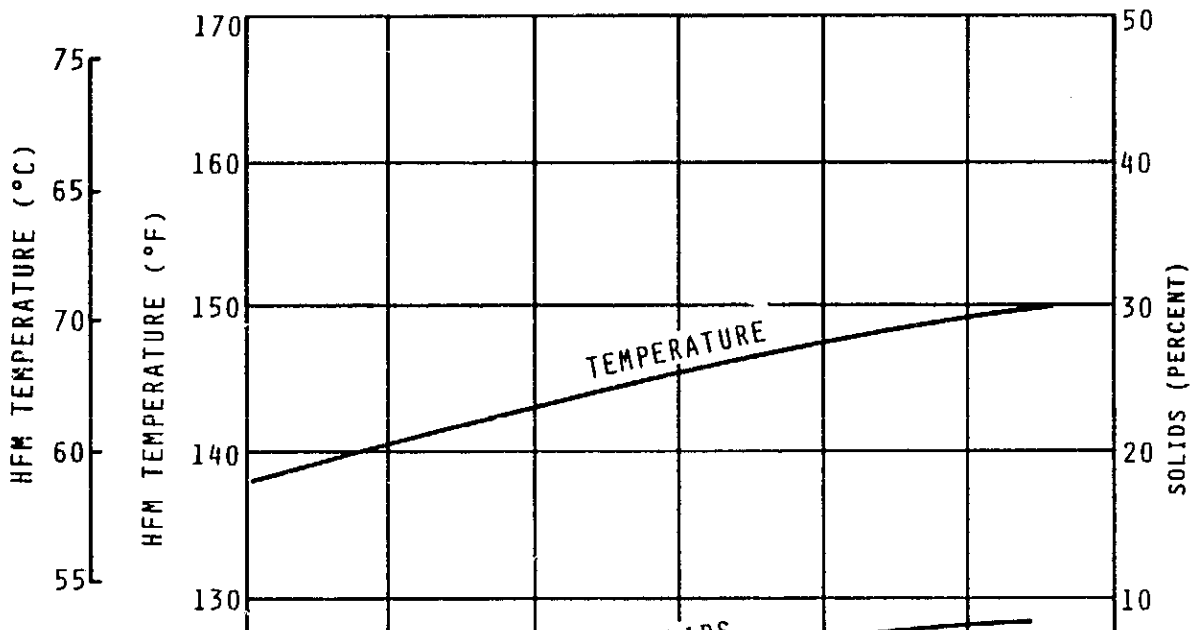

FIGURE 92

URINE/WASH WATER TESTING
OXONE PRETREAT

As noted in the previous paragraphs, the pH of the wash water/urine mix in the recycle loop drifted up to neutral values, yielding product water with high conductivity valves, as seen in Figure 79. The subsystem performance was not affected, however, until 1,655 hours when a concentrated injection of acid was added to lower the recycle pH and conductivity. At this point, the detergent (Bio-Soft HD-100) decomposed, resulting in membrane fouling and subsequent HFM performance decay.

In all, 672 hours of waste water processing was performed using Oxone powder and H_2SO_4 as the pretreatment chemicals. Aside from the manual powder handling procedure necessary, no major problems were noted with this pretreatment formulation once ventilation precautions were established for the off-line mixing procedure.

MEMBRANE REJUVENATION CONCEPTS

Objective

Nafion membrane material has been selected for use on TIMES but data on this material relative to evaporative waste water processing is very limited. The objective of this task is to evaluate a number of concepts for membrane refurbishment while installed in the subsystem.

Background

After completing several hundreds of hours of urine testing in addition to the 850 hours of urine and wash water Acceptance Testing, an obvious change in the membrane water transport rate became evident. Whether the change was due to chemical interaction between the waste water and the membrane, or mechanical clogging, or a combination of both, was undetermined. An obvious approach is to investigate the effect that various chemicals have on subsystem water production rate. Prime candidates would be strong acids or bases that are compatible with the materials of construction. Mechanical cleaning does not appear to be a viable approach, and has not been considered as a serious candidate.

Results

The HFM evaporator may be cleaned in place using a 5-10% solution of sulfuric acid. This solution was found not only to dissolve the inorganic fouling encountered during pretreated urine processing, but also is capable of exchanging hydrogen ions for cations at the Nafion ion exchange sites, thereby rejuvenating the membrane material chemically.

The use of soaps or detergents requires that the pH of the recycle fluid be held closer to neutral conditions to prevent decomposition of these solutes. When surfactant precipitates formed during the testing, 5-10% sodium hydroxide was found to dissolve the contaminants.

A more complete membrane rejuvenation was accomplished outside of the subsystem by soaking the membranes in 20% nitric acid. Both inorganic and organic contaminants were removed by this process.

Discussion

The HFM tubes had been inspected during the replacement of the silicone rubber headers with new Viton-GF headers at the end of the Acceptance Testing, and were found to be clean. After 230 hours were accumulated on the first urine concentrating run (to 41%), evidence of HFM tube clogging was observed (low production rate). The evaporator was removed and the liquid capacity measured only 560 cc (34 in^3) instead of its normal capacity of 900 cc (55 in^3). Disassembly of the HFM did reveal many clogged tubes. The material was assumed to be a chromium precipitate since it was green in color.

Syringe Cleaning

After a day of soaking in hot water, some of the material oozed out of the tubes, but this procedure was very time consuming. It was decided to use a syringe filled with water to force the loosened sludge out of the tubes. This procedure was also time consuming, but at least provided an accurate assessment of when a tube was totally clear. After all 1,656 tubes were subjected to this procedure, there remained at least 10% of the tubes clogged. The unit was resoaked in water for several more days. Finally, the HFM was reassembled, and a 27 kg/h (60 lb/h) flow was pumped through the unit. The liquid capacity was retested and found to be 900 cc (55 in^3) once again. The HFM was then reinstalled into the subsystem.

Water Purge Cleaning

At the end of the second urine concentrating run (to 28%), all the maintainable recycle loop elements were removed for an inspection. A large amount of green sludge was observed on the bottom of the recycle tank, but the HFM showed no clear evidence of clogged tubes. The tubes did, however, have a green coating on the inside wall. It was noted that a water spray from a squeeze bottle would wash off the residue from the HFM bottom urine header which was also coated. So, the HFM was reassembled and purged with a DI water flow, then reinstalled into the subsystem.

Detergent Cleaning

A third urine concentrating run was initiated, and the water production rate appeared normal. When the solids reached 12.5%, a pretreated ML-11 soap and water feed was introduced into the recycle loop. No apparent performance losses were noted. The subsystem was shutdown at 465 hours and the HFM again removed for inspection. A thick coating of green sludge was seen on the top urine header, and several bundles had at least 10% tube clogging. In addition, a coating was again noted on the tube inside walls. The liquid capacity was 780 cc (47 in^3).

This time the HFM was reassembled and flushed for one hour, and then allowed to soak with the detergent solution in the tubes overnight. In the morning, the detergent solution was drained and the HFM was flushed, reassembled, and reinstalled into the subsystem. Urine was introduced into the recycle loop to check baseline performance. Water production rates were worse.

The urine was drained from the subsystem and DI water was introduced and flushed through the recycle loop. Then a pretreated sodium lauryl sulfate (SLS) detergent solution was introduced as feed to the recycle loop. Performance was improved very slightly.

Sulfuric Acid Cleaning

At the 583 hour mark, the subsystem was again shutdown and the HFM removed for inspection. This represented 90 hours of operation on the detergent. The liquid capacity was measured at 820 cc (49 in^3). A visual inspection revealed no clogged tubes, but a green coating was still visible on most tubes. It was found that a moderately concentrated solution of H_2SO_4 (5-10%) was effective in spot removing the green precipitate, so the HFM was allowed to sit with a 1% H_2SO_4 solution in the evaporator shell overnight. The next morning, the acid was flushed out of the shell. The HFM was reassembled and flow purged with a 0.5% H_2SO_4 for one hour. The solution turned green, probably due to replacement of Cr^{+3} ions with the H^+ ions at the ion exchange sites of the Nafion membrane. The liquid capacity was rechecked and found to be back to the original volume. The unit was reinstalled.

The subsystem was started up with a 1% H_2SO_4 acid solution by volume as the feed. The unit was operated for twenty-four hours and the production rate returned to the original baseline level.

Urine was then introduced into the recycle tank. The pretreatment proportions were changed to reduce the amount of chromium trioxide while maintaining the same sulfuric acid level required for pH control. The subsystem was operated for 155 hours with no apparent degradation of the production rate when compared to the original baseline urine run.

Urine processing continued until 1,220 hours had been accumulated with no apparent performance degradation. At this point, the pretreatment chemicals were changed from the chromium trioxide/sulfuric acid mix to oxone/sulfuric acid. An additional 250 hours were accumulated using this pretreatment with no apparent adverse effect.

At the 1,475 hour point, a pretreated wash water/urine mix was employed as the feed. The mixture composition was 10% urine/90% wash water consisting of BioSoft-HD-100, a concentrated liquid detergent blend. No problems were encountered until 1,655 hours when a concentrated H_2SO_4 flow was introduced into the recycle loop at the filter housing in an otherwise successful attempt to bring the loop pH down from 7.5. The lower pH (2.8) was necessary to reduce the high product water conductivity levels. Within several hours after this adjustment, the production rate fell off drastically. At 1,755 hours, a 1% H_2SO_4 solution was flushed through the HFM in place in the subsystem for sixteen hours. In the morning, the circulate was green and sudsy. The subsystem was restarted, but this time no performance recovery was observed. Finally at the 1,860 hour mark, the HFM was again disassembled. No clogged tubes were evident, but the tubes were green-black in color and had salt-like deposits on the outside surfaces. It was decided to terminate waste water processing and just use tap water to try to determine the cause of the degraded performance and if it could be remedied.

It was presumed that the detergent had decomposed at the low pH levels that occurred after the sulfuric acid ingestion for pH control. Now the problem was to try to remove the contaminants from the HFM tubes.

Sodium Hydroxide Flush

The HFM was flushed in place with 1% H_2SO_4 again overnight. By morning, the solution was green and sudsy as seen before. The spent solution was flushed and new acid solution introduced. The subsystem was started up and improved performance was observed initially. After twenty-four hours, performance was degraded somewhat. The HFM was again removed and a slimy, brown material was found in the headers. It dissolved in a 1% NaOH solution. The same solution was used to circulate through the HFM in place. The solution immediately turned brown and had a distinct amine smell.

The subsystem was restarted and some improvement was noted. Finally, a 0.5% (by weight) $CrCl_3$ solution was flushed through the subsystem, and subsequent to that, full recovery was noted. The recovery was due to replacement of salts with chromium which imparts a greater water transport capability to the membrane.

Nitric Acid Rejuvenation

After the testing was completed, the HFM was removed and the membranes were observed to be black in color and extremely stiff. The bundles were removed from the HFM and several tubes were subjected to solutions including bleach, nitric and sulfuric acids, and concentrated pretreatment solution. Only a 20% HNO_3 mix was able to remove the contaminant and return the membrane to a more flexible state over a period of twenty-four hours.

TIMES II STUDY EFFORT

SUMMARY

There are four tasks described in this section reflecting studies performed to develop a preliminary design concept for a next generation TIMES. The overall results of the study are the completion of major design analyses, and preliminary configuration layout drawings.

In conjunction with the study, it was necessary to refurbishment the TIMES I packages, including an upgrading of the computer generated graphics display. All the processing components were installed into the processing package, while tanks and post filters were installed into the collection package. New insulation panels were also installed on the processing package.

Thus outfitted, the subsystem was operated on urine and water feeds to establish a performance baseline, and to ensure proper operation. After this checkout, the subsystem was shipped to NASA/JSC where a urine processing test program was completed. The test results from that program will be included in a NASA/JSC report.

THERMOELECTRIC REGENERATOR IMPROVEMENT

Objective

In order to meet the goals of lower specific energy, greater ease of maintainability, and enhanced reliability, an improved TER configuration is necessary. The objective of this task is to study those areas where improvements may be realized, such as thermoelectric module selection, electrical network wiring, and condensing section design.

Background

The present TER configuration was selected to provide the required water production capacity from the condensation of the steam load and reutilization of the latent heat load of the process. To ensure condensate transport through the porous plates, an adequate pressure differential had to be mantained. This ΔP was a function of the operating temperature differential across the TER heat pump. The TER efficiency is inversely proportional to the ΔT, so in order to decrease specific energy, the ΔT has to be decreased as well. One way of doing this is to decrease the TER electrical current. However, the heat pumping capacity is directly proportional to current, therefore the number of thermoelectric modules must be increased to maintain a given condensation load.

Another way is removal of the porous plate which serves two purposes; 1) overall TER reliability is increased, and 2) ΔP requirements are lower for transport of condensate from the condenser to the output pump. However, the output pump must be capable of separating the gas load from the condensate, in order to ensure gas-free product water delivery.

It is necessary to redesign the TER assembly in order to incorporate the above mentioned modifications in an energy and weight efficient configuration.

Results

A water production rate of 0.67 kg/h (1.48 lb/h) was obtained using an existing EMU gas/water separator in place of the accumulator and burper. This was lower than that obtained for the baseline run, but the subsystem at least demonstrated stable operation with the separator installed.

The TER was operated at a reduced voltage of 15 VDC, and the specific energy demonstrated was 85.3 W-h/kg (38.8 W-h/lb). The water production rate at this operating condition was 0.53 kg/h (1.16 lb/h). This test demonstrated the potential for operating the thermoelectrics at reduced power conditions in order to decrease the specific energy.

It was determined that a reconfigured TER could be operated at significantly reduced specific energy levels if the total number (area) of the thermoelectrics was increased four-fold. An equivalent performance, larger area thermoelectric module is available that will minimize the number of electrical interconnections required for this arrangement. A preliminary TIMES II TER would include 234 thermoelectric modules arranged in a rectangular sandwich configuration. Two arrays of 117 thermoelectrics would provide an active area of 0.40 m^2 (4.34 ft^2).

A gas/liquid separator design would require a larger rotating drum than the one included in the present EMU design. The rotational speed would be 7000 RPM. A single motor could drive the separator and the recycle pump.

The main condenser would consist of small passages so that flow velocities can be kept high enough to avoid stagnation. An aftercooler would be necessary to recondense the steam not condensed in the main condenser, in order to provide a means of additional cooling.

Discussion

Gas Separator Testing

In order to determine the applicability of substituting a gas/liquid separator for the porous plates on TIMES, a test was conducted using a gas/water separator designed for the EMU space suit. The performance charactersitics of this separator were close enough to the gas and liquid output required of the TIMES condensate stream to allow the interconnecting of the two units as shown in Figure 93.

In an actual application, there would be no need for porous plates to act as the main condensing/transport surface in the TER, but it was not possible to modify the existing TER to eliminate their presence. However, the main point of the test was to evaluate the operating performance of typical separator design in handling two phase fluid flow in the proportions typical of a TIMES process.

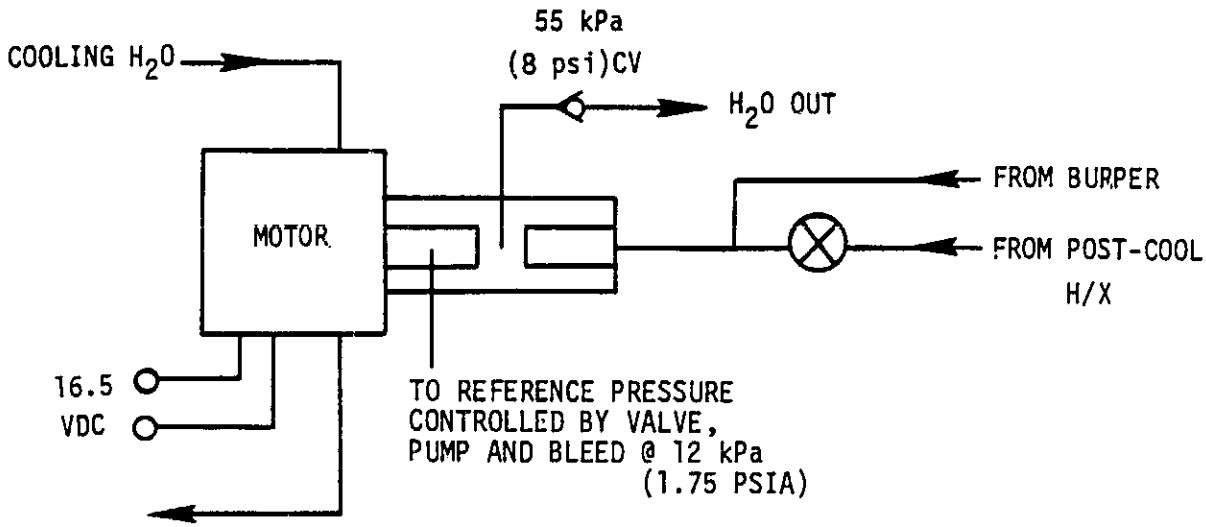

FIGURE 93

GAS/LIQUID SEPARATOR/TIMES SCHEMATIC

The test was conducted after the newly refurbished TIMES (including new membranes for the HFM) had accumulated 65 hours of operation on a urine feed. For this test the feed was changed to tap water, in order to keep the recycle fluid properties constant. Both the burper line, and the condenser were combined at the separator inlet. Thus, the total loading of gas and liquid generated by transport through the membrane walls is present at that point, and for all purposes, any effect of the porous plate is negated.

The test was initiated by first starting up the subsystem, which then automatically entered the "warming-up" state. The separator motor was then started, the reference pressure shut off valve opened, and the condensate shut off valve opened. The separator motor current was 1.95 - 2.00 amps, giving a power draw of 33 watts.

The test was conducted over a two day period. The results are given in Table 34 and are compared to a performance level obtained on tap water feed operation immediately preceding the initiation of the separator test.

The plumbing schematic was modified on the second day by moving the inlet valve ahead of the burper line as well, so that the separator could be completely isolated. In addition, the reference pressure was reduced to 10 kPa (1.45 psia) from 10.8 kPa (1.55 psia). Results are given with and without the product water check valve. The check valve backpressures the separator to allow efficient separation to occur. The burper line solenoid valve was kept open 100% of the time, instead of its normal 5% duty cycle.

The water production rate using the separator, in place of the accumulator and burper was lower than that obtained for the baseline run performed with the normal subsystem configuration. The evidence for this includes higher HFM inlet and ΔT temperatures, and lower TER currents. It is entirely likely that this is attributable to the choice of reference pressure. The total water produced was 0.67 kg/h (1.48 lb/h), but the loss to vacuum was 14% of this total, which indiates the separator back pressure from the check valve was too high.

TIMES I TER Power Requirements

The subsystem was operated on urine at 26.5 and 29.0 VDC over two nominal 40 hour concentrating cycles. Water production, power and specific energy, are plotted in Figures 94 through 101. The average specific energy values for 26.5 and 29.0 VDC are 200.2 W-h/kg (91 W-h/lb) and 224.4 W-h/lb (102 W-h/lb) respectively. Of those totals, nearly 80% is due to the TER power requirement as seen in Table 35. In order to fulfill the goal of low subsystem specific energy, it would therefore be necessary to reduce this large TER contribution. According to thermoelectric operating principles, the easiest way of accomplishing this is to lower the current required for the heat pumping process. The TIMES was utilized to evaluate this approach by performing a test where the TER voltage was reduced to 15 VDC, thereby reducing the current and power requirement.

Table 34

EMU SEPARATOR TEST

Parameter		Subsystem Baseline	Run #1	Separator Run #2 Check Valve Off	Separator Run #3 Check Valve On
Reference Pressure,	kPa (psia)	---	10.7 (1.55)	10.0 (1.45)	10.0 (1.45)
HFM T	°C (°F)	57.2 (135.0)	60.4 (140.7)	60.7 (141.3)	61.7 (143.0)
ΔT	°C (°F)	4.1 (7.3)	4.0 (7.2)	3.6 (6.5)	3.8 (6.9)
Recycle Temperature,	°C (°F)	50.08 (123.5)	54.3 (29.8)	54.9 (130.9)	55.8 (132.5)
Steam Pressure,	kPa (psia)	13.1 (1.9)	15.9 (2.3)	16.6 (2.4)	17.2 (2.5)
Current:					
TER 1, amps		1.87	1.81	1.77	1.79
TER 2, amps		1.92	1.87	1.82	1.83
TER 3, amps		1.80	1.80	1.75	1.77

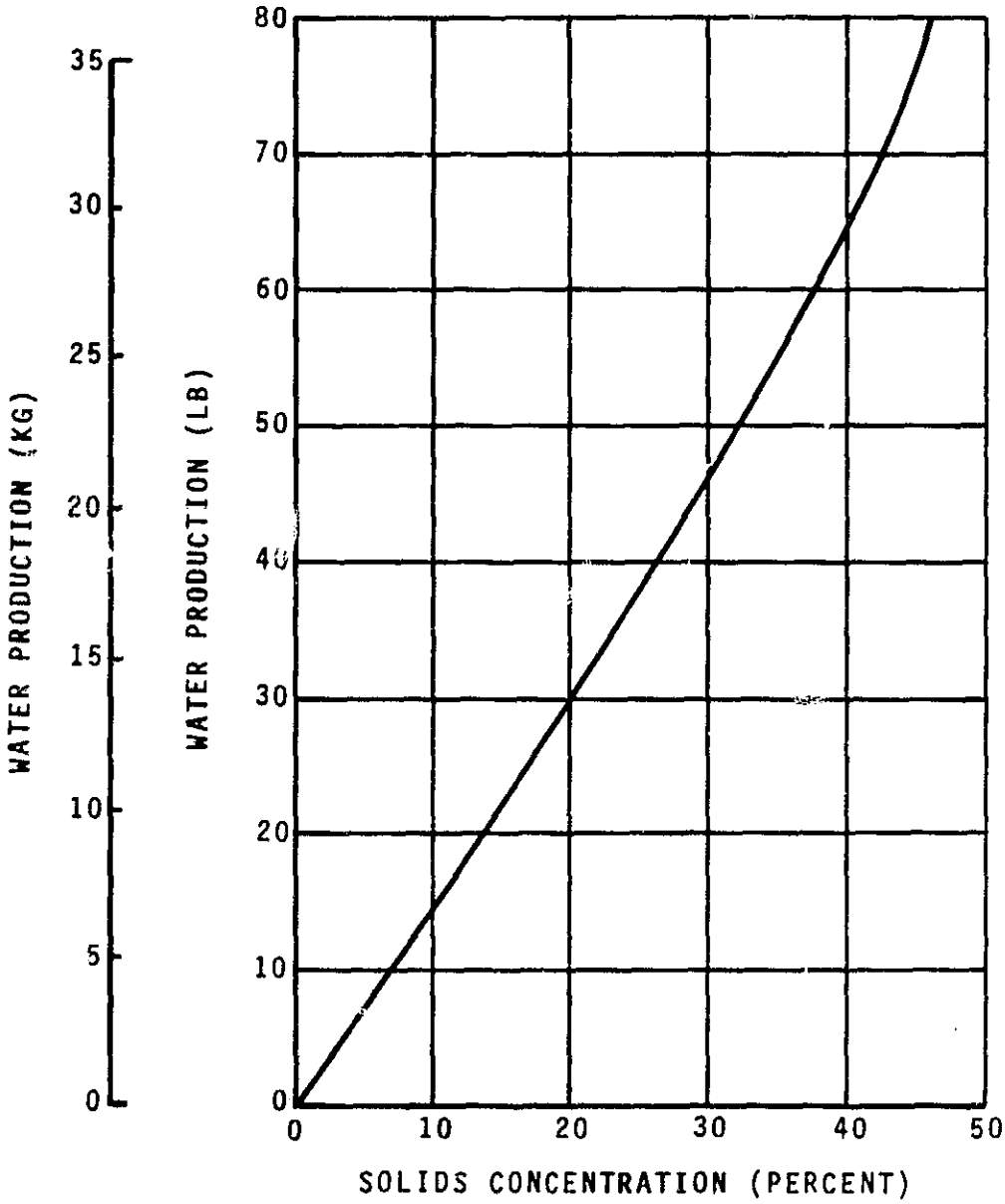

FIGURE 94

WATER PRODUCTION VS SOLIDS CONCENTRATION
26.5 VDC

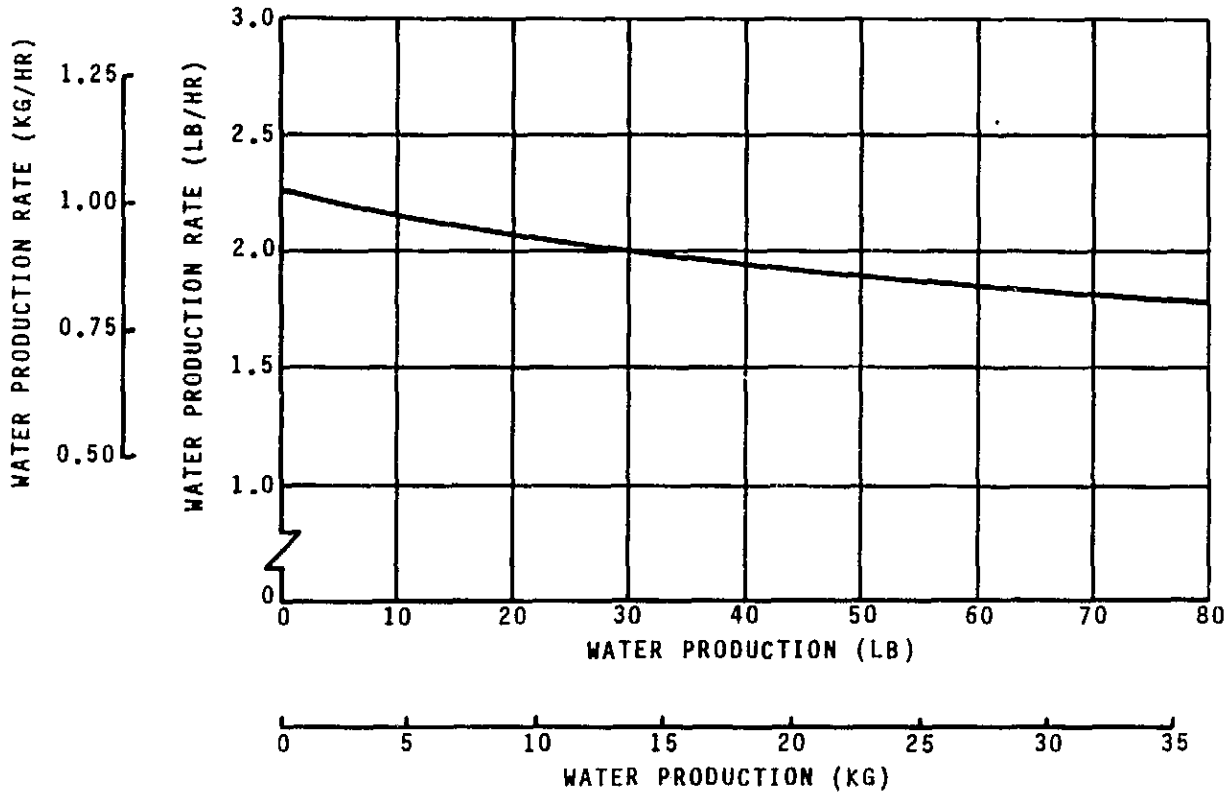

FIGURE 95

WATER PRODUCTION RATE VS WATER PRODUCTION
26.5 VDC

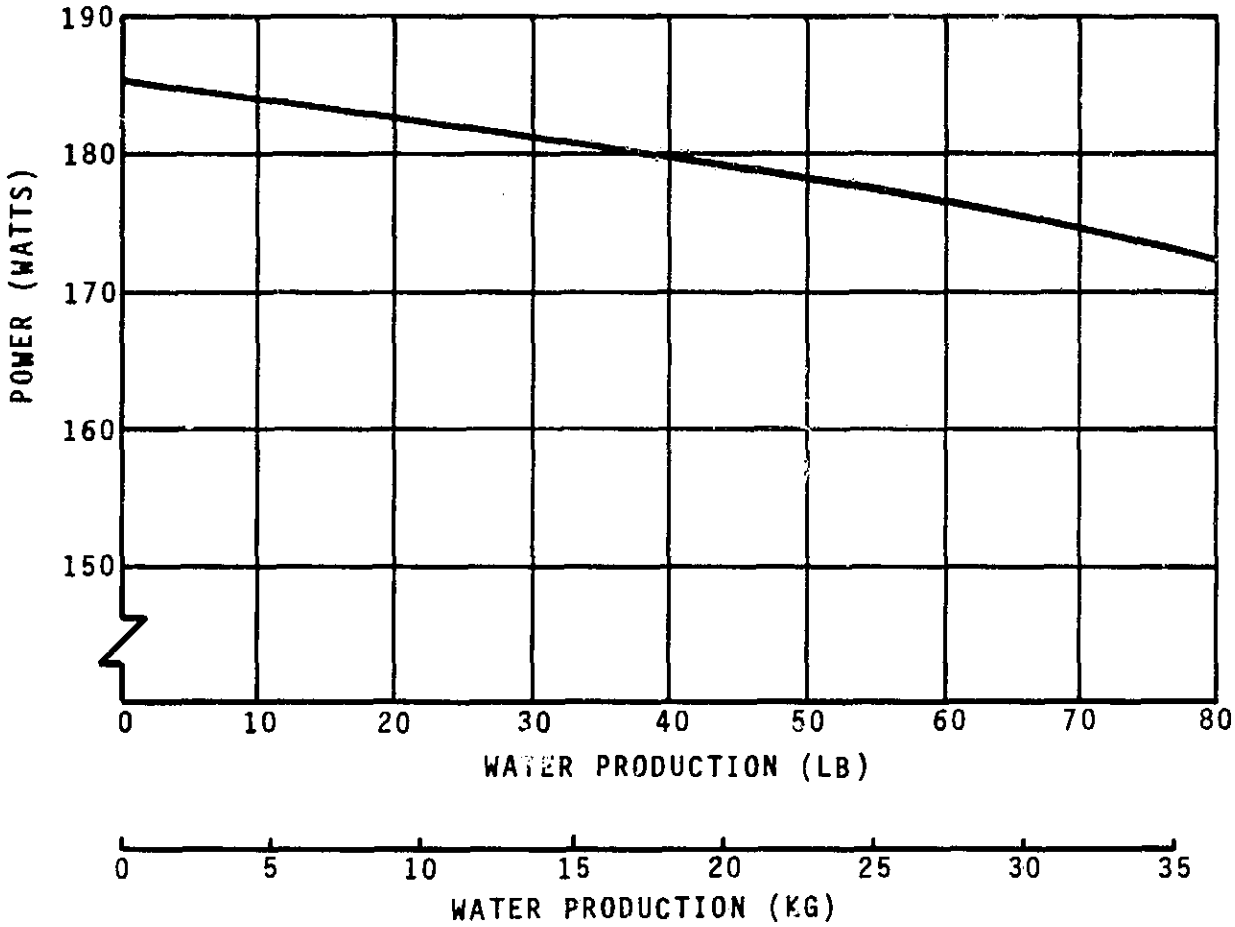

FIGURE 96

POWER VS WATER PRODUCTION
26.5 VDC

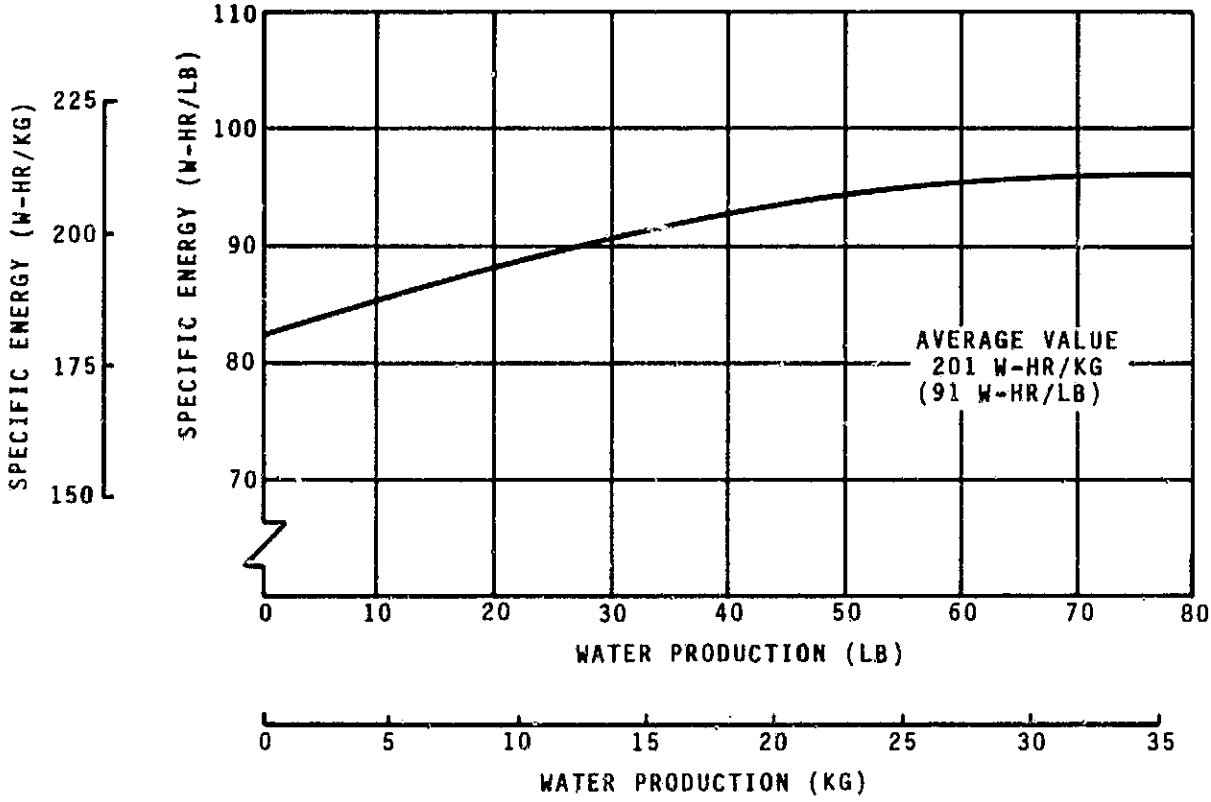

FIGURE 97

SPECIFIC ENERGY VS WATER PRODUCTION
26.5 VDC

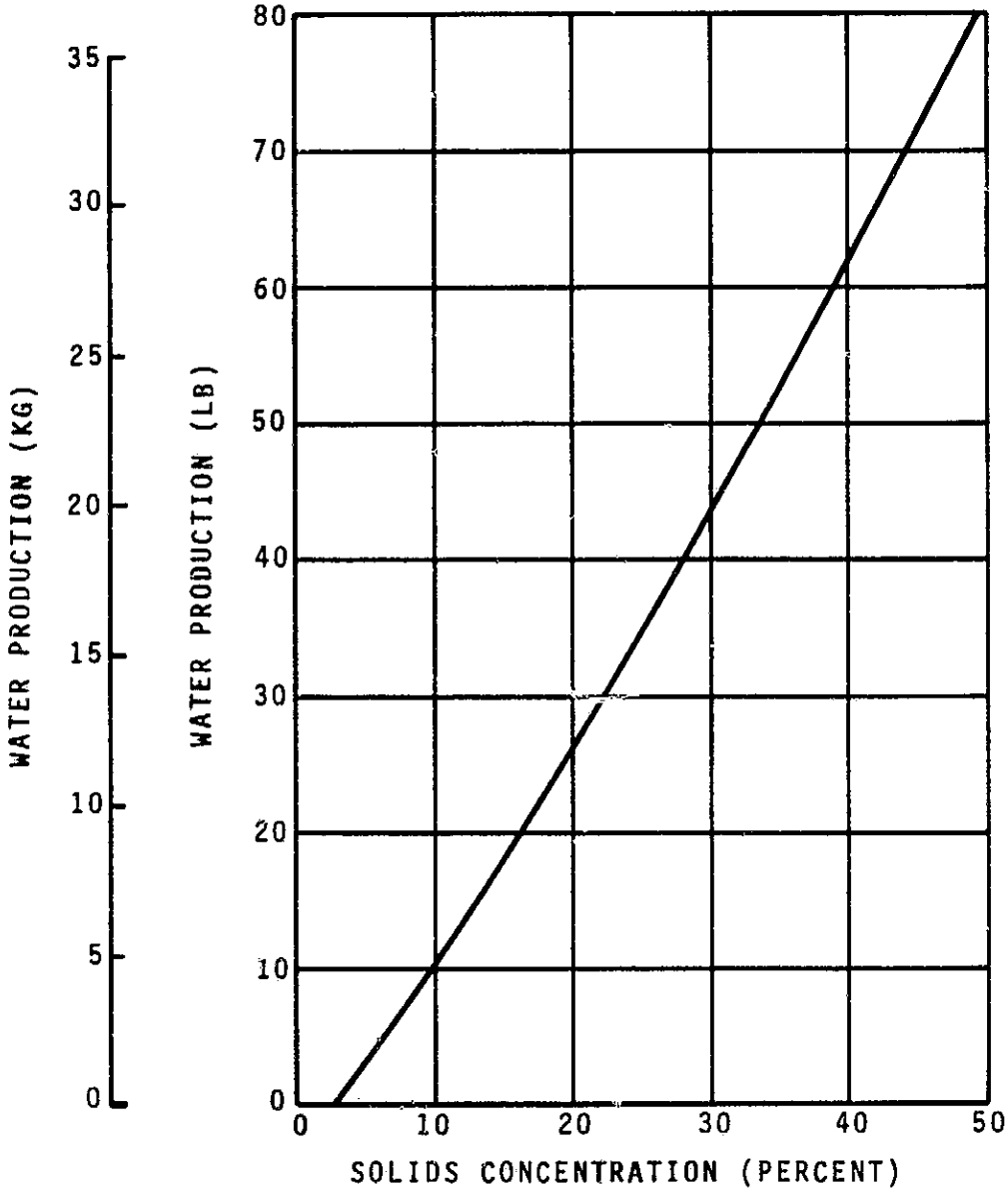

FIGURE 98

WATER PRODUCTION VS SOLIDS CONCENTRATION
29 VDC

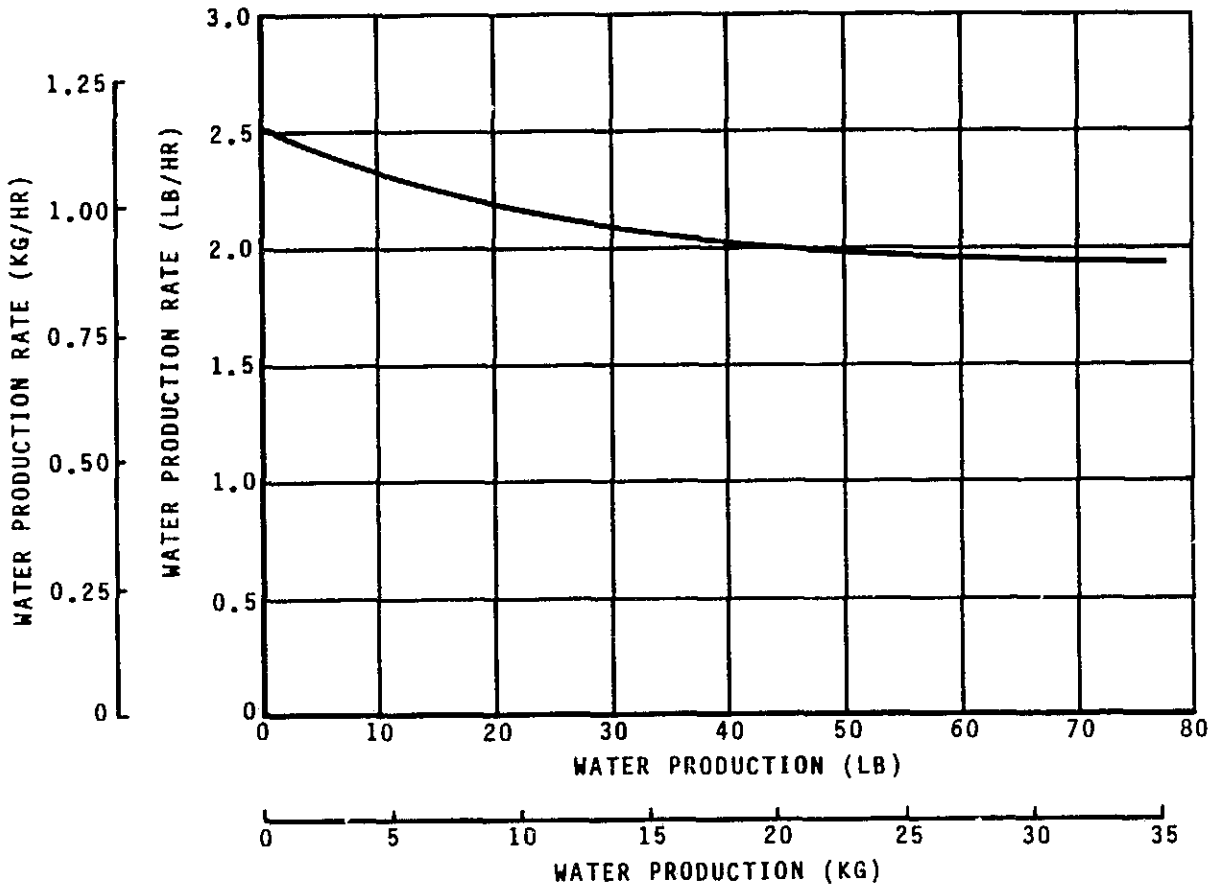

FIGURE 99

WATER PRODUCTION RATE VS WATER PRODUCTION
29 VDC

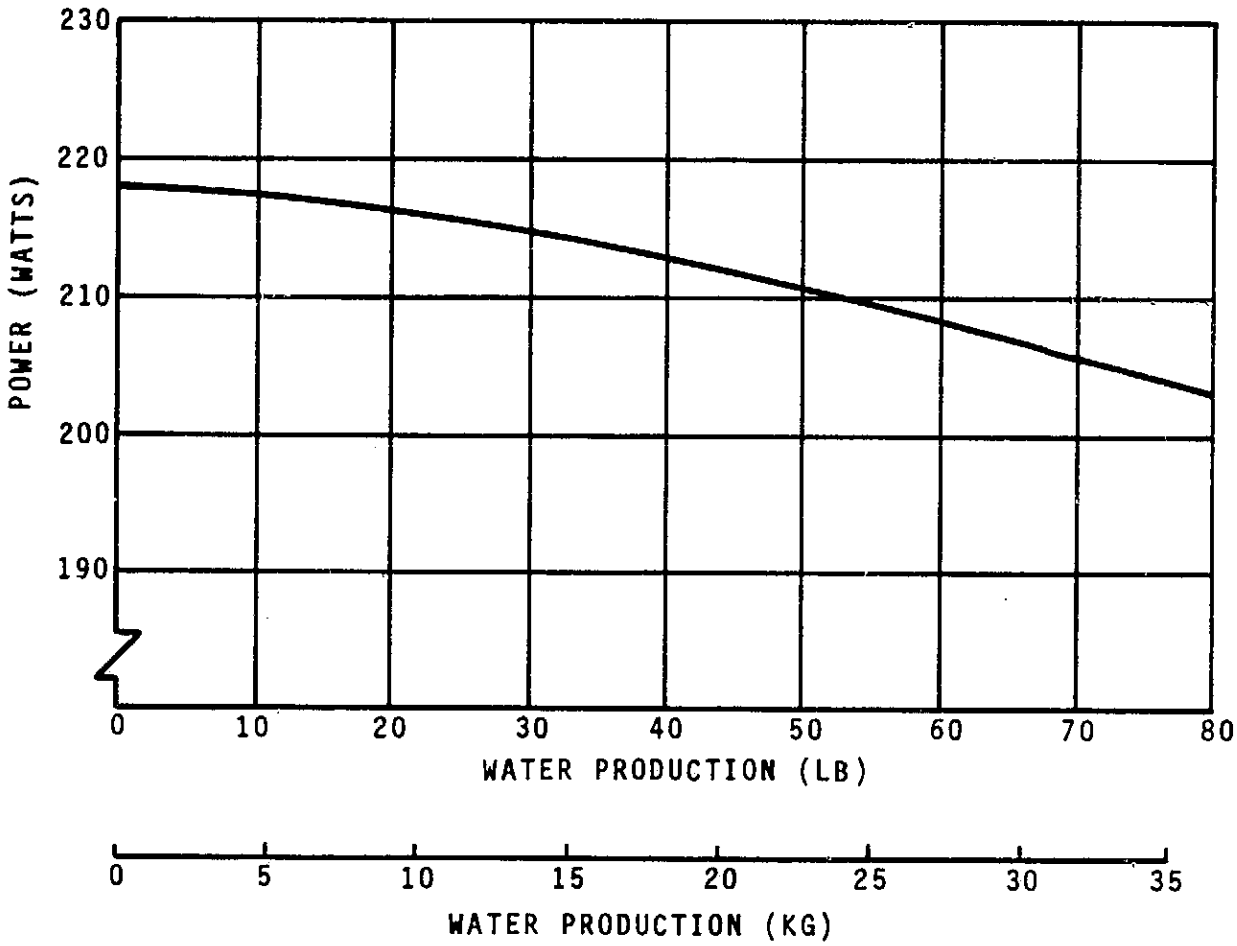

FIGURE 100

POWER VS WATER PRODUCTION
29 VDC

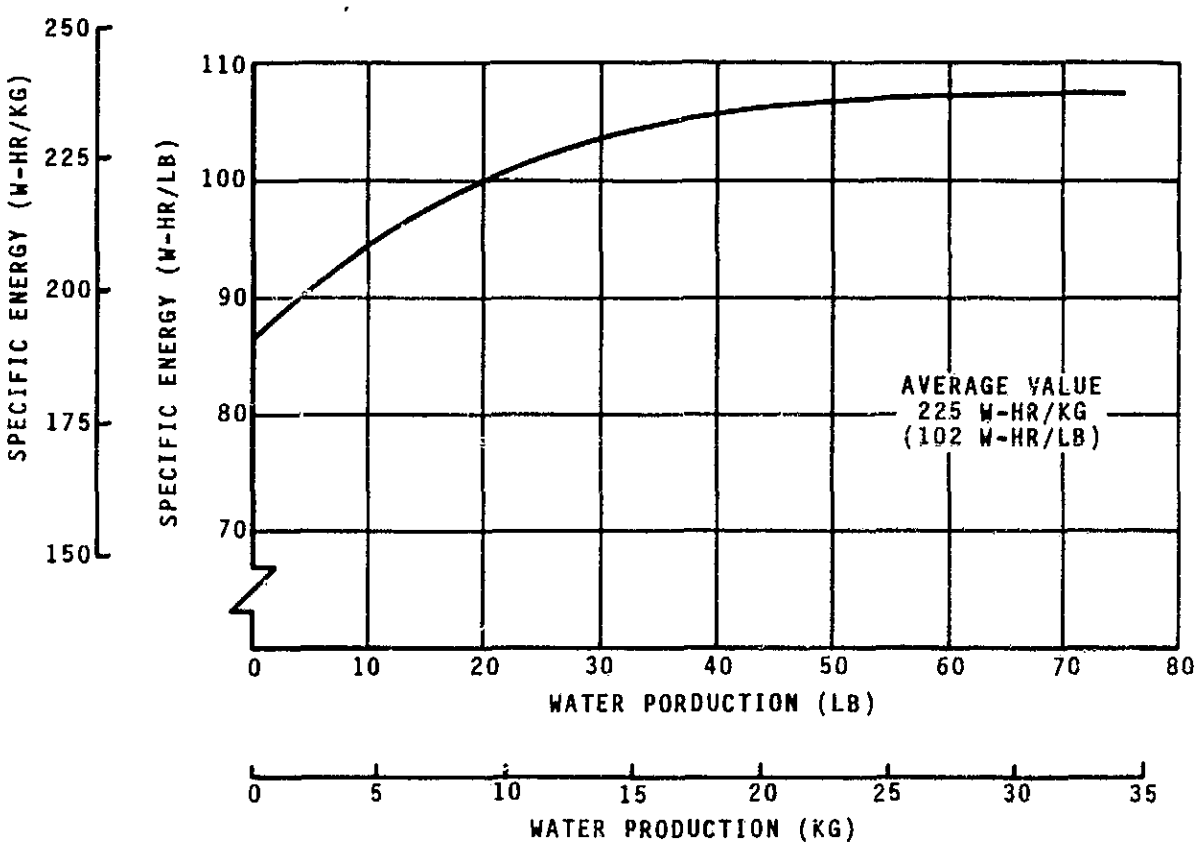

FIGURE 101

SPECIFIC ENERGY VS WATER PRODUCTION
29 VDC

Table 35

NOMINAL POWER REQUIREMENTS

- 26.5 Volts DC
- Water Production = 0.9 kg/h (2.0 lb/h)
- Unconcentrated Urine

Item	Current (A)	Duty Cycle (%)	Effective Power W (BTU/h)	Specific Energy W-h/kg (W-h/lb)
TER	5.5	100	144.3 (492.4)	157.0 (71.2)
Recycle Pump	1.2	100	32.0 (109.2)	35.3 (16.0)
H/X Fan	0.2	100	5.3 (18.1)	5.3 (2.4)
Filter Heater	1.5	2.5	1.0 (3.4)	0.9 (0.4)
Burp Valve	0.7	5.0	0.9 (3.1)	0.9 (0.4)
Condensate Pump	1.3	2.0	0.7 (2.4)	0.7 (0.3)
Accumulator Valves	0.7	2.0	0.4 (1.4)	0.4 (0.2)
		Total	184.6 (630.0)	200.5 (90.9)

A separate power supply and current meter were connected to the TER. The subsystem was started up with a water feed and allowed to heat up.

After 6.5 hours, the HFM inlet temperature was still only 50°C (122°F) due to the reduced amount of heat pumping occurring at 15 VDC. No product water was evident at this temperature (not enough ΔP to drive the membrane transport mechanism) so the test was stopped. A software change was made to allow the filter heater to remain on during automatic processing, and the TER voltage was initially set at 29 VDC. Within one hour the voltage was reduced to 15 VDC, and after 4 hours the filter heater was shut off. The HFM inlet temperature at this point was 53°C (128°F) and stabilized here for the next two hours. The HFM ΔT leveled off at 2.3°C (4.2°F), and total water production (product and burp) was 0.53 kg/h (1.16 lb/h). The TER current was 3.0 amps, giving a specific energy of 85.3 W-h/kg (38.8 W-h/lb).

Sizing For Low Specific Energy Operation

The results of the low voltage tests confirmed that the Cambion thermoelectric element used for TIMES I could be more efficiently operated at lower power. An effort then was made to calculate the number of thermoelectric elements needed to provide the same design water production rate at lower power.

Using the concept of total equivalent weight (TEW) as the basis for comparson, a map of TER specific energy versus TEW was generated for several multiples of the present number of thermoelectric elements, and present membrane area. The results are graphically displayed in Figure 102. The TEW calculation is shown in Table 36 and is based on a 227 kg/kW (500 lb/kW) penalty for a projected total specific energy requirement of 143 W-h/lb (65 W-h/lb). The map is generated by proportioning the projected membrane and TER weights based on the TIMES I assembly weights. A water production rate of 0.77 kg/h (1.7 lb/h) is used as a basis for comparison since this is the TIMES I design requirement.

Referring to Figure 102, it is seen that the present design employs 96 thermoelectric modules and has a membrane PA = 5. A 44% decrease in the TER specific energy could be theoretically realized, and the COP_{TER} increased from 4.5 to 8.0, by doubling both the number of modules and PA, and decreasing the module voltage from 0.73 to 0.38 VDC. In order to generate a higher water production rate at a given COP_{TER} level requires that the module and membrane area be increased proportionately. For example, in order to obtain a production rate of 1.54 kg/h (3.4 lb/h) at a COP_{TER} = 8, the number of modules = 384 and the PA = 20. The water production rate can also be increased at the expense of the COP_{TER} if the voltage/module is increased for a given number of modules and membranes. This result is illustrated by the map of thermoelectric characteristics given in Figure 103. It should also be noted that decreasing COP_{TER} by lowering the voltage (hence current) per module causes the ΔT generated across the module to decrease as well. Depending on the actual subsystem design application, low ΔT's and associated COP's may be difficult to realize. Thus from a practical standpoint, a COP_{TER} = 8 may not be realizable, while a COP_{TER} = 6 should be considered the maximum value for the actual best design point.

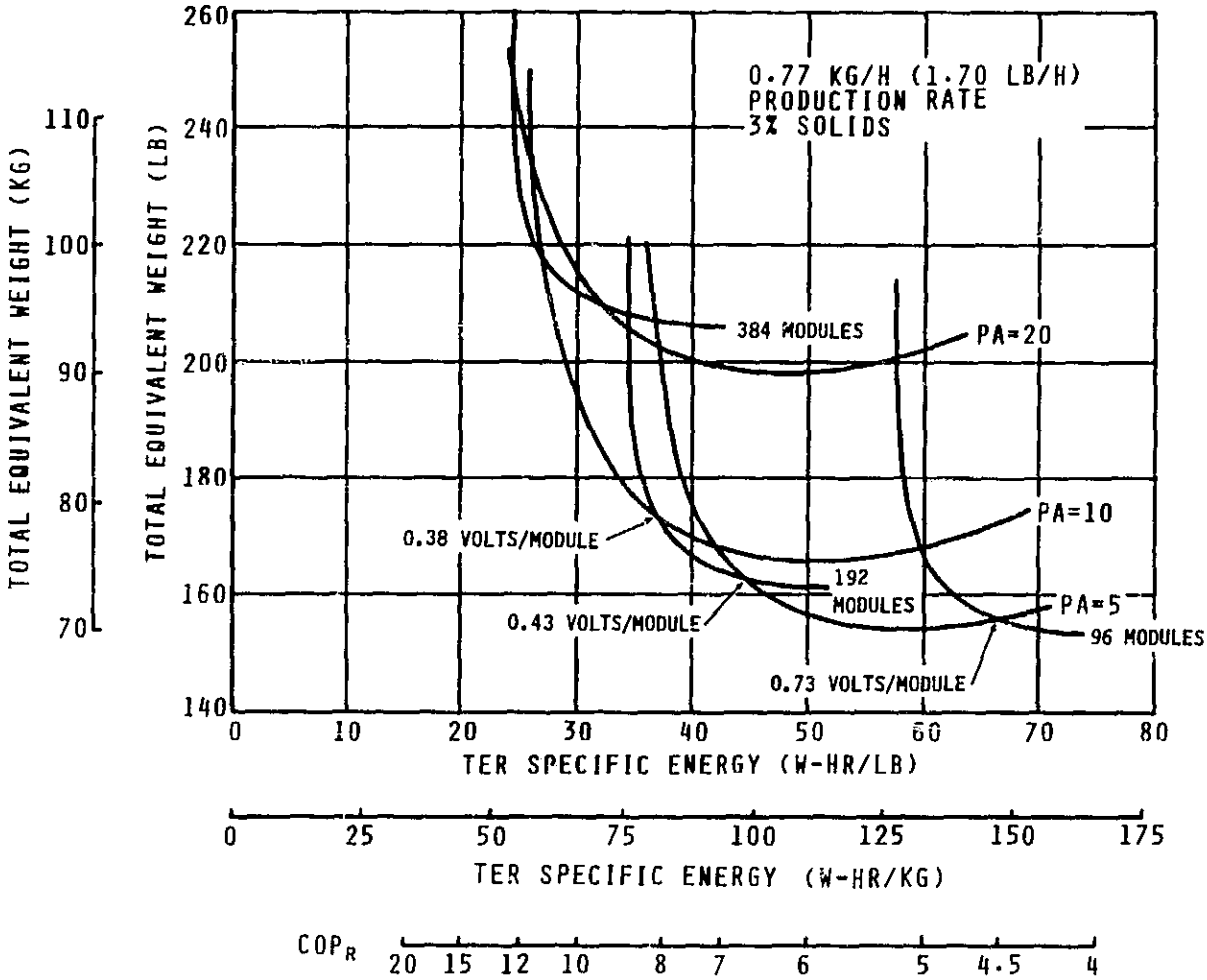

FIGURE 102

TIMES II PRELIMINARY SIZING

Table 36
TOTAL EQUIVALENT WEIGHT

		Equivalent Weight kg (lb)	
1)	0.5 lb/W X 65 $\frac{W\text{-}h}{lb}$ X 1.7 lb/h =	25.1	(55.3)
2)	Accumulator	2.4	(5.3)
3)	Recycle Tank	1.4	(3.1)
4)	Recycle & Delivery Pumps	2.3	(5.0)
5)	Valves	2.3	(5.0)
6)	HFM	7.8	(17.2)
7)	TER	11.0	(25.0)
8)	Controller	17.8	(39.2)
		70.0	(155.0)

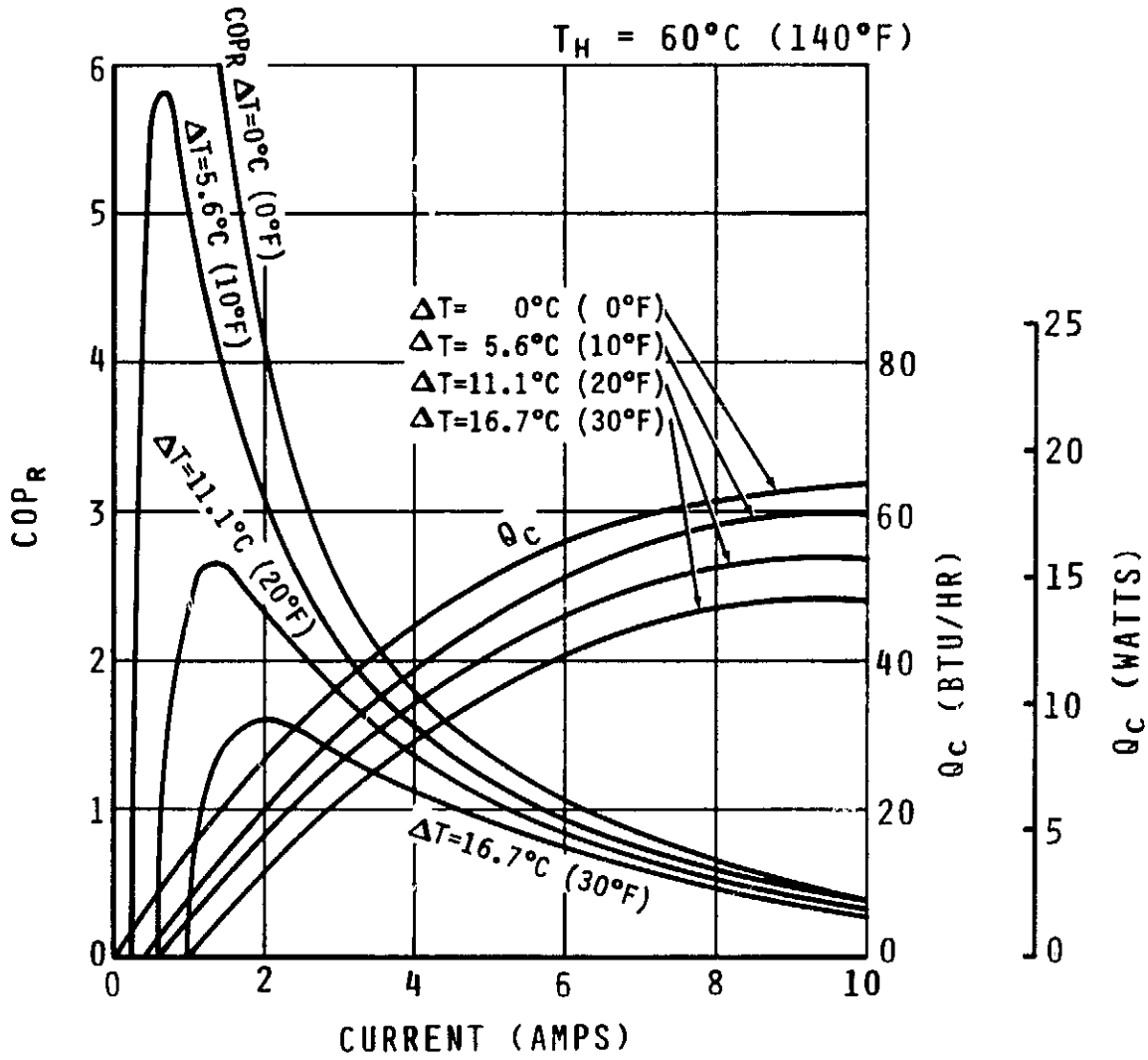

FIGURE 103

TIMES I
THERMOELECTRIC MODULE CHARACTERISTICS

Thermoelectric Module Comparison

The preceding section indicated that for all practical purposes at least a four-fold increase in the number of thermoelectric modules would be needed to produce 1.4 - 1.9 kg/h (3.1 - 4.2 lb/h) of water at a COP_{TER} = 6. As a result, a review of the available data on thermoelectric modules was conducted in order to optimize the performance of the thermoelectric heat pump in the TIMES II design. Performance data was provided by the following vendors:

1. Cambion Division/Midland-Ross Corp.
2. Melcor
3. Marlow Industries, Inc.
4. Borg-Warner Thermoelectrics/Borg-Warner Corp.

The Cambion thermoelectric module 801-3958-01, currently used in TIMES, was compared to Marlow Industries's MI 1142 and to Melcor's CP2-31-10L. These modules were selected for comparison since they were roughly of the same size and had an equal number of thermoelements per module. Data on the Borg-Warner modules lacked completeness, and was therefore excluded from this study.

The modules were compared at T_h = 27.0°C (80.6°F) and T_{TED} of 0° and 5.5°C (10°F), since data for these conditions was readily available. The results were plotted in Figures 104 and 105. A plot of COP_R, Qc/A vs. current, I, was done for the Cambion 801-3958-01 at T_h = 27.0° and 60.0°C (80.6 and 140°F), and at T_{TED} = 0, 5.5, 11.1, and 16.7°C (0°, 10°, 20° and 30°F), to determine performance changes as operating temperatures are varied (see Figures 106-107). The COP_R was found to be insensitive to temperature, while Qc/A increased for a given current at the higher operating temperatures. As a first order approximation, since the COP_R for the Cambion module was insensitive to temperature, the COP_R for the other modules would likewise be insensitive to temperature. Therefore, performance maps done for T_h = 27.0°C (80.6°F) would be sufficient to show performance trends of the various modules at different operating temperatures.

As a result of these plots, it appears that there are modules available that would improve performance of the thermoelectric regenerator in the TIMES. For example, the Marlow MI 1142 thermoelectric module apparently achieves a higher COP_R for a given P/A than the Cambion 801-3958-01 over the entire range of P/A inputs considered.

The data provided by Melcor included the dimensions of the thermoelements contained in the module. This data indicated several interesting trends in thermoelectric performance (see Figures 108-110).

1. For a given thermoelement cross-section and a constant number of couples, "thinner" modules (shorter thermoelement length) were found to be more efficient (higher COP_R for a given P/A input).

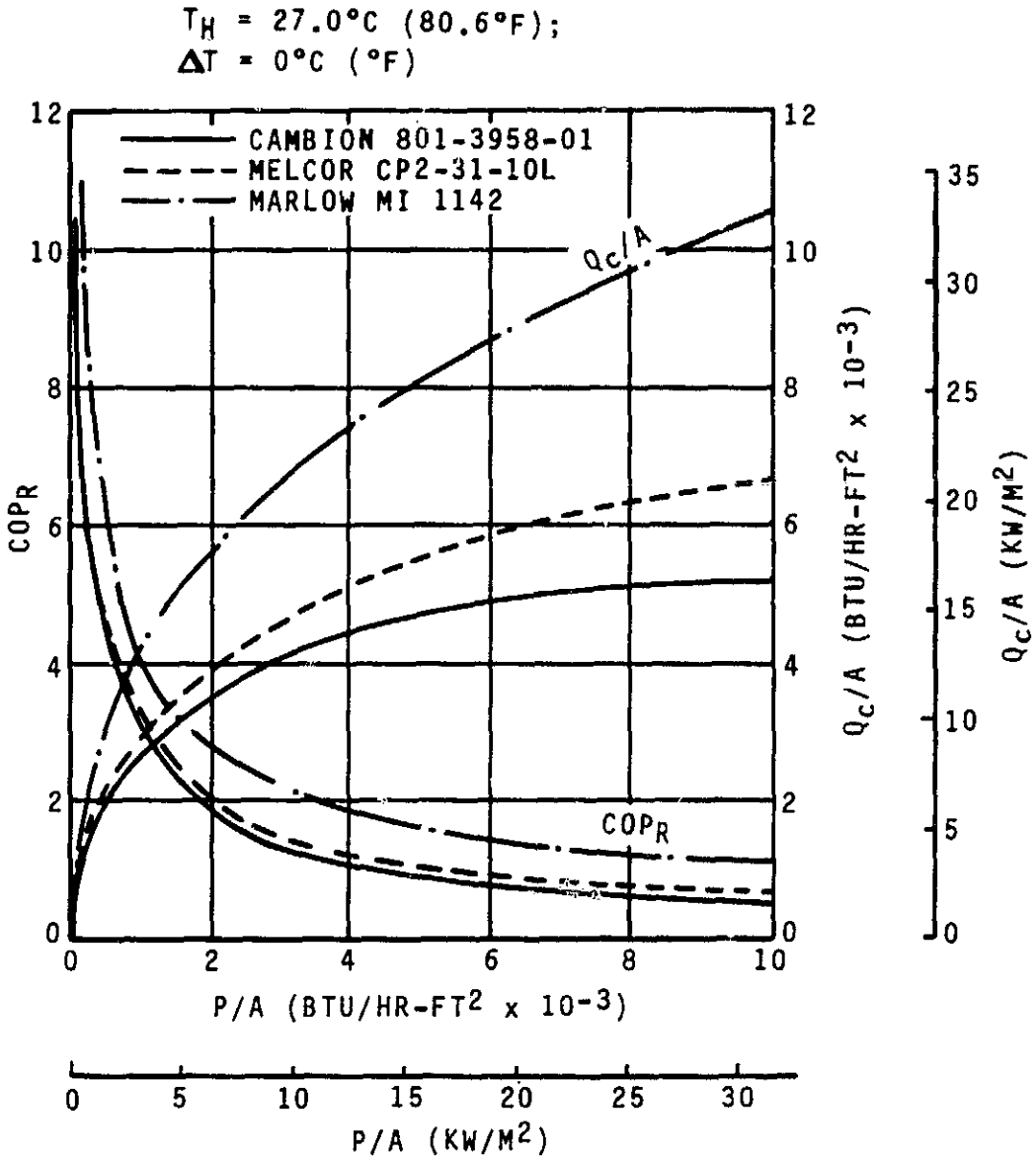

FIGURE 104

THERMOELECTRIC MODULE COMPARISON

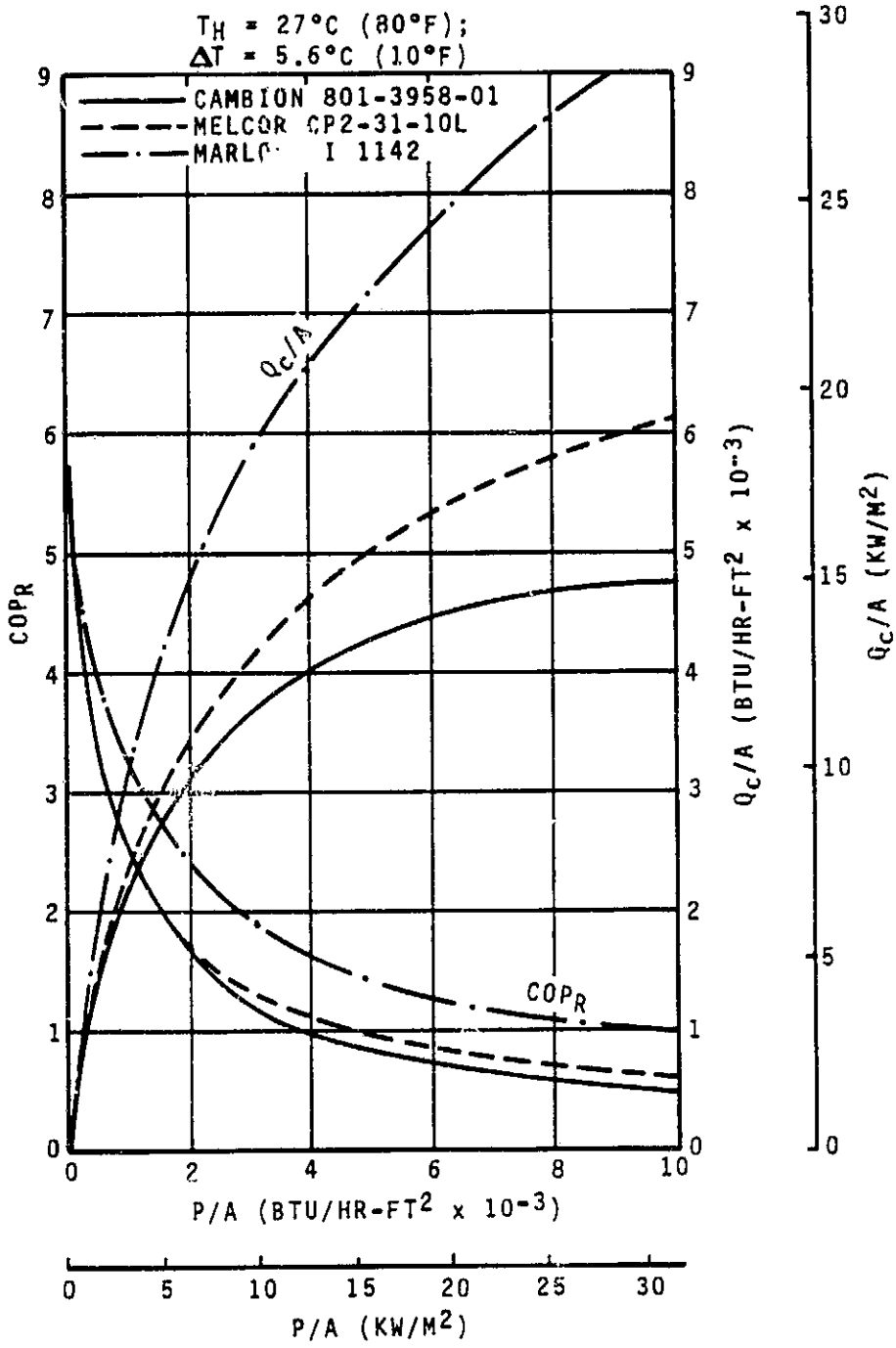

FIGURE 105

THERMOELECTRIC MODULE COMPARISON

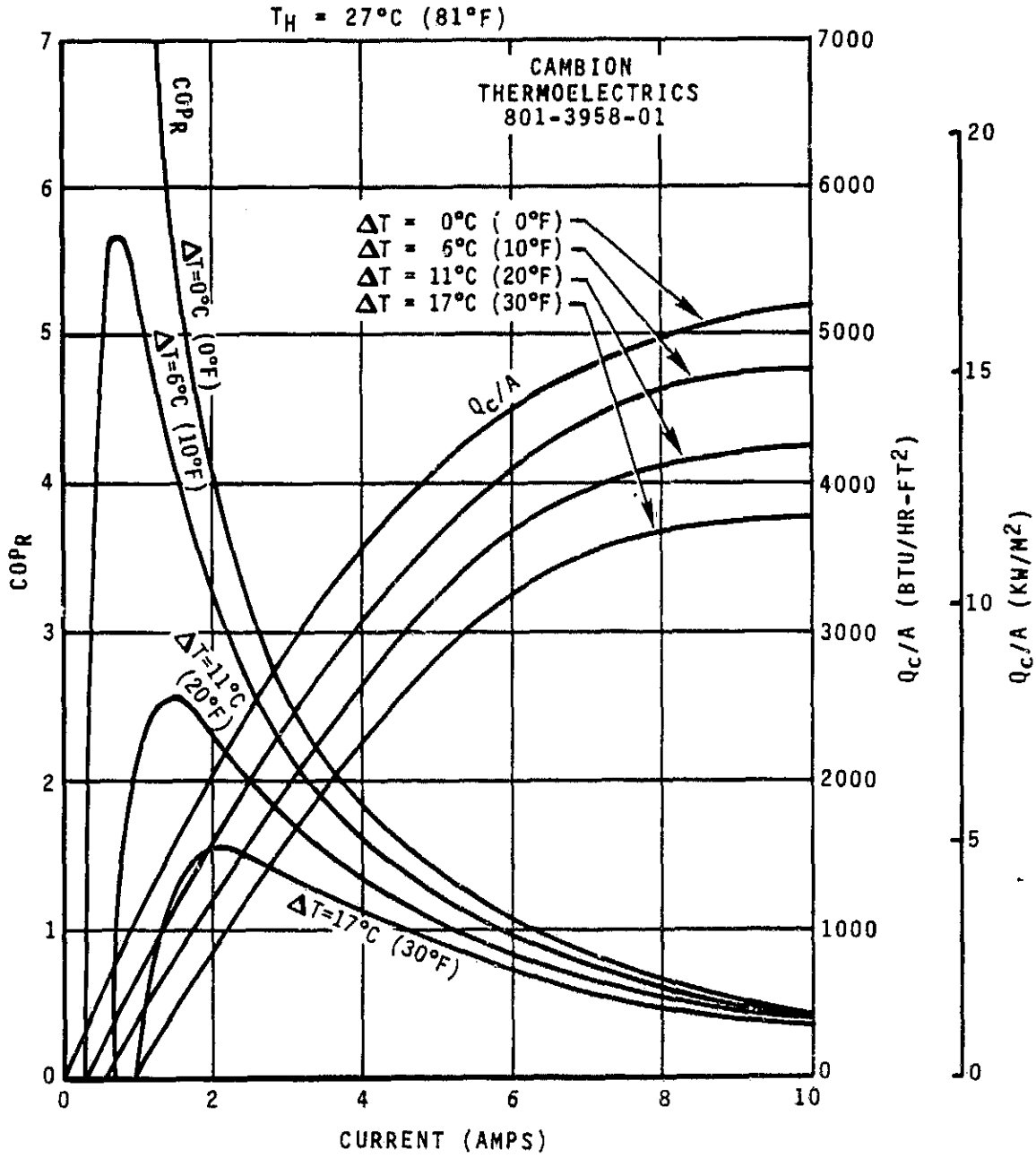

FIGURE 106

CAMBION THERMOELECTRIC PERFORMANCE

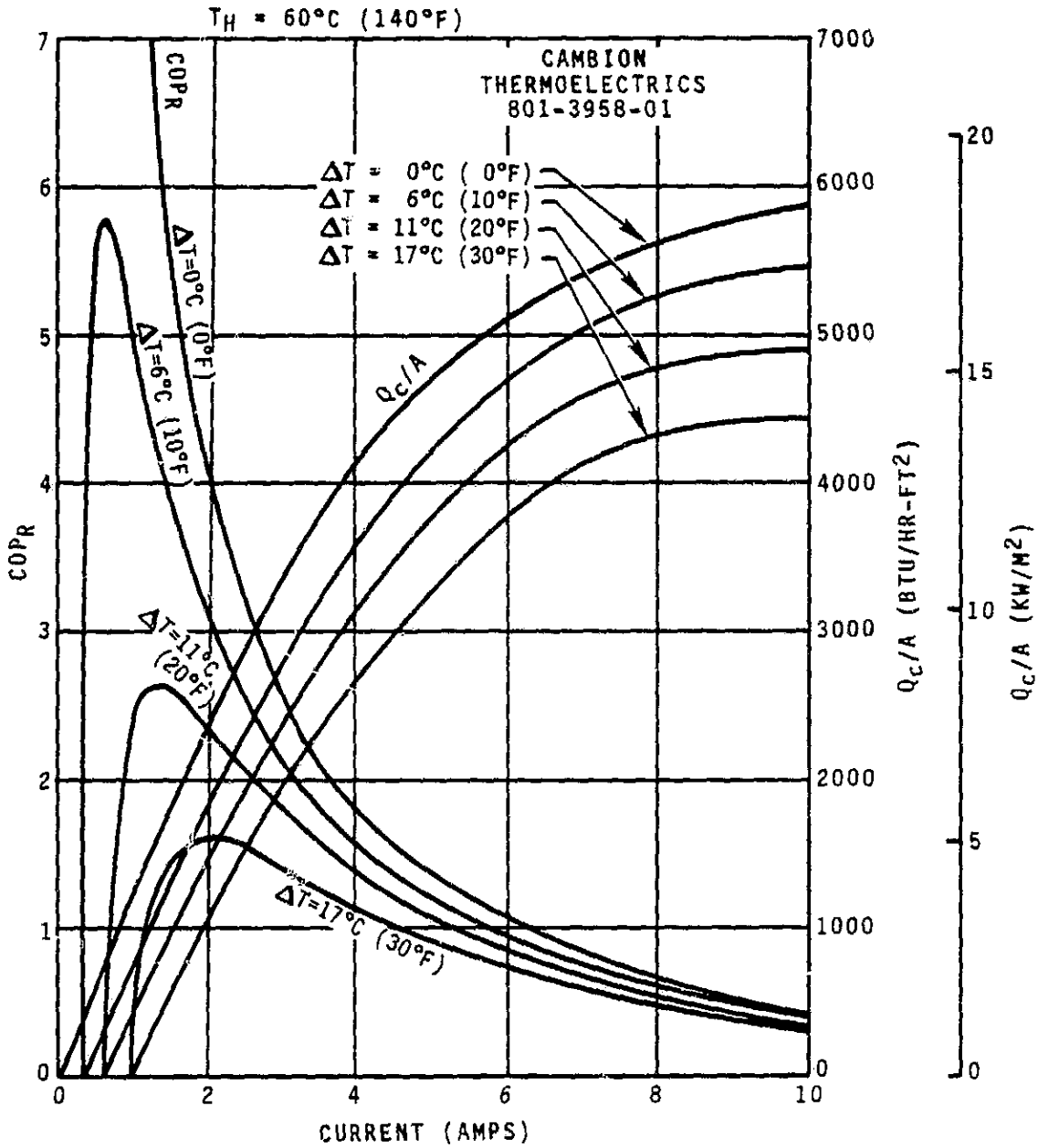

FIGURE 107

CAMBION THERMOELECTRIC PERFORMANCE

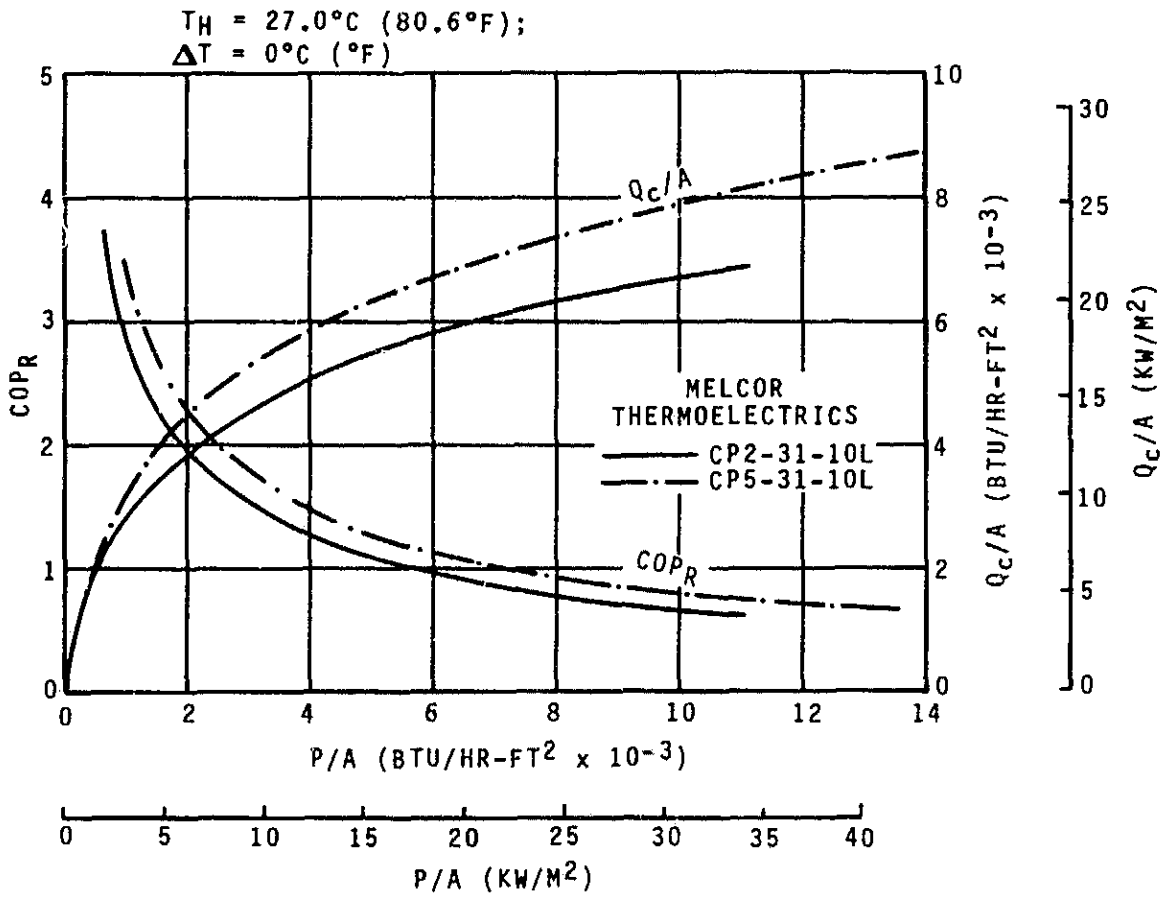

FIGURE 108

MELCOR THERMOELECTRICS PERFORMANCE

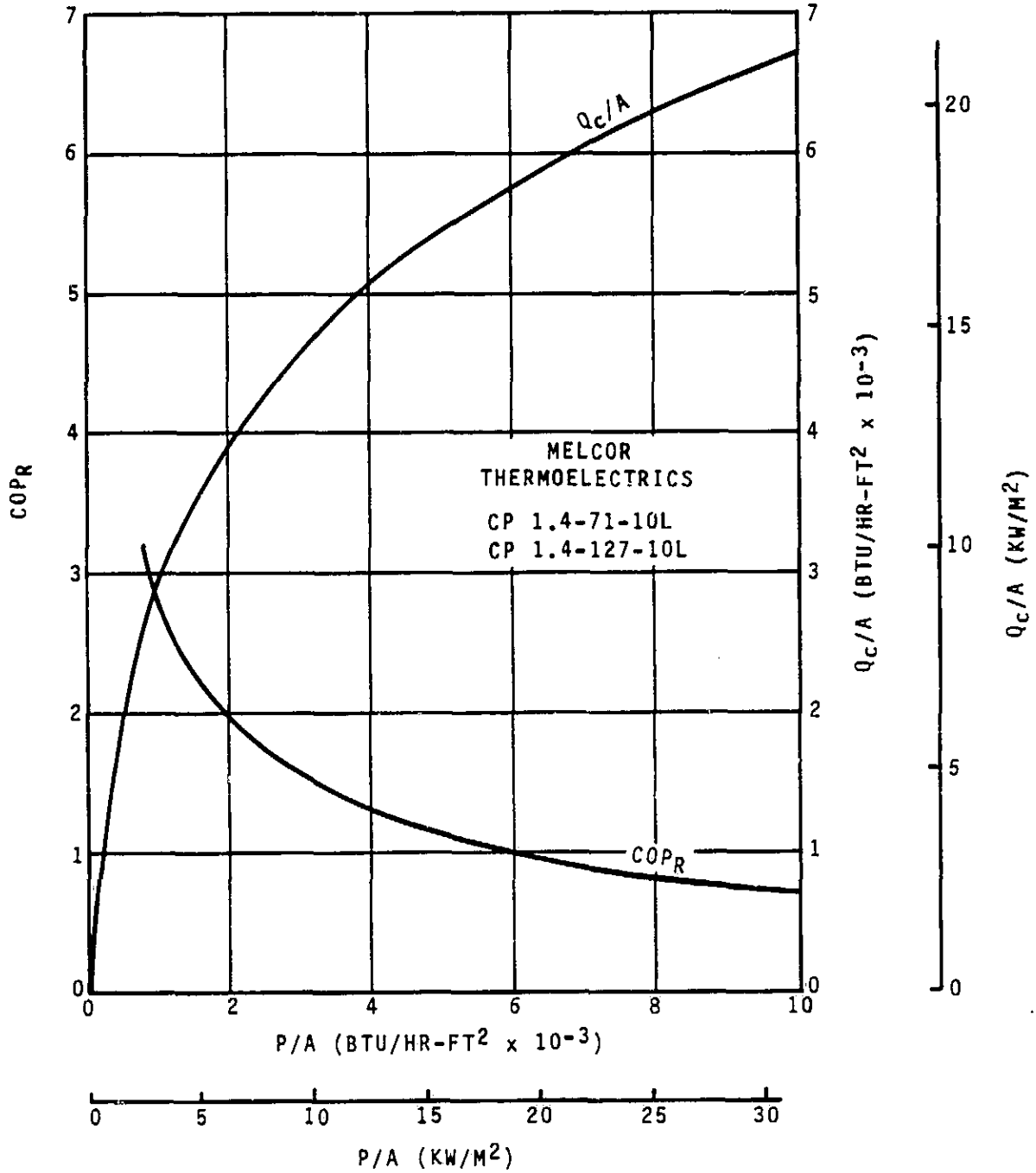

FIGURE 109

MELCOR THERMOELECTRICS PERFORMANCE

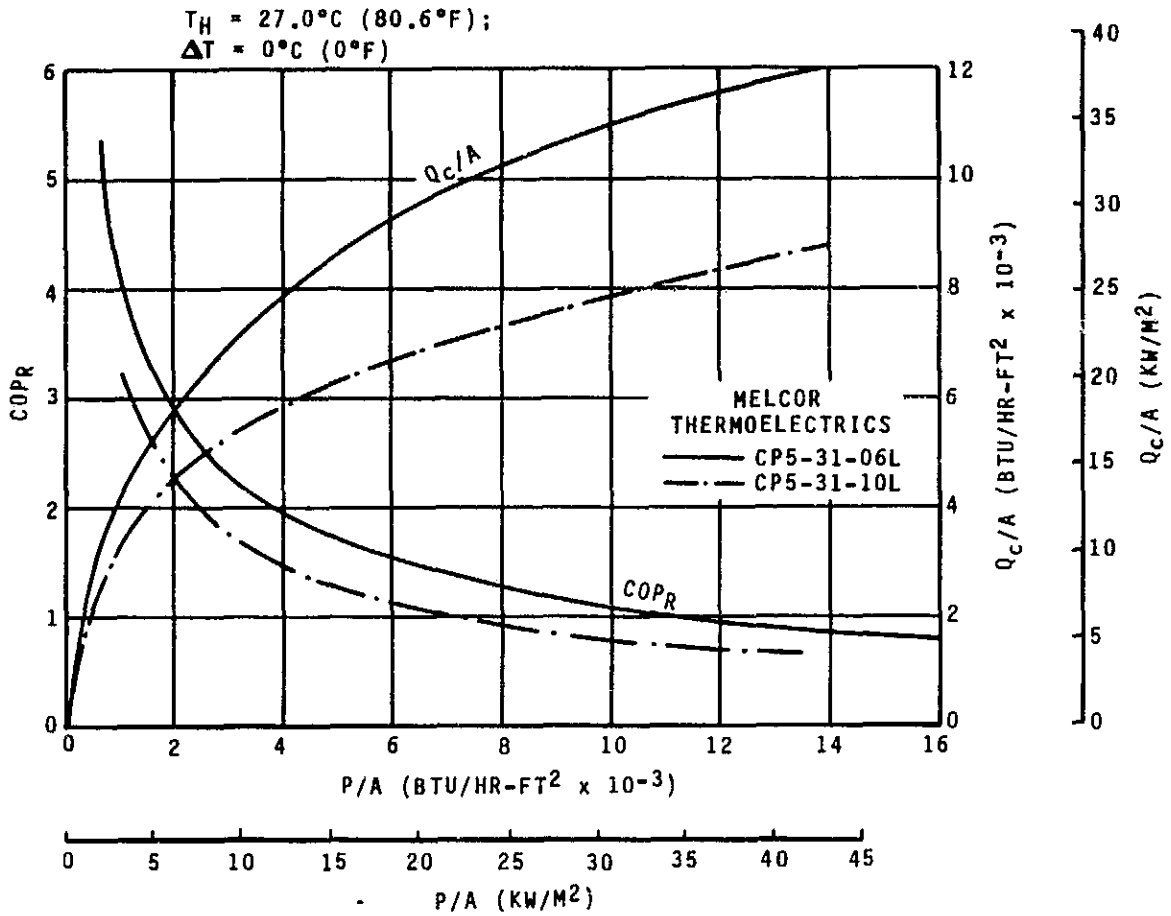

FIGURE 110

MELCOR THERMOELECTRICS PERFORMANCE

2. For a given number of couples and thermoelement length, modules with a larger thermoelement cross-section were found to be more efficient.

3. Varying the number of couples while holding constant thermoelement cross-section and length led to no change in module performance.

These results indicate that thermoelement cross-section and length are important parameters to consider when selecting a module. Also, when comparing modules of similar performance, the larger modules should be selected in order that the number of module electrical interconnections can be held to a minimum.

Although the above graphical methods yield the desired results, it is very lengthy and time consuming to plot performance curves for all the modules available over the range of operating temperatures possible. For this reason, a short, concise method of module selection was developed. This procedure indicates which module to use, how many modules are to be wired in series in a bank, and the total number of banks required to pump a given heat load while maximizing COP_R.

Module Selection Procedure

Given: T_h, Tc, Qc, Voltage

Determine: Type of module, total number of modules, and number of banks to maximize COP_R

Define: N = number of couples/module
λ = L/A
L = thermoelement length
A = thermoelement cross-sectional area

1. From T_h, find ΔT_{max}, V/N_{max} and $Q\lambda/N_{max}$ from Figures 111-113.

2. $\Delta T_{normalized} = \Delta T/\Delta T_{max}$

3. Using $\Delta T_{normalized}$ and Figure 114, determine the optimum (maximum COP_R) and maximum (maximum heat pumping) values for $I\lambda$ and normalized heat load.

4. Using these values for optimum and maximum conditions, the following table can be filled out:

Parameter	Optimum, Maximum
$I\lambda$(amps/cm)	From Figure 114
Normalized Heat Load (N.H.L.)	From Figure 114
$Q\lambda/N$ (w/cm)	= N.H.L. X $Q\lambda/N_{max}$
Normalized Voltage (N.V.)	$= \Delta T/\Delta T_{max}$
V/N (volts)	= N.V. X V/N_{max}
COP_R	$= (Q\lambda/N)/((V/N)(I\lambda))$

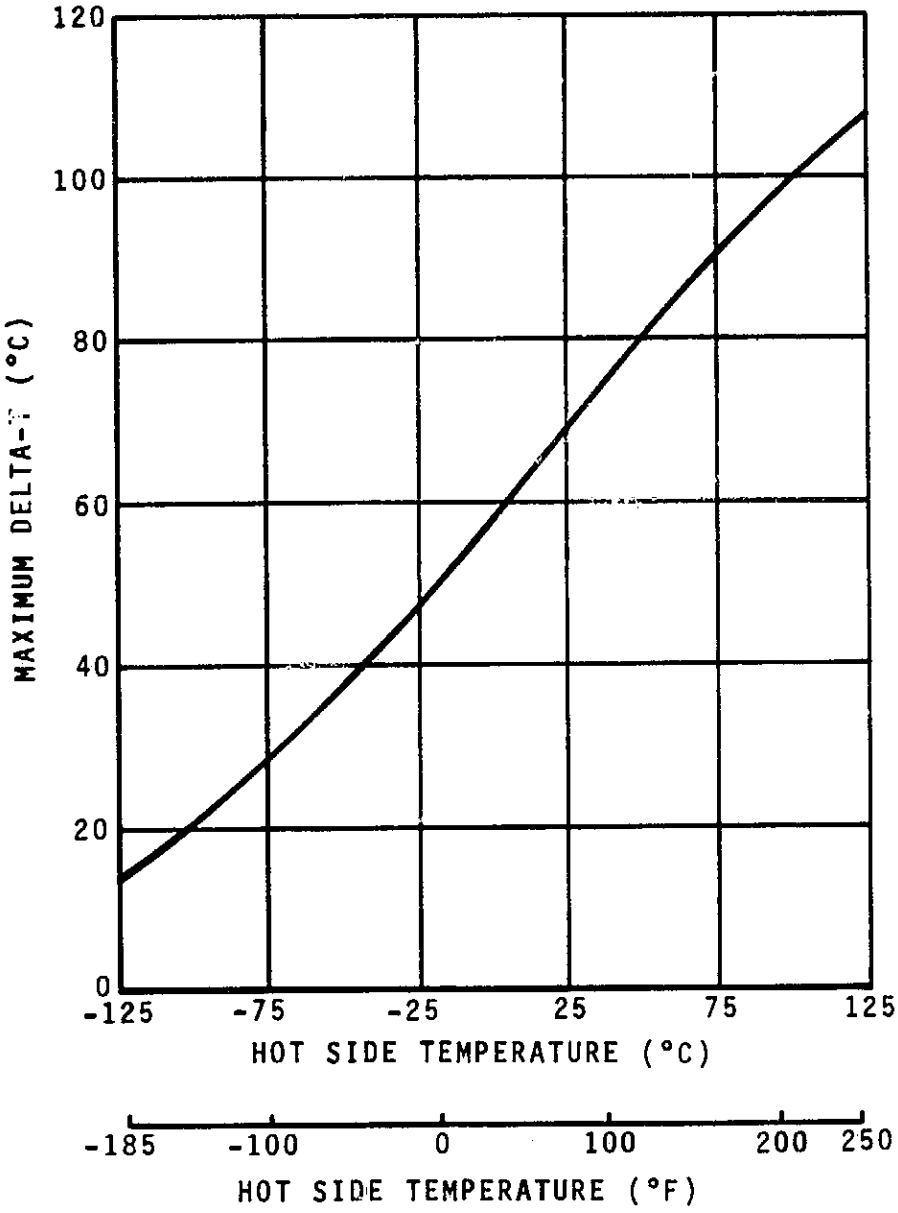

FIGURE 111

ZERO HEAT LOAD MAXIMUM DELTA-T
VS HOT SIDE TEMPERATURE

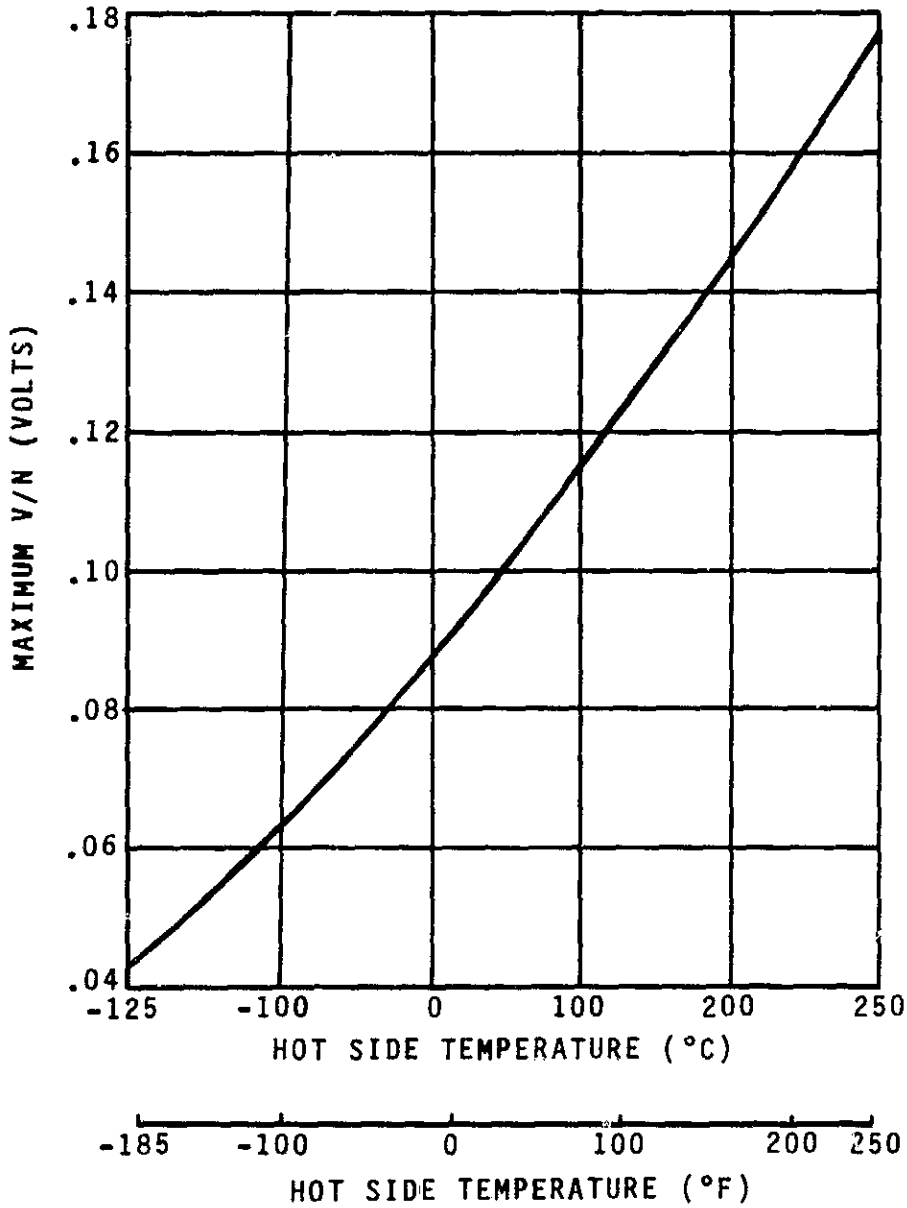

FIGURE 112

MAXIMUM VOLTAGE PER THERMOELECTRIC COUPLE VS HOT SIDE TEMPERATURE

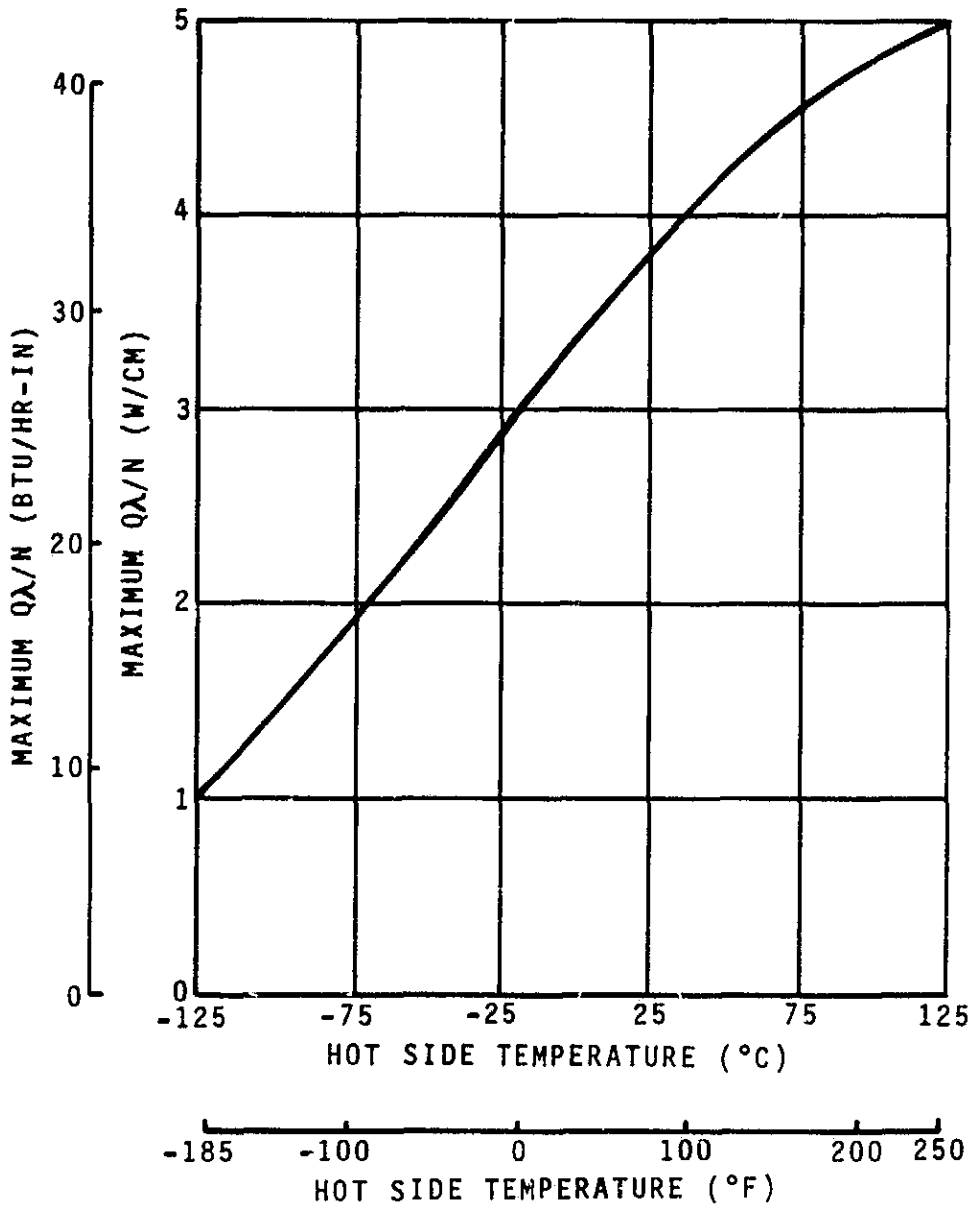

FIGURE 113

MAXIMUM Qλ/N VS
HOT SIDE TEMPERATURE

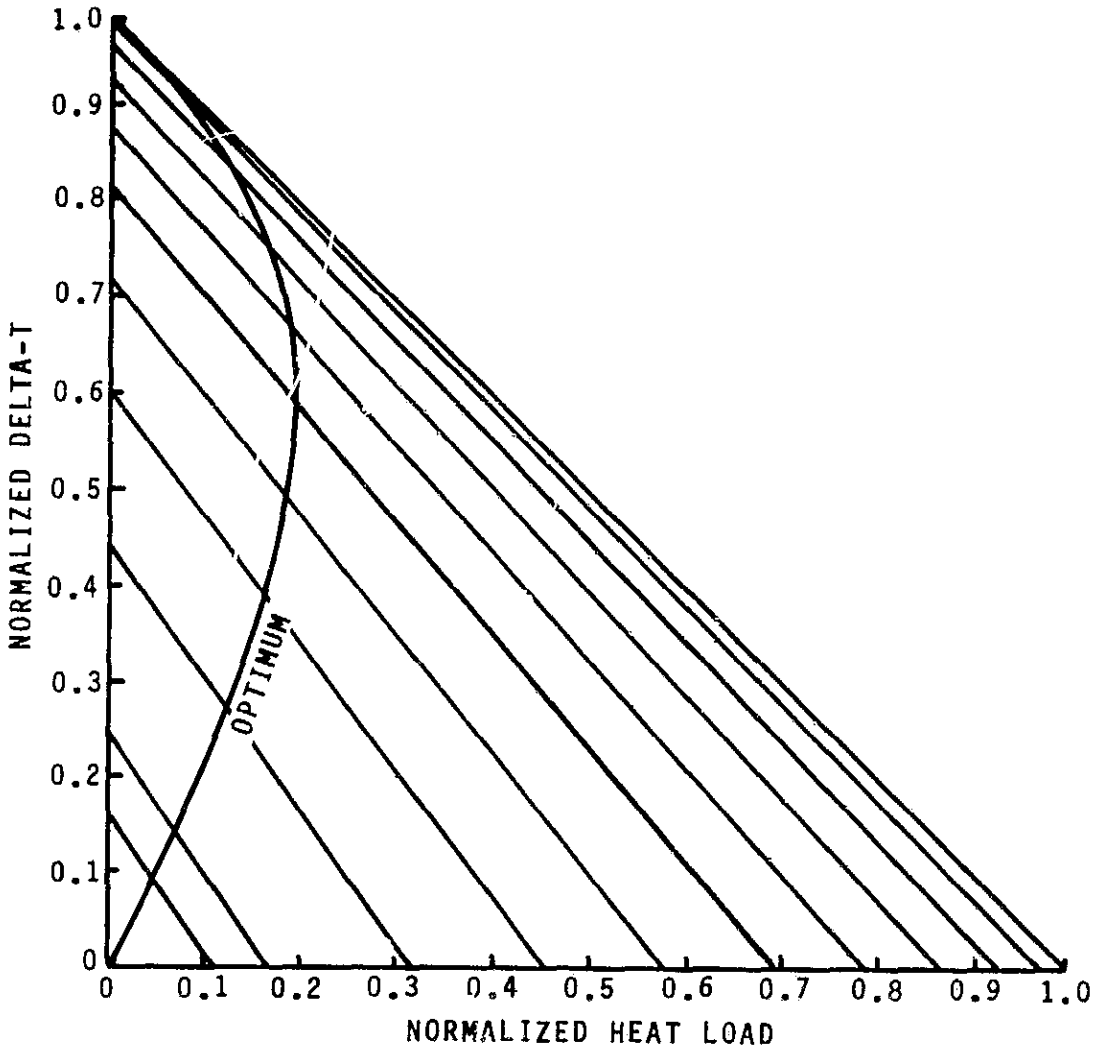

FIGURE 114

NORMALIZED DESIGN/PERFORMANCE CHART

5. The module, total number of modules, and number of banks can now be determined:

$$\frac{\text{Voltage Supplied}}{\text{Volt/Couple}} = \frac{\text{Volts}}{V/N} = \text{M couples in series}$$

$$\frac{Qc}{M} = Q/N = \text{heat load per couple}$$

$$\frac{Q\lambda/N}{Q/N} = \lambda \text{ required}$$

TIMES II TER

Consideration of the major criteria in the thermoelectric element selection process leads to the recommended use of a larger area module so that the number of electrical interconnections are minimized. Cambion thermoelectric module 801-1010 was chosen for the following sizing calculations, since it is larger [4.15 cm (1.635 in) square] than the currently employed element, and Cambion has demonstrated a high degree of reliability in the TIMES application.

At the proposed design operating point, a ΔT of 5°C (9°F) across the thermoelectric elements is expected. The performance characteristics for the Cambion module at this ΔT are given in Figure 115. Using this information, for a $COP_R = 6$, current draw is 0.5 amps, yielding a heat load capability of 3155 watts/m^2 (1000 BTU/h-ft^2). For a design point of 1.93 kg/h (4.25 lb/h) the heat load will be 1270 watts (4335 BTU/h), yielding a total area of 0.40 m^2 (4.34 ft^2). The total number of thermoelectric modules necessary to provide that area is 234. The resulting TER specific energy is then 100 W-h/kg (50 W-h/lb), a 30% less than the existing TIMES.

To accommodate this quantity of thermoelectric elements, the TER has to be configured in a flat rectangular sandwich design. The thermoelectric modules can be arranged in two arrays, each 9 X 13, to provide the necessary area. Using the electrical generating characteristics given in Figure 116, the necessary voltage/chip is 1.5 - 2.0 volts. If the subsystem generating voltage is specified to be 28 VDC, each row of 13 modules can be wired in series, and connected in parallel to the other banks of chips.

Proposed Gas/Liquid Separator Operation

The test of an EMU type separator demonstrated that utilization of a similar device on TIMES II to place the porous plates function was indeed practical. The EMU design could be modified to use a lower speed rotating drum, in conjunction with the stationary pitot tube water pickup. Decreasing the speed of the rotating drum would permit the combination of the separator and the presently employed recycle pump on a common shaft motor. To compensate for the lower speed, the drum diameter would have to be increased to generate the required fluid pressure head (created by the rotational speed) at the pitot inlet.

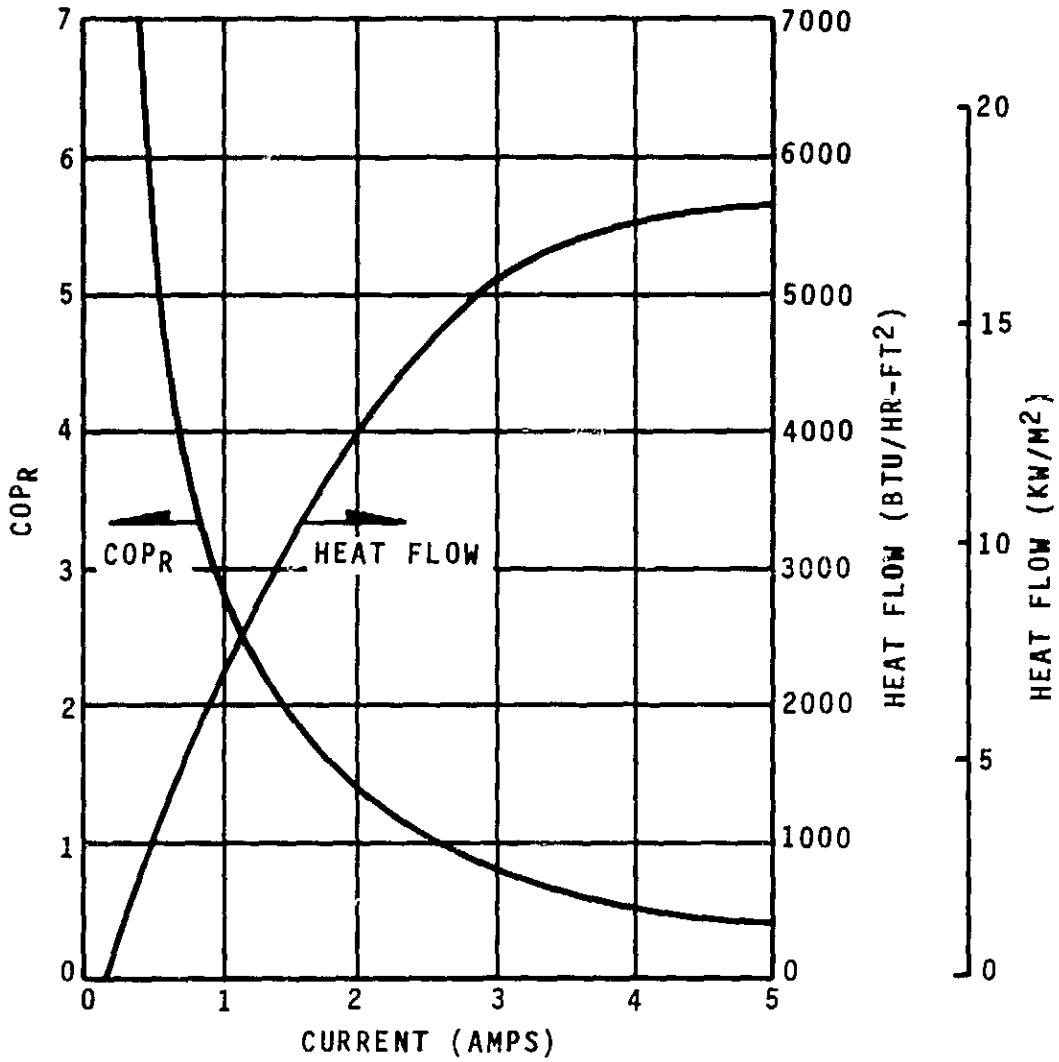

FIGURE 115

CAMBION MODULE 801-1010 PERFORMANCE

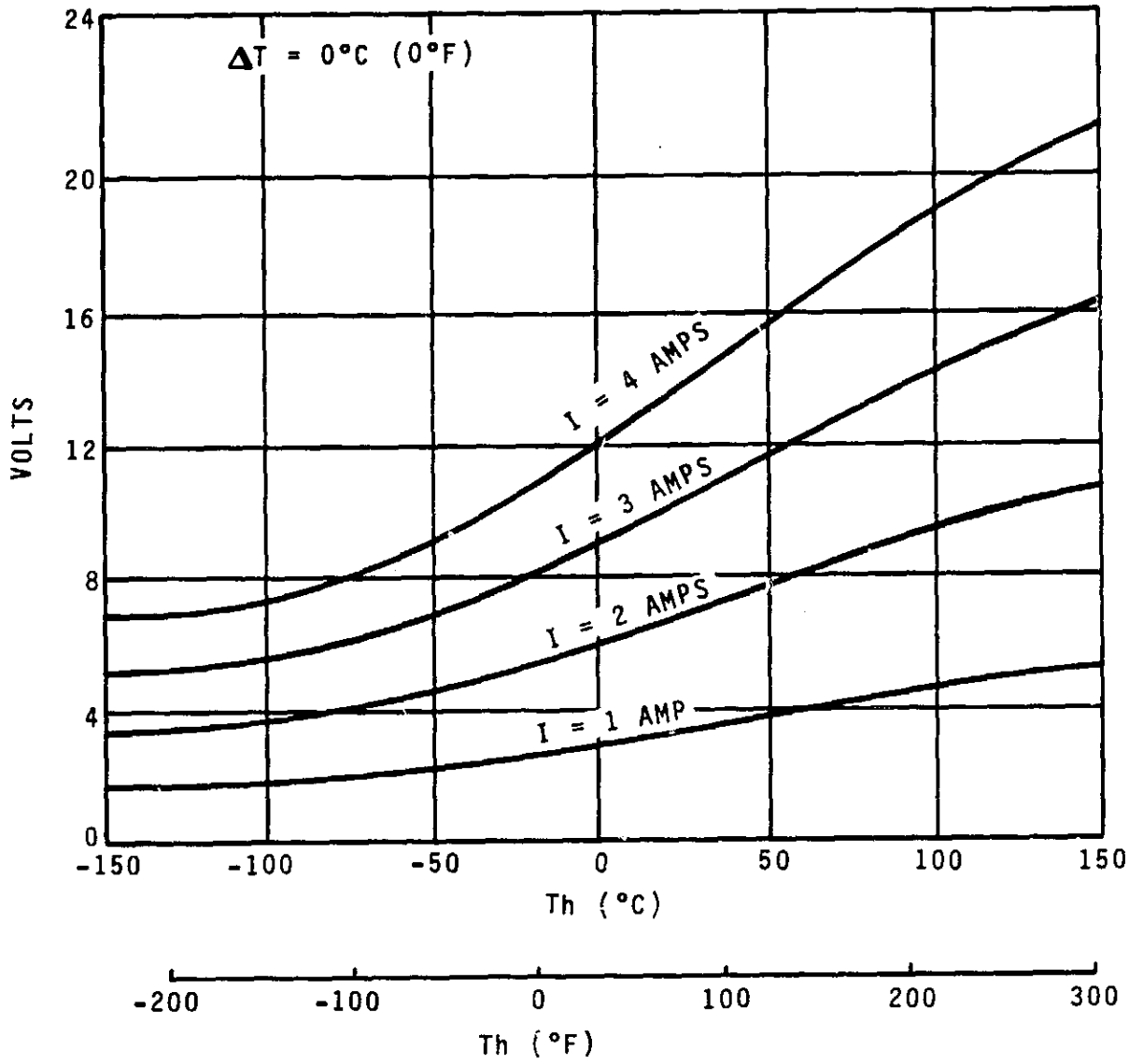

FIGURE 116

CAMBION MODULE 801-1010
ELECTRICAL CHARACTERISTICS

Analytical Relationships:

Acceptable water separator performance occurs when system resistance does not exceed the pumping capacity of the pitot, thereby preventing liquid carryover in the gas outlet. Unacceptable performance is encountered when system resistance is low and the pitot passes a mixture of gas and water.

This latter condition, gas inclusion in the product water, is elminated when the pitot opening is running just under the water level in the trough (Figure 117a). The pressure head developed at the pitot inlet for this situation is equivalent to the velocity head of the liquid in the trough:

$$\Delta P_V = \rho \frac{W^2 R_p^2}{2g}$$

where:

ΔP_V = Trough velocity head
ρ = Fluid density
g = Gravitational Constant
W = Fluid rotational speed
R_p = Radial distance between pitot and rotational center line

As the water level in the trough rises (Figure 117b), a centrifugal force is added to the velocity head so that total head at the pitot inlet is:

$$\Delta P_T = \Delta P_V + \Delta P_C$$

and:

$$\Delta P_C = \rho \frac{W^2}{2g} (R_s^2 - R_p^2)$$

where:

ΔP_T = Total head at pitot inlet
ΔP_C = Head due to centifugal force at pitot inlet
R_s = Radial distance to free water surface in trough

These relationships may be combined so that:

$$\Delta P_T = \rho W^2 R_p^2 \left[2 - \frac{R_s}{R_p}^2\right]$$

It should be noted that the fluid rotational speed will be less than the separator drum speed due to slip at the wall. Analytical predictions of separator performance would resemble the curves in Figure 118. Delivered head at any flow is total head at the pitot inlet, ΔP_T, less the pressure loss through the pitot assembly itself.

a)

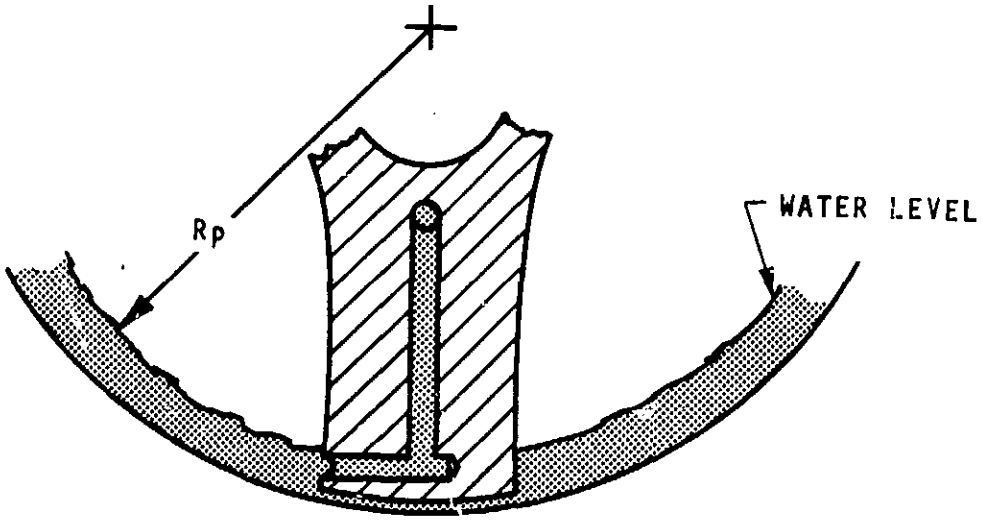

VELOCITY HEAD ONLY

b)

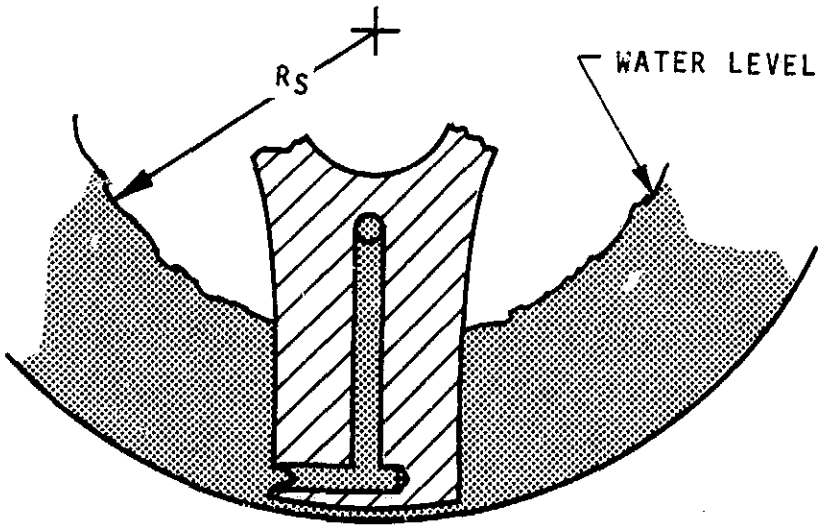

VELOCITY HEAD PLUS CENTRIFUGAL FORCE

FIGURE 117

WATER SEPARATOR GEOMETRY

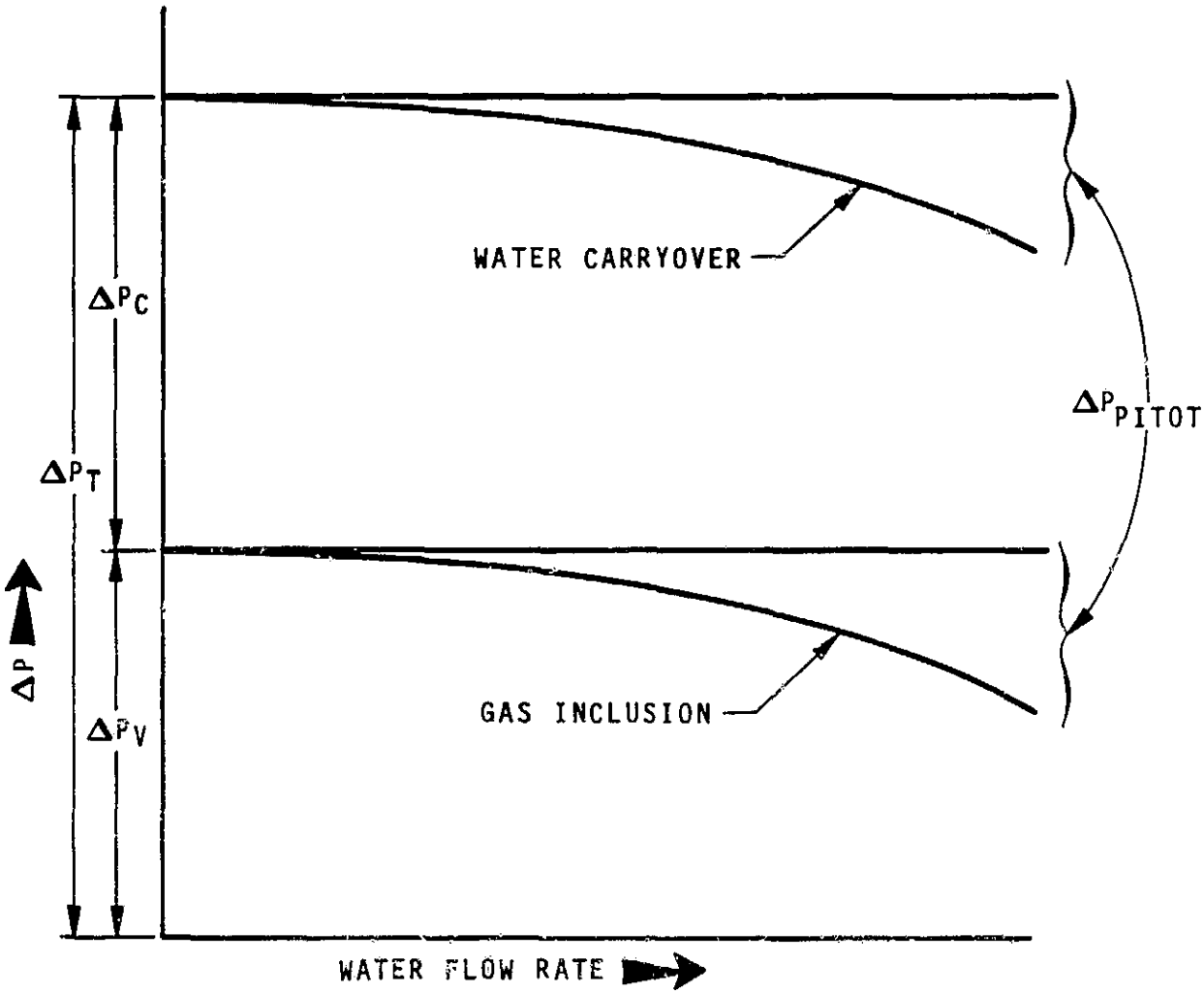

FIGURE 118

WATER SEPARATOR
PERFORMANCE CHARACTERISTICS

TIMES II Main Condenser And Aftercooler Preliminary Design

A condenser circuit concept was developed for TIMES II that eliminates the porous plate, product water pump and condenser burper. This concept uses a plate-fin condenser, finned tube convective aftercooler and rotary separator. Preliminary sizing of the condenser and aftercooler was completed.

Description:

Blockage and corrosion of the porous plate in the existing TIMES condenser plus a desire to reduce the total number of system parts resulted in a systems review to determine possible alternate condenser circuits. The following assumptions and performance requirements were used:

- Average product water rate of 1.4 kg/h (3 lb/h)
- Thermoelectric COP of 6
- Evaporating temperature of 60°C (140°F)
- Condensing temperature of 54°C (130°F)
- Parasitic thermoelectric and pump losses to be minimized
- Water vapor loss of 1% or less by weight
- Average 0.025 m^3/sec (0.015 ft^3/min) of noncondensable gas would exist

The amount of vapor that could be condensed by the thermoelectric modules is limited by the assumed COP. Complete condensation and additional subcooling to eliminate water vapor loss must be accomplished in a downstream heat exchanger (aftercooler). To eliminate additional subsystem interfaces such as liquid loops, the aftercooler should be cooled by cabin air. Finally, the condensed liquid and noncondensable gas must be separated and the noncondensable gas vented.

The resulting condenser circuit concept is presented schematically in Figure 119. In this system, water vapor and noncondensable gases from the evaporator are cooled in the thermoelectric-chilled condenser. The required 892 W (3042 BTU/h) to evaporate 1.4 kg/h (3 lb/h) of water at 60°C (140°F) is accomplished by a power input of 122 W (417 BTU/h) to the thermoelectrics. This provides 734 W (2504 BTU/h) to condense vapor on the cold side of the module, resulting in 1.1 kg/h (2.4 lb/h) of condensate at 54°C (130°F).

The remaining 0.3 kg/h (0.6 lb/h) of vapor is condensed and all of the liquid subcooled to 27°C (80°F) in the aftercooler. The total heat rejection in the aftercooler is 205 W (700 BTU/h). At the 27°C (80°F) aftercooler exit temperature, the 0.026 m^3/sec (0.015 ft^3/min) of noncondensable gas will entrain 0.006 kg/h (0.0014 lb/h) of water vapor. This is a water vapor loss of 0.05%, which is well within the target loss of 1% or less.

The liquid water and noncondensable gas are separated in an EMU-type rotary separator. This separator will provide a 138 kPa (20 psid) head to the product water. The noncondensable gas is then vented into an optional gas volume and a timed solenoid switch burps the noncondensable gas to vacuum.

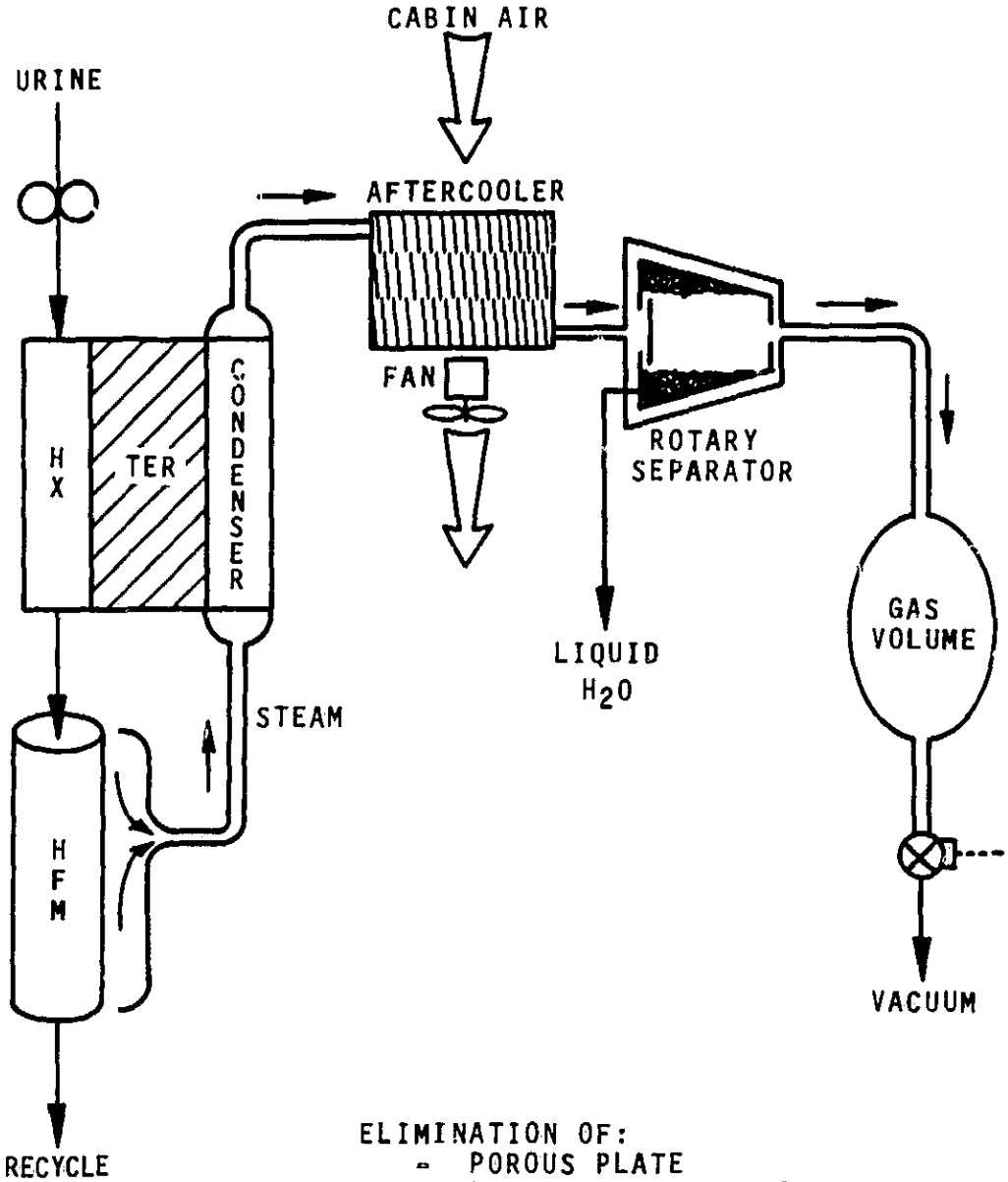

ELIMINATION OF:
- POROUS PLATE
- PRODUCT WATER PUMP
- CONDENSER BURPER

FIGURE 119

TIMES II
CONDENSER CIRCUIT SCHEMATIC

System control is provided by maintaining condenser line pressure via the gas volume and burping sequence. The pressure is maintained to hold the condensing temperature of 54°C (130°F). There is sufficient margin to avoid flashing at the aftercooler outlet even with some condenser line pressure variation.

Component Sizing:

Both the thermoelectric cooled condenser and the air cooled aftercooler were sized. The condenser primary heat transfer area of approximately 0.40 m^2 (4.3 ft^2) was determined by the face area of the 234 thermoelectric modules. The condenser was sized as a single passage unit with two parallel paths, both 30.5 cm (12 in.) wide by 61 cm (24 in) long. Ruffled stainless steel fins, 0.19 cm (0.075 in) high, 0.005 cm (0.002 in) thick with 7 fins/cm (18 fins/in) were selected to minimize flow area and increase vapor velocity. Based on 0.025 m^3/sec (0.015 ft^3/min) of noncondensable gas at a conenser temperature of 54°C (130°F), the mass porportion of noncondensable gas to steam is 0.3%. This results in a reduction of approximately 1/3 in the condensing heat transfer coefficient. Empirical data was obtained at a condensing temperature of 60°C (140°F) and indicated a heat transfer coefficient of 0.08 cal/sec-cm^2°C (600 BTU/hr-ft^2-°F) when the effects of the noncondensable gas were included. This heat transfer coefficient, when used in conjunction with the primary heat transfer area, indicates a safety factor of more than 5 to accomplish the required condensation.

However, this approach is expected to result in flow distribution and condensate removal difficulties. The inlet vapor velocity is ony 2.7 m/sec (8.7 ft/sec) and the outlet velocity is only 0.7 m/sec (2 ft/sec). The calculated pressure loss is only 0.12 kPa (0.017 psi) if vapor is assumed to exist throughout the heat exchanger. This pressure drop is not high enough to force condensed liquid out of the heat exchanger. The final condenser design may require multiple passes to increase the vapor velocity and pressure drop to effect condensate transport.

A preliminary design of the aftercooler has also been completed. The possibility of incorporating the aftercooler with the condenser in the form of a section of free convection air cooled external fins was also evaluated. This approach is unacceptable because:

1) There is insufficient heat transfer area to reject the heat to the air with a free convection heat transfer coefficient of 1.4×10^{-4} cal/sec-cm^2°C (1 BTU/h-ft^2-°F).

2) If complete condensation and subcooling is obtained, the hot side thermoelectric temperature will be affected.

3) The existing noncondensable gas velocity is so low 0.8 cm/sec (0.3 in/sec) that condensate flow maldistributions will exist.

For these reasons, a separate finned tube air cooled aftercooler was sized. Air at 21°C (70°F) was assumed to flow over the finned tubes at a velocity of 4.6 m/sec (15 ft/sec). The total heat rejection rate is 205 W (700 BTU/h), which includes condensation of the remaining 0.25 kg/h (0.54 lb/h) of water vapor and subcooling of the 1.4 kg/h (3.0 lb/h) of liquid to 54°C (80°F). Finned tubes were selected with the following characteristics:

- tube O.D. of 1.0 cm (0.42 in)
- fin O.D. of 2.2 cm (0.861 in)
- fin thickness of 0.05 cm (0.019 in)
- 3.4 fins/cm (8.7 fins/in)

With a tube wall thickness of 0.025 cm (0.010 in), the inlet vapor velocity is 8.3 m/sec (27.3 ft/sec) and the exiting noncondensable gas velocity is 0.09 m/sec (0.30 ft/sec). This is expected to produce a liquid slug flow similar to that observed in TIMES I.

In the condensing portion of the aftercooler, the air side heat transfer coefficient of 2×10^{-3} cal/sec-cm^2-°C (16 BTU/h-ft^2-°F) is controlling. This results in 35 cm (14 in) of tube to condense the remaining water vapor. The length of the subcooling section was calculated by combining the air side coefficient with an assumption of a minimum Nusselt value of 3.66 for parabolic flow of the liquid in the tube. To subcool the liquid to 54°C (80°F) requires an additional 58 cm (23 in) of tube length, resulting in a total aftercooler length of 94 cm (37 in). The tubes are to be arranged in a cross-counterflow configuration. The temperature distribution of this component assuming 58 m^3/sec (35 ft^3/min) of air flow is presented schematically in Figure 120, as a preliminary packaging sketch.

For this package, the air flow rate required to maintain a 4.6 m/sec (15 ft/sec) velocity through the tube bank is 68 m^3/sec (41 ft^3/min) assuming the flow to face area is 50%. This is reasonably close to the 58 m^3/sec (35 ft^3/min) used in the current unit.

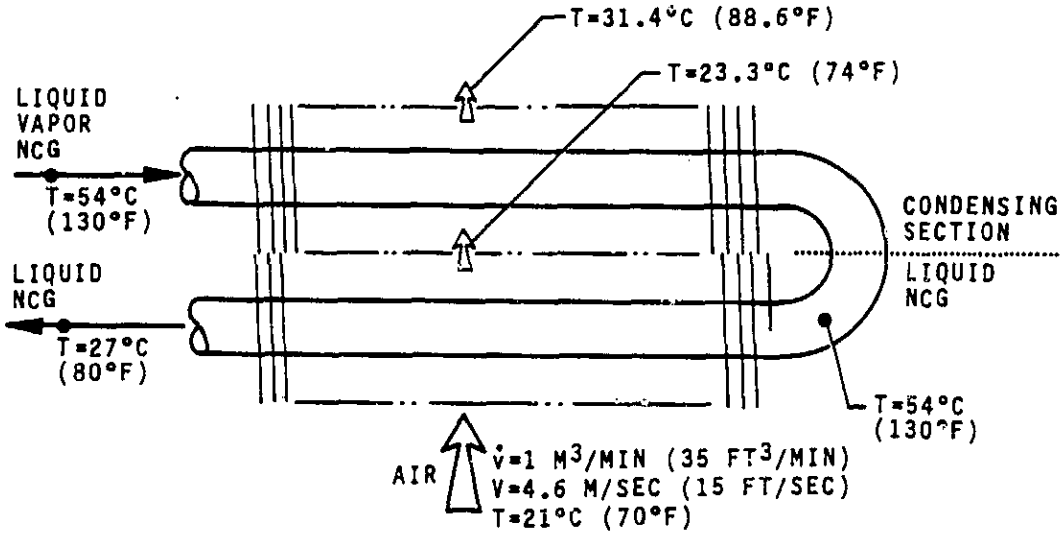

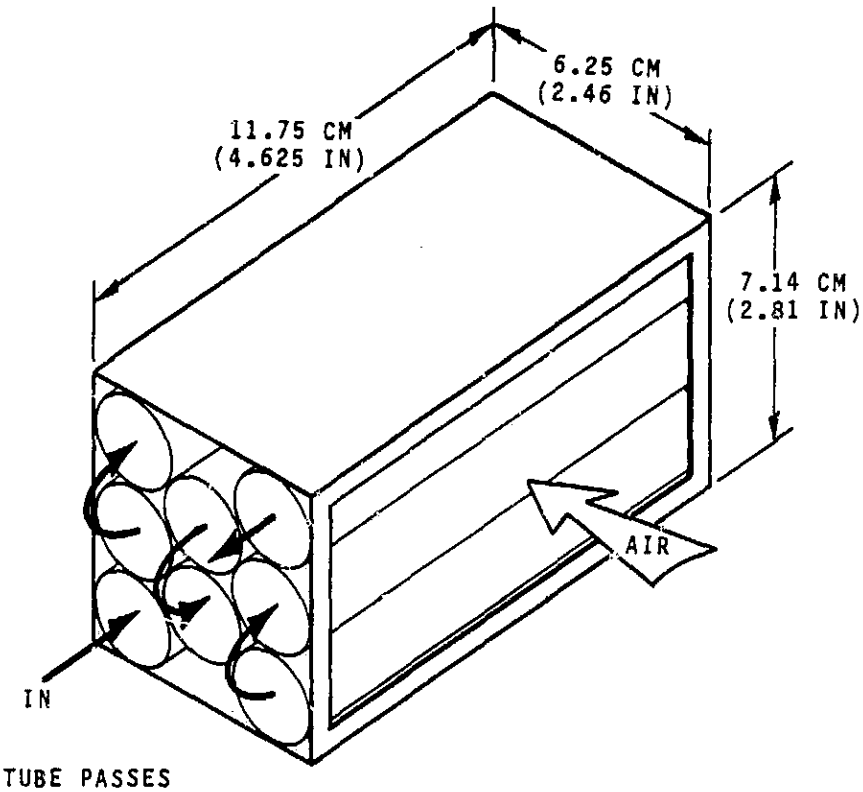

8 TUBE PASSES
3 PASSES CONDENSING SECTION = 35.24 CM (13.875 IN)
5 PASSES SUBCOOLING = 58.74 CM (23.125 IN)

FIGURE 120

TIMES II AFTERCOOLER

RECYCLE LOOP pH OPERATIONAL CRITERIA

Objective

Pretreatment of incoming wastewater is necessary to inhibit microbiological growth and fix the free dissolved ammonia. The objective of this task is to study the effect of wastewater pH with respect to subsystem operating conditions. Elimination of processing loop pH control components is the goal.

Background

The present subsystem design incorporates a collection package that is capable of pretreating incoming wastewater and storing it for later use in the processing loop. A pH sensor is installed in the recycle loop to control addition of sulfuric acid, in order to maintain a given pH level in the loop. It would be desirable to elminate this pH control, and be able to accept whatever wastewater fluid was introduced directly into the recycle loop. In this way, the processing package could be functionally separated from a wastewater collection and pretreatment package, providing a greater degree of flexibility.

Results

With the present subsystem configuration, no pH control scheme was necessary since under normal operating conditions, pH levels averaged 2.5 using the Oxone/sulfuric acid pretreatment. It is clear that care should be taken to ensure the pH of wash water solutions using soaps or detergents is either neutral or slightly acidic, otherwise chemical degradation of the surfactant will occur.

Urine Feed

Urine testing was performed at HSD and NASA/JSC to indicate the stability of the wastewater (urine) pH during actual subsystem operation. The pretreatment mix that was used consisted of the following:

COMPONENT	% BY WEIGHT	MG/CC OF URINE
Conc. H_2SO_4	17.0	2.32
Oxone	36.8	5.00
Water	46.2	6.28

Testing revealed that during actual processing, the residence time of the urine batch in the recycle loop was on the order of 50 hours. At the dosage utilized, the pH remained between 2.0 - 3.0. It became clear that automatic addition of mildly concentrated sulfuric acid from the pretreat tank would not be necessary, since that logic was based on a control band of pH 3.8 - 4.2.

While from a control point of view, the recycle pH should be kept at 2.0 or slightly below, under actual operating conditions a level of 2.5 - 3.0 is more acceptable. This is the result of water quality considerations previously discussed. In addition, the use of pure titanium or titanium alloys are recommended for the recycle fluid since even 300 series stainless steels are subject to corrosion, especially AISI 347.

Testing also revealed that despite pH control during operating modes, apparent loss of control occurred during some quiescent periods. This was evidenced by the discovery of fungal growth inside the evaporator, in areas of low flow velocity. This phenomena apparently has been observed in other urine processing subsystems and needs to be investigated more fully.

Wash Water Consideration

While pH on the order of 2.0 is necessary for urine processing, previous testing at HSD had determined that wash water using a liquid detergent blend, Biosoft HD-100, was subject to decomposition at low pH levels.

There are four categories of surfactants that are based on the hydrophilic or solubilizing groups appended to a longer hydrocarbon chain. They are anionics, nonionics, cationics, and amphoterics. Of the anionics, the carboxylates represent the soaps, which are the salts of otherwise insoluble fatty acids. Soaps are not tolerant at all to low pH because they hydrolyze back to the insoluble fatty acid. Beside the soaps, there are sulfonates, sulfates, and phosphates. Of these, the sulfonates are the least sensitive to low pH because the carbon-sulfur linkage is not susceptible to hydrolysis or oxidation under normal conditions. Sulfates on the other hand, are not as stable because the carbon-oxygen-sulfur bond is more easily hydrolyzed.

It is recommended that for a wastewater feed consisting of urine and wash water, ony the urine be pretreated. The resultant pH obtained after dilution by wash water will then be closer to neutral conditions and therefore less apt to chemically react with the detergent employed.

RECYCLE LOOP COMPONENT OPTIMIZATION

Objective

Both the geometry and operation of the recycle loop components contribute to overall wastewater processing efficiency. The objective of this task is to optimize the loop components in a way such that increases in mechanical and fluid management efficiencies are realized.

Background

The recycle loop volume of the TIMES has already been reduced by 80 percent by removing the recycle tank. This was done to create a nominal 40 hour cycle for 95 percent water recovery. By doing so it was felt that the average specific energy would be lower than the previous large volume loop configuration that allowed excessive urea breakdown to occur, resulting in degraded water quality and performance capabilities. A disadvantage of the present configuration is that the filter and filter tank make up 50 percent of the total recycle loop volume. This filter volume causes excessive mixing of fresh and concentrated fluid, so that some quantity of solids are left in the loop after each dump/flush cycle. As a result, decreased water recovery on the subsequent cycle occurs if the wastewater is not concentrated to a higher solids level, and the specific energy is therefore proportionately increased.

The major source of parasitic energy consumption on the existing subsystem, however, is the recycle pump motor. The currently employed brush, DC motor is probably the least efficient of the commercially available fractional horsepower motors.

Results

It was determined that operating the TIMES with a small recycle loop volume in order to obtain concentrating cycles of 40-50 hours will not diminish the desired 85% water recovery efficiency, provided the proper initial to final dissolved solids level ratio is maintainable for each cycle.

A 400 Hz AC induction motor can be utilized to replace the present permanent magnet DC brush type. The AC motor will operate at least 50% more efficiently and will provide more reliability and longer life.

Discussion

Recycle Loop Volume

For a dynamic process such as TIMES where water is produced from a constant volume recycle loop, the relationship expressing water recovery in terms of water produced is:

$$\% \text{ Rec.} = \frac{\text{Mass of water produced}}{\text{Mass of water inputted + mass water initially in loop}} \times 100$$

or:

$$\% \text{ Rec.} = \frac{{}_{w} V_{H_2O}}{\rho_{in} V_{in} (1-X_{in}) + \rho_i X_i (1-X_i)} \times 100$$

Where:
- ${}_{w}$ = Density of water
- ${}_{in}$ = Density of fluid feed
- ρ_i = Density of initial recycle fluid
- V_{H_2O} = Volume of water produced
- V_{in} = Volume of fluid feed
- V_i = Volume of recycle loop
- X_{in} = Solids fraction of fluid feed
- X_i = Solids fraction of initial feed

Expressed in terms of initial and final weight fractions, X_i and X_f, respectively, the relationship can be expressed as:

$$\% \text{ Rec.} = \frac{\text{Mass of water inputted - mass of water final}}{\text{Mass of water inputted + mass of water initial}} \times 100$$

or:

$$\% \text{ Rec.} = \frac{(1-X_{in}) M_{T_{in}} - (1-X_f) \rho_f V_i}{(1-X_{in}) M_{T_{in}} + (1-X_i) \rho_i V_i} \times 100$$

Where: X_i, X_{in}, ρ_i, defined as before

and:
- ρ_f = Density of final recycle fluid
- X_f = Solids fraction of final recycle fluid
- $M_{T_{in}}$ = Total mass of fluid feed

The relationship of processing duty cycle with water production rate, percent water recovery, and recycle loop volume with a 2% solids feed is given in Figure 121. It should be clear that a higher average production rate and smaller volume lead to a reduction in cycle time.

The percent water recovery becomes important to the specific energy requirements of the subsystem since the relationship of specific energy with power, duty cycle, and total water produced is expressed as follows:

$$\text{Specific energy} = \frac{\text{total power X cycle time}}{\text{total water produced per cycle}}$$

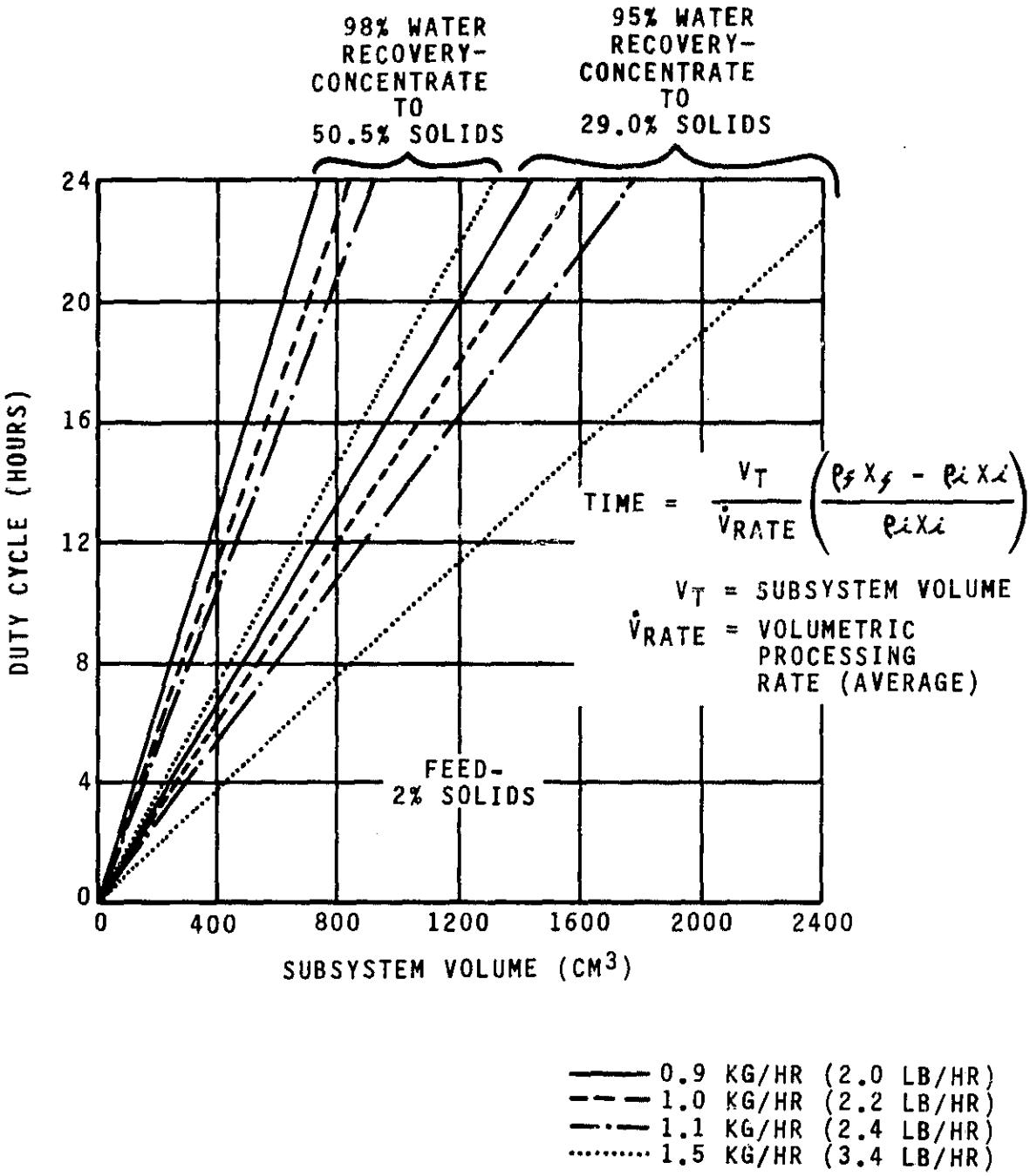

0.9 KG/HR (2.0 LB/HR)
1.0 KG/HR (2.2 LB/HR)
1.1 KG/HR (2.4 LB/HR)
1.5 KG/HR (3.4 LB/HR)

FIGURE 121

DUTY CYCLE VS SUBSYSTEM VOLUME

It can be seen that the specific energy will decrease if the percentage water recovery (expressed as total water produced per cycle) decreases. Cycle time only affects specific energy if the total water produced per cycle varies.

While the above mentioned parameters may be manipulated to generate a desired processing cycle time, the question of waste management becomes more critical as the cycle time decreases. For example, a problem that can occur with the present solids dump and flush procedure is that the same initial dissolved solids level may not be reached in the recycle loop after a dump/flush due to volumetric inefficiencies of the purge process. As a result, solids can accumulate after each cycle, and each subsequent run must reach a higher final solids concentration to obtain the same water recovery. However, as the final solids level increases it becomes increasingly more difficult to flush out the loop and reach the original initial solids level. In effect, water recovery will decrease after each processing cycle. With a large removable solids tank, the problem remains, but is less obvious since a greater amount of time is required to concentrate the solids. A comparison of the two concentrating cycles is given in Table 37. It can be seen then, that if no other changes are made to the component geometries, the same water recovery may be obtained independently of the number of cycles, provided the final solids concentration increases as the initial solids level increases.

While the above reasoning says water recovery may be held constant over a number of cycles, eventually the loop must be totally flushed until a baseline initial solids level is again reached. This is true whether a large or small recycle tank is employed, and it is this final flush that defines the overall cycle efficiency.

All flush cycles are dependent on the amount of mixing that can occur between the high density fluid already in the loop and the low density fluid being introduced. Component geometries and residence time affect the mixing factor. Decreasing flow velocities enough to prevent turbulence, and minimizing large areas where flow stagnation can occur, will both decrease the extent of mixing. An obvious target is a filter tank where velocities may be low and multiple flow paths abound. To this end, employing a filter with less surface area would be appropriate, at the expense of increasing filter change-out cycles. A Balston type 33 filter assembly was selectd for evaluation. The volume is approximately 0.3 liters (0.01 ft^3), or 24% of the TIMES I filter tank. The 25 micron filter tube is 6.4 cm (2.5 in) long and is constructed from Borosilicate glass microfibers with a chemically resistant fluorocarbon resin binder.

Recycle Pump Motor

The present recycle pump motor is a 28 VDC permanent magnet, brush type. It drives the Teflon gear pump at a speed of 6800 RPM, and requires approximately 35 watts (0.047 HP) of power. The theoretical power requirement of a pump that provides 182 kg/h (400 lb/h) at 138 kPa (20 psi) is 6.8 watts (0.0091 HP). Thus the present overall pump/motor combination efficiency as defined by:

$$\eta = \frac{\text{Pump output}}{\text{Pump motor power input}} = \frac{6.9}{35} = 0.197$$

Table 37

WASTEWATER CONCENTRATING CYCLE COMPARISON

1) Single Cycle

X_i = 2% and X_f = 30% for 95% recovery

if 10:1 dilution upon removal of recycle tank, get

X_i = 3% for next run

2) Multiple Cycle 10:1 dilution each cycle

1)	X_i = 2%	X_f = 30%	R = 95%
2)	X_i = 3	X_f = 38	= 95
3)	X_i = 3.8	X_f = 45	= 95
4)	X_i = 4.5	X_f = 49	= 95
5)	X_i = 4.9	X_f = 51	= 95

C-2

If the pump is assumed to operate at an efficiency of 50 percent, then the motor efficiency is: $\frac{0.197}{0.50} \times 100 = 40\%$

The relationships for the power required, and the torque generated by a direct current motor are given by:

$$P = 2 \quad NT \quad \text{and} \quad T = \frac{EI}{2\pi N}$$

Where: T = torque
P = power
E = voltage
I = current (armature)
N = speed

The graphical representation of the presently employed DC motor is given in Figure 122, and is typical for this type of motor when new. With time, the efficiency will decrease due to increased frictional losses.

While the advantages of a DC motor are its small size, speed variability, and low cost, the disadvantages are:

- The brush-commutator assembly, which contains life limiting (although replaceable) brushes.
- The bearings, which are affected by the brush dust, and which exhibit accelerated degradation as the speed and ambient temperature rise.
- Low efficiency, due primarily to the relatively high friction losses of the brush-commutator assembly.

There are two basic types of motors that are available in the fractional horsepower levels, which can replace the permanent magnet DC motor. They are the brushless DC and alternating current, or AC, motors.

Brushless DC motors may be divided into two main classifications. The first type has an inverter combined with the motor winding driving an AC induction motor. The second type is a DC motor with an electronic commutator. With the latter, rotor position is sensed, then the excited circuits in the armature are changed to correspond to the rotor position, similar to the way that an ordinary commutator-brush DC motor operates. The advantages of both brushless DC motors are small size, long life, speed variability and control, and high efficiency. The main disadvantages are the high cost, and less than off-the-shelf availability. Electronically commutated motors have typical performance characteristics as shown in Figure 123.

AC motors also are classified into several types, but for our application the induction motor is of primary interest. In the generally accepted sense, an induction motor refers to a motor whose stator accepts AC power, and whose rotor turns at some rate less than that of the stator's field. The stator rotates at some speed, N_S, as given by:

$$N_S = F/P$$

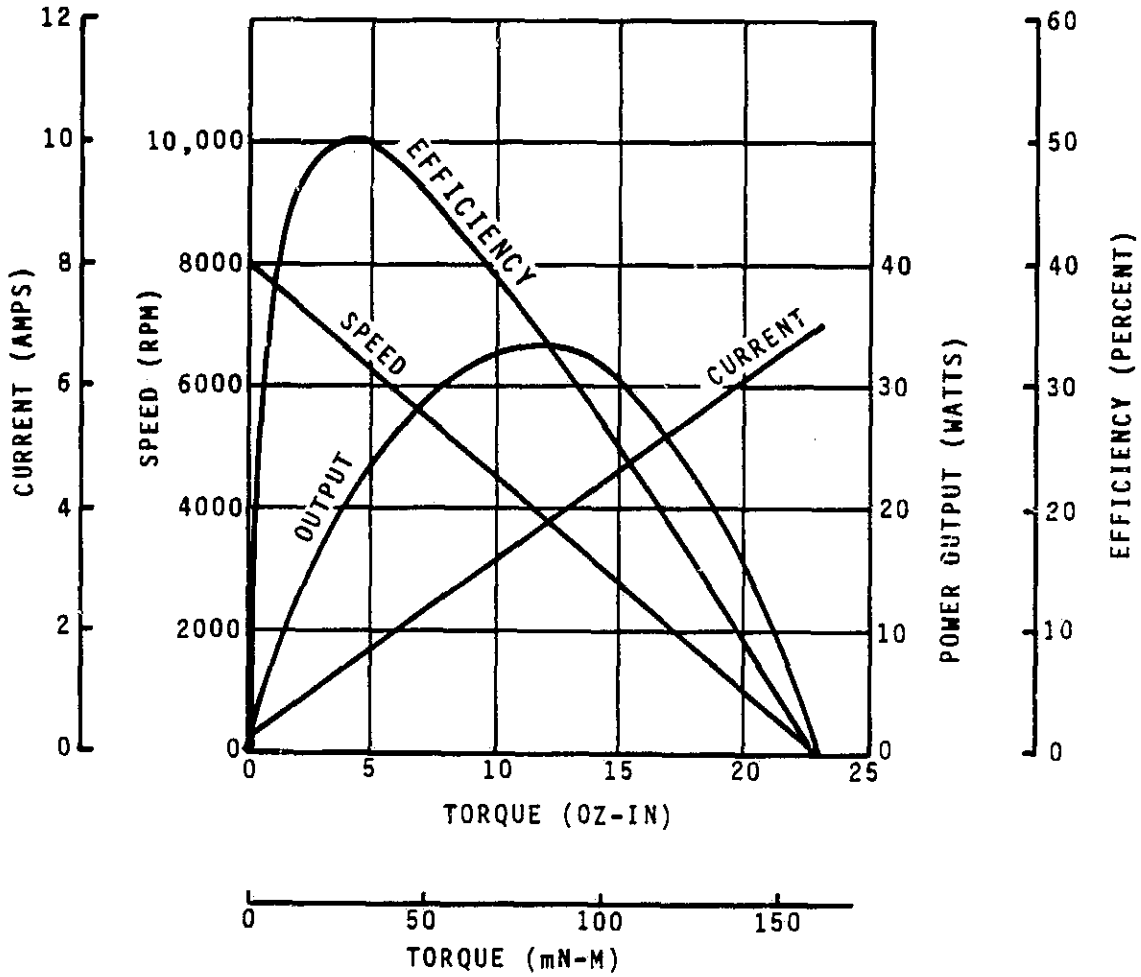

FIGURE 122

GLOBE BRUSH DC MOTOR #100A108-9
PERFORMANCE CURVES

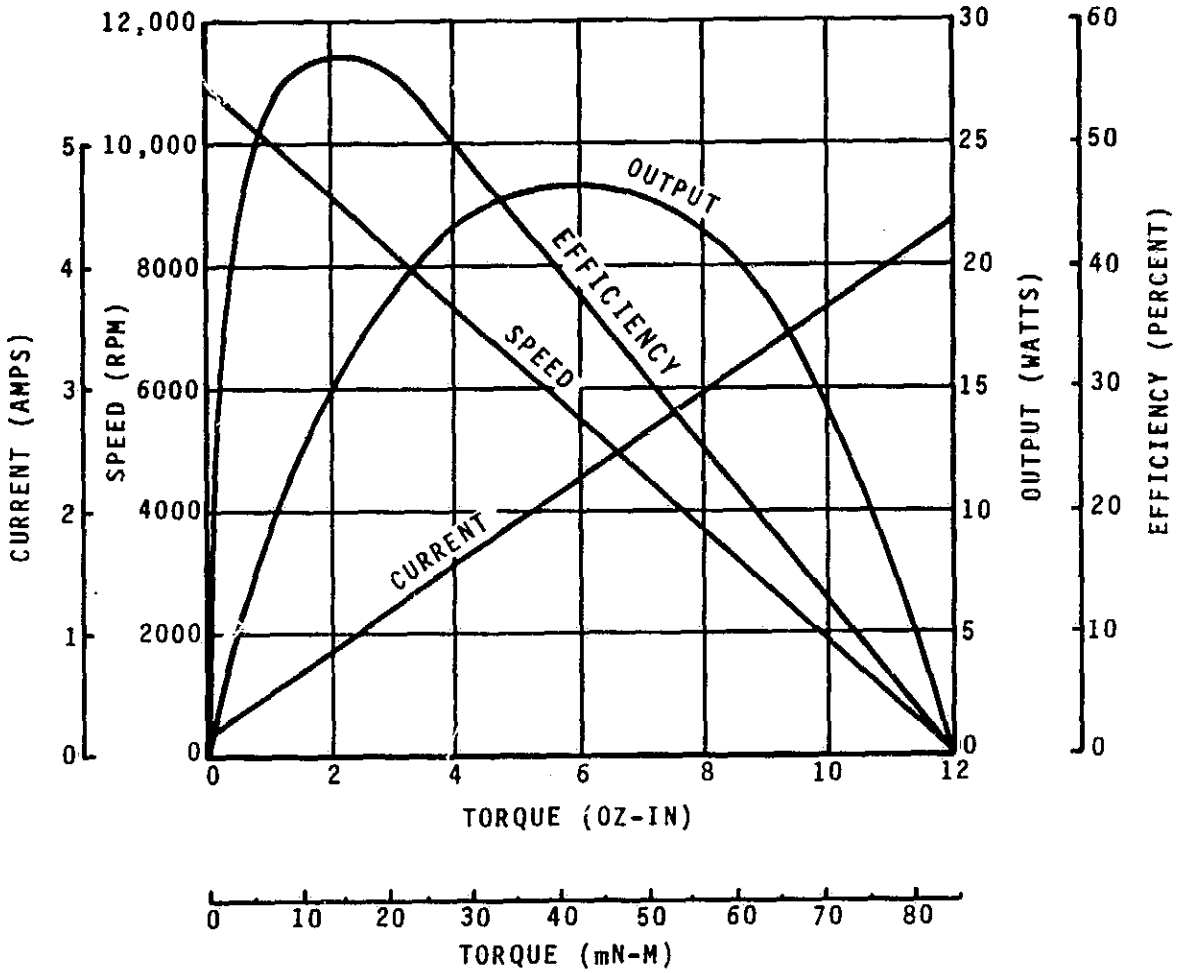

FIGURE 123

AEROFLEX BRUSHLESS DC MOTOR #BM15C-1
PERFORMANCE CURVES

where F is the input frequency and P is the number of poles. Commonly available motors operate at either 60 Hz or 400 Hz. The advantages of an AC motor are its simple, brushless design, high efficiency, long life, and high reliability. The disadvantages, depending on the chosen frequency, can be large size and weight. A typical AC induction motor performance curve is shown in Figure 124, and would equally apply to an inverter/induction brushless DC motor.

Manufacturer Survey

A number of manufacturers were contacted regarding the availability and performance capabilities of motors for our appication. The manufacturers are listed in Table 38.

TIMES II Recycle Component Requirements

The proposed TIMES II configuration would employ two rotating pieces of equipment: 1) a gas-liquid separator, and 2) the recycle fluid pump. It was decided to combine the rotational components with a single motor, for this improves overall reliability.

The proposed TIMES II recycle fluid flow is 272 kg/h (600 lb/h), and the pressure rise is 103 kPa (15 psid). The theoretical pumping requirement at processing conditions would be 8.5 W (0.006 HP).

The general conclusions to be drawn from the motor replacement study are:

1) A 400 Hz AC motor will be smaller and lighter than a 60 Hz motor.

2) A 400 Hz motor will be more available and less expensive than a brushless DC motor.

3) Both 400 Hz and brushless DC exhibit high efficiencies and long life.

Based on these results, a preliminary choice for the separator/recycle pump combination assembly would be a 400 Hz motor, due to its proven reliability, availability, and lower cost.

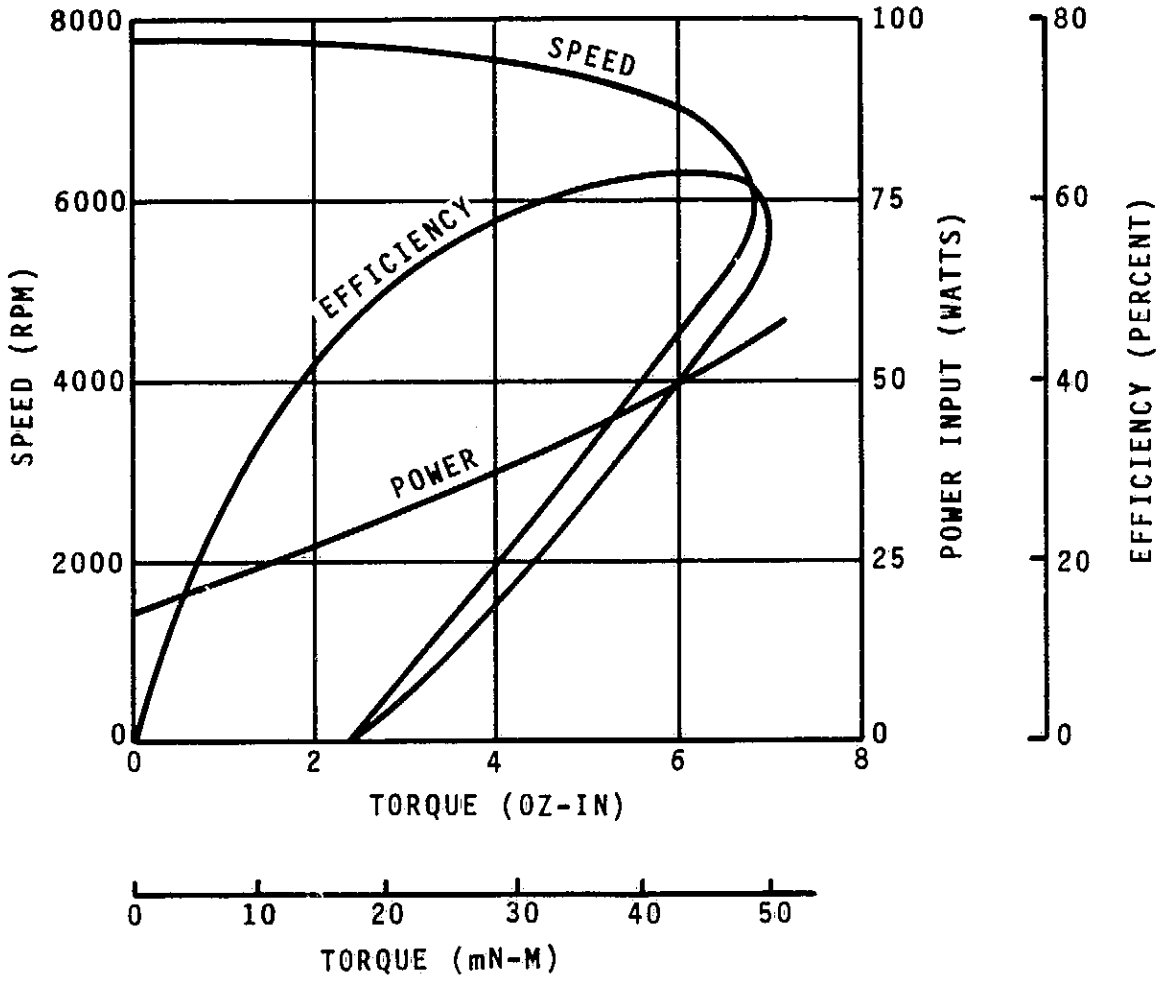

FIGURE 124

SINGER AC MOTER # E2161-17
PERFORMANCE CURVES

Table 38

MOTOR MANUFACTURERS

Major Type	Manufacturer
AC	Singer Co., Kearfott Division
DC, AC	Globe Industries
AC	Western Gear
AC	IMC Magnetics Corp.
BDC	Honeywell
DC	Reliance
BDC	Sierracin/Magnedyne
BDC	NuTech Industries
BDC	Easter Air Devices
BDC	Robbins and Myers
BDC	EDO Corp., Elinco Division
BDC	Kollmorgen
BDC	Clifton Precision
BDC	MPC Products
BDC	Aeroflex

HOLLOW FIBER MEMBRANE EVAPORATOR IMPROVEMENT

Objective

In order to provide a greater degree of maintainability and ease of assembly, the HFM assembly must be redesigned. The objectives of this task are to study the means by which these goals may be reached, as well as to fabricate, and implement an improved HFM evaporator design into the TIMES I unit.

Background

The present HFM evaporator must be removed as a unit and partially disassembled in order to perform maintenance on the 1656 tubes fixtured into 18 bundles. While testing the TIMES I preprototype at NASA/JSC during 1983-1984, the unit accumulated 1,650 hours of urine processing. However, problems in the areas of the membrane bundle headers and steam shell seals occurred that resulted in subsystem downtime. Disassembly of the HFM evaporator to remedy these problems was difficult, and often led to additional repairs having to be made to the hardware.

It was clear that improvements to the HFM evaporator design in the aforementioned areas would result in improved operation as well as provide more efficient maintenance. As a result, a spare HFM evaporator for the existing TIMES I was requested by NASA/JSC. It was decided that a redesigned HFM evaporator would provide valuable information for the TIMES II application, and more reliable operation than a duplicate unit while employed for TIMES I.

In striving to minimize specific energy for TIMES II by reducing TER power, the total area of the membranes necessarily must increase. The present TIMES I design would grow to an unwieldy size in order to accommodate this extra membrane area, so a reconfiguration is necessary. There are two ways to meet the area requirement, and they are either to increase the length of the tubes, or to increase the number of bundles.

Results

A redesigned HFM evaporator was fabricated that replaces the existing subsystem hardware. The major subassemblies are shown in Figure 125. The following drawings describe the assembly and subassemblies:

SVSK 108622	Evaporator, Hollow Fiber Membrane
SVSK 108623	Housing, Evaporator
SVSK 108624	Tube, Outlet, Steam
SVSK 108625	Header & Tubes, Upper
SVSK 108626	Cover
SVSK 108627	Support, Membrane

The HFM evaporator assembly envelope is 22.3 cm (8.8 in) in diameter by 37.6 cm (14.8 in) high. The assembly weighs 9.5 kg (21.0 lb) dry. The HFM evaporator/subsystem fluid interfaces are 1) two short fluid line sections that connect (with additional line lengths) to the inlet and outlet recycle fluid ports; and 2) the steam shell that bolts onto the existing subsystem steam cone. The additional line sections are the only subsystem hardware modifications required in order to interface with the HFM evaporator.

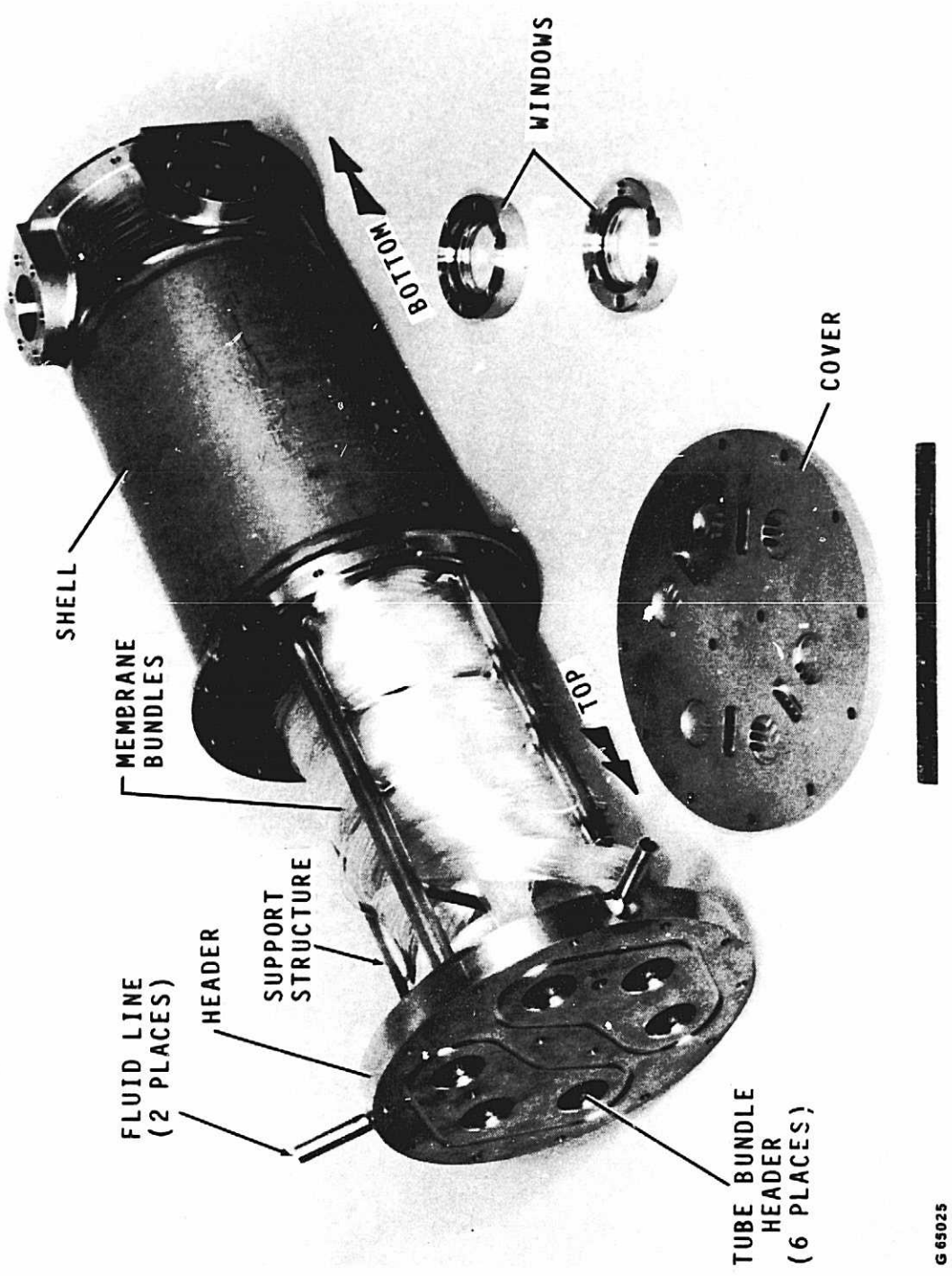

FIGURE 125
REDESIGNED TIMES I HFM EVAPORATOR

ORIGINAL PAGE
BLACK AND WHITE PHOTOGRAPH

In order to provide a minimum water production rate of 1.8 kg/h (4.0 lb/h) for unconcentrated wastewater, the TIMES II configuration must contain twice the surface area of membrane tubing than is currently employed on TIMES I. The membranes would be configured into six bundles, each 2.3 m (7.5 ft) in length. It is necessary to build two identical evaporator sections to allow a structurally satisfactory arrangement for the proposed TER/HFM evaporator assembly design. All the membrane bundle headers would be connected at one end of the evaporator, so that removal for maintenance is facilitated. In addition, only O-ring face seals should be employed to reduce the potential for leakage.

Discussion

TIMES I Evaporator

The TIMES I evaporator employs 18 bundles that are grouped into a number of parallel and series paths with the use of flow distribution headers. The arrangement is as shown in Figure 84. The pressure drop across the evaporator is 21.4 kPa (3.1 psid) and the average tube velocity is 0.23 m/sec (0.75 ft/sec). There is an average of 2.5 bundles/pass connected in 7 passes for a total series length of 2.6 m (8.8 ft). The disadvantage of this design, regardless of how the flow is distributed among parallel groupings of membrane bundles, is that there are 36 bundle headers for a total of 3312 individual tube connections. The number of tube connections can be decreased if the number of bundles connected in parallel decreases. However, the length of each bundle would have to increase to provide the same total surface area. Table 39 gives the results of reducing the number of bundles, keeping surface area constant. It is obvious that the ΔP increases rapidly as the number of bundles is decreased at a given flow.

The preliminary criteria for the replacement HFM evaporator were such that the unit should: 1) be completely interchangeable with the present unit; 2) incorporate improvements to the O-ring seal areas to reduce the leakage potential; 3) demonstrate a more maintainable membrane tube section; and 4) reduce the number of tube bundle headers while maintaining the same membrane area, which simplifies assembly and maintenance, and increases the reliability of the tube bundle assembly. To accomplish the above requirements, the unit was redesigned as follows:

O-Ring Seals

All O-ring seals are made compressively between mating flange surfaces, instead of radially between cylindrical sections as in the original design. The face-type seal is much less subject to leakage due to expansion, contraction and abnormalities in the mating surfaces. In addition, all mating pieces are fabricated from one material, titanium, rather than the TIMES I design which mates a plastic, polysulfone, to titanium. This material discontinuity resulted in the different rates of expansion and contraction during temperature transients, contributing to leakage around the radial seal.

Viton O-rings (MIL-R-83248, Type 1, Class 1) are used to seal all mating surfaces. Viton has demonstrated excellent material compatability with pretreated urine, and is mechanically suitable for the low pressure steam environment.

Table 39

INCREASED LENGTH MEMBRANE PRESSURE DROP

- 92 Tubes/Bundle, 18 Bundles Total
- Total Bundle Length $\simeq$ 6.9m (22.5 ft)
- 40% Solids
- 67°C (150°F)

# Bundles	ΔP, kPa	(psid)
1	131.0	(19.00)
2	32.7	(4.74)
3	14.5	(2.11)
4	8.2	(1.19)
5	5.2	(0.76)
6	3.7	(0.53)
7	2.9	(0.39)
8	2.1	(0.30)
9	1.6	(0.23)
10	1.3	(0.19)

Membrane Bundle Header Assembly

The membrane bundle header assembly is located at the top end of the evaporator shell. The tubular membrane bundles are formed into looped sections that have inlet and outlet headers contained in a single header manifold. This greatly simplifies assembly and maintenance by allowing the membrane bundle assembly to be removed as a unit from the evaporator shell. Once removed, the tube bundles are clearly exposed allowing for complete inspection and repair, if necessary.

The membrane bundle header assembly consists of three sections:

Cover, SVSK 108626
Membrane Support Structure, SVSK 108627
Header, SVSK 108625

Cover - The cover is fabricated from titanium alloy. It is mated to the header manifold and provides a uniform flow distribution of recycle fluid through the membrane bundles. The cover remains intact in the event that the evaporator needs to be disassembled, thereby minimizing spillage of waste fluid out of the header manifold and membrane bundles. In addition, the tube header plug fluid inlet and outlet ports are designed so that tube header plug retention is positive even during a possible pressure reversal at the steam/manifold interface.

Membrane Suppport Structure - The membrane support structure is fabricated by welding titanium alloy tubing into a tree-like structure. The structure is then welded to the bottom of the header manifold. The Nafion membrane tube bundles are wound through and around the structure, with the end being fed through the header manifold for insertion into the header plugs. Tube headering (inlets and outlets) is accomplished from the same end of the evaporator.

Header - The header manifold is fabricated from titanium alloy. Fluid inlet and exit lines are fabricated from titanium tubing and welded to the header. Fluid ports in the header are aligned with the cover to allow uniform flow distribution through the membrane tube bundles. Bundle inlet and outlet ports are isolated from each other as well as from the outside by racetrack O-ring seals.

Evaporator Shell Assembly

The evaporator shell (SVSK 108623) is fabricated from titanium alloy. It is designed to fit precisely into the allotted space of the presently employed HFM evaporator, with only slight modifications necessary to the existing subsystem inlet and outlet recycle fluid line connections.

The body of the shell is formed by rolling titanium alloy sheet s[illegible] into a cylinder; the mating edges are joined by welding. The top and bottom [illegible] are machined from a titanium alloy billet, and welded to the shell. Since [illegible] shell is metal, two vacuum service viewing ports made from type 304 stainless steel with type 7056 glass windows are employed. Through these ports any significant buildup of liquid in the shell can be observed and drained. A Viton gasket completes the seal between the shell and the viewing port flange.

Tube Bundle Headers

The most significant departure from the present evaporator design is the reduction of the number of Viton tube bundle headers from 36 to 6. This is accomplished by increasing the length of each bundle from 0.38 m (1.25 ft) to 2.29 m (7.50 ft), thereby maintaining the equivalent total membrane tube length. IR&D supported testing in 1983 of Nafion membrane bundles had demonstrated that the water transport rate of a 92-tube Nafion bundle increases proportionally with length. The redesigned evaporator takes advantage of this finding.

The number of actual tube-to-header connections is reduced from 3312 to 552, significantly increasing the ease of maintenance and overall reliability of the assembly. The perforated metal retainers used in TIMES I to prevent the tube bundle header from being forced through the header manifold (as a result of the operating ΔP) have been eliminated in the new HFM evaporator design. This change allows the Viton header plug to form a facial seal (in addition to the inherent radial seal) with the header manifold.

Functional Checkout

After assembly of the membrane bundles and subsequent installation into the header manifold was completed, the cover plate was attached. A hydrostatic test was conducted using triple distilled water at room temperature and 274 kPa (25 psig). No leaks were observed after approximately five minutes. A water flow of 182 kg/h (400 lb/h) at 12.8 kPa (3.8 psig) was then established through the membrane bundle/header assembly. The membrane bundle assembly was gradually backpressured using a needle valve downstream of the unit until a flow of 145 kg/h (320 lb/h) at 274 kPa (25 psig) was again established. These conditions were held for two hours with no leaks observed. Finally, a reduced pressure level of 11 kPa (1.60 psia) was established in the steam shell with the membranes and header bolted in place. After three hours no vacuum decay was noted.

Following the hydrostatic and vacuum leak check, the membranes were conditioned with pretreated urine (oxone and sulfuric acid). A 182 kg/h (400 lb/h) flow was established and allowed to circulate for 225 hours. This procedure reduces the possibility of flooding the evaporator shell with water during initial subsystem startup, due to the relatively high initial water permeability of the Nafion membrane material.

The urine was then flushed from the assembly and distilled water was again circulated for an additional 100 hours. Finally, another hydrostatic check to 274 kPa (25 psig) was performed with no indication of leaks. The unit was then drained and prepared for shipment.

Preliminary Sizing For TIMES II Evaporator

As indicated in the discussion of the combined TER/HFM performance characteristics, a corresponding membrane PA of 10 at the design point of 1.93 kg/h (4.25 lb/h) (see Figure 126) is required. The present evaporator provides a PA = 5, representing a membrane surface area of 2.5 m^2 (27 ft^2) which must be doubled to 5.0 m^2 (54 ft^2) to give a PA = 10. Simultaneously, the number of membrane bundles should be kept to a minimum to facilitate assembly and maintenance. The envelope dimensions and volume of the evaporator shell(s) are dependent on the area of the thermoelectric elements necessary to provide a COP_{TER} = 6. Due to proposed design considerations, an optimal number of membrane bundles was determined to be six (12 headers). To obtain the required surface area, each of the six bundles would have to be 2.3 m (7.5 ft) in length. The calculated pressure drop of such an assembly is shown in Figure 127. To obtain the same average Reynold's number as is presently employed, 436 kg/h (960 lb/h) would be chosen as the recycle flow, at a pressure drop of 22.4 kg/h (3.25 psid). However, practical considerations such as recycle pump sizing would dictate a flow of 272 kg/h (600 lb/h), at a 13.8 kg/h (2 psi) pressure differential.

Because of the longer tube length, the bundles would have to be looped several times and constrained in order to fit into the available evaporator volume. This is actually no different than the arrangement now utilized in the TIMES I evaporator, where, in effect, the individual bundles are "looped" into an equivalently longer bundle through the use of the flow distribution headers.

Evaporator Layout and Package Integration

The goals of the evaporator reconfiguration are:

1) Increase membrane area
2) Facilitate assembly of membrane bundles into evaporator
3) Provide for facilitated maintenance on the evaporator
4) Integrate the evaporator with the TER

There were two approaches considered for a reconfigured evaporator envelope. The first was similar to the present design where a vertical structure, either cylindrical or polygonal in shape, would form the evaporator shell. The second took the form of a flat rectangular box or boxes. In both concepts the membrane bundles would be headered from only one end of the enclosure, so that preassembly of the headers and bundles into a header retention plate could be accomplished independently of the evaporator shell. In addition, the thermoelectric elements, wastewater heat exchanger(s), and main condenser(s) would be integrated with the evaporator shell(s), in contrast to the separate assemblies now employed on TIMES I. In this way, heat transfer could be optimized to conduct heat into the evaporator shell where the heat could be used to prevent steam condensation on the walls during processing. Furthermore, the package insulation would now be fitted directly on the appropriate assemblies, providing increased thermal efficiency.

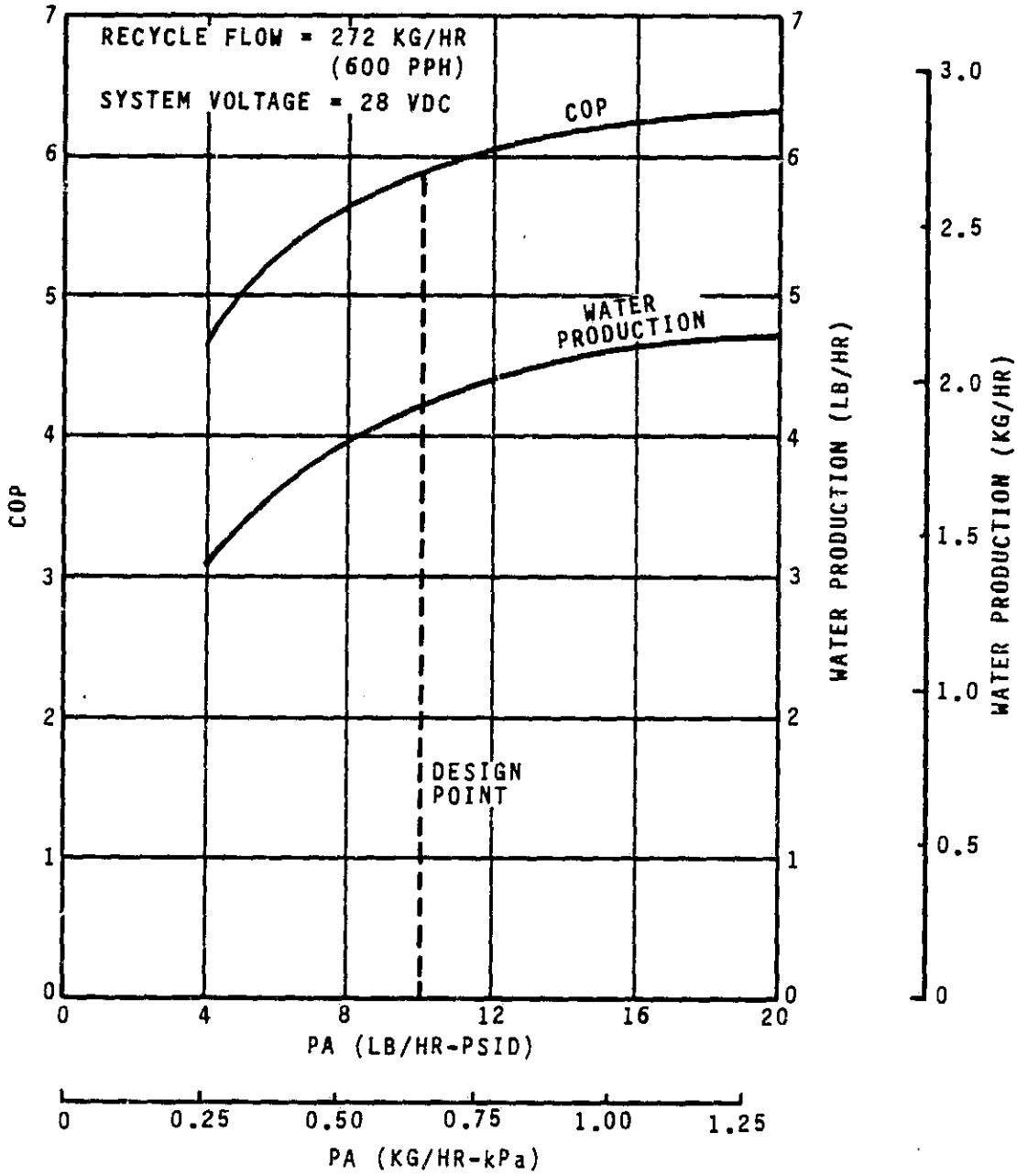

FIGURE 126

SUBSYSTEM MEMBRANE PERFORMANCE

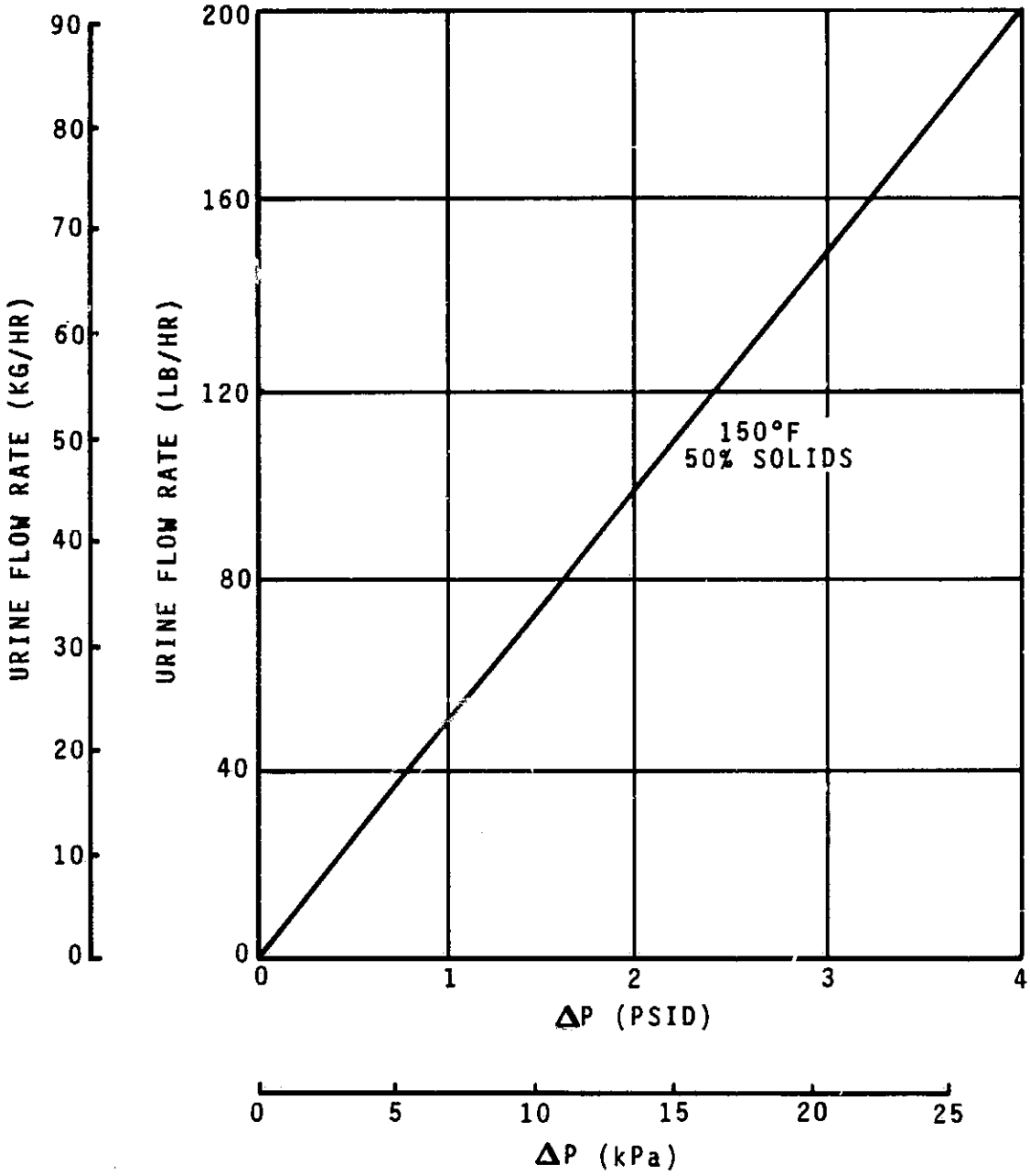

FIGURE 127

7.5 FT MEMBRANE BUNDLE
FLOW CHARACTERISTICS

After consideration of the two geometries, it became clear that the flat, rectangular design, assembled into a sandwich arrangement could best satisfy the design criteria of a TIMES II subsystem. The initial design concept included a single evaporator sandwiched between two banks of thermoelectric elements and heat exchangers. The goal here was to thermally isolate the hot evaporator as much as possible. The main steam condensers would be located on the outside of the package where heat transfer to ambient surroundings was not accruable as a loss of efficiency. While the thermodynamic concept was sound, manufacturing considerations indicated that the design would not be easily fabricated, and that the overall package dimensions would be marginally satisfactory.

The concept was then modified to the selected design, where the main steam condenser is sandwiched between two banks of thermoelectrics and two evaporator shells. While this design requires that more insulation panels be utilized to reduce heat transfer from the exposed evaporator shells, the fabrication and assembly of the major components will be more straightforward.

TER/HFM Assembly

The basic dimensioning of the TER/HFM assembly is dependent on the area required by the thermoelectric elements. The 9 X 13 array occupies an area of 0.40 m^2 (4.34 ft^2). The layout of the assembly is shown in Figure 128; all titanium construction will be used to minimize weight. Integral to the two evaporator shells will be the wastewater heat exchangers, each of which will consist of channels milled into a flat plate. The evaporator shell/heat exchanger sections will surround a thermoelectric heat pump section consisting of the two 9 X 13 arrays of thermoelectrics sandwiching a milled-channel main condenser. The entire sandwich will be clamped together within a framework suitable for mounting ancillary equipment (see Figure 129).

Evaporator Header Manifolds

The membrane bundle header manifolds will consist of two removable retention plates, one for each evaporator shell, each bored out to accept six headers, in an alternating inlet and outlet succession. The retention plate will mate with a flange on the evaporator shell, and an O-ring face seal will be employed. A cover plate, also with an O-ring face seal, will complete the manifold section. This arrangement allows the entire membrane header manifold to be removed from the evaporator shell for complete maintenance. In addition, the face sealing O-rings eliminate the suspected leakage problems encountered with the radial seals on the present evaporator.

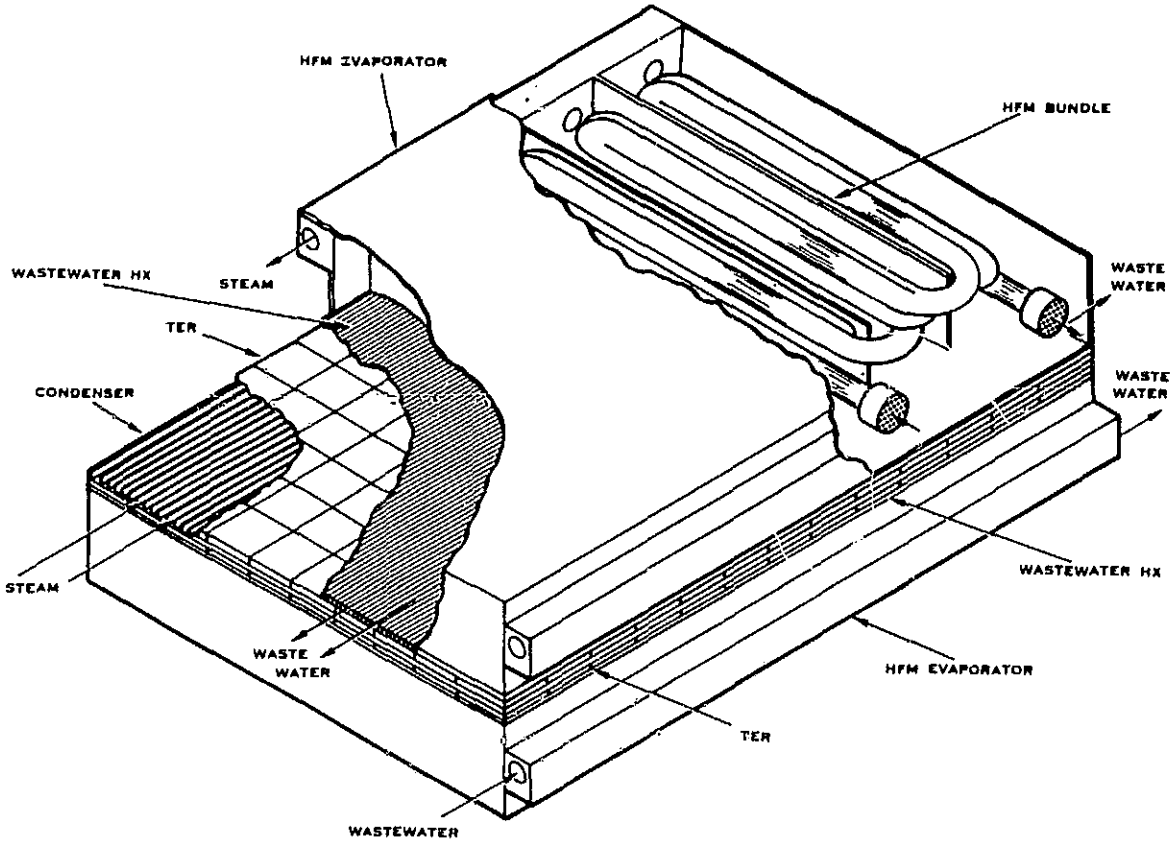

FIGURE 128

TER/HFM LAYOUT

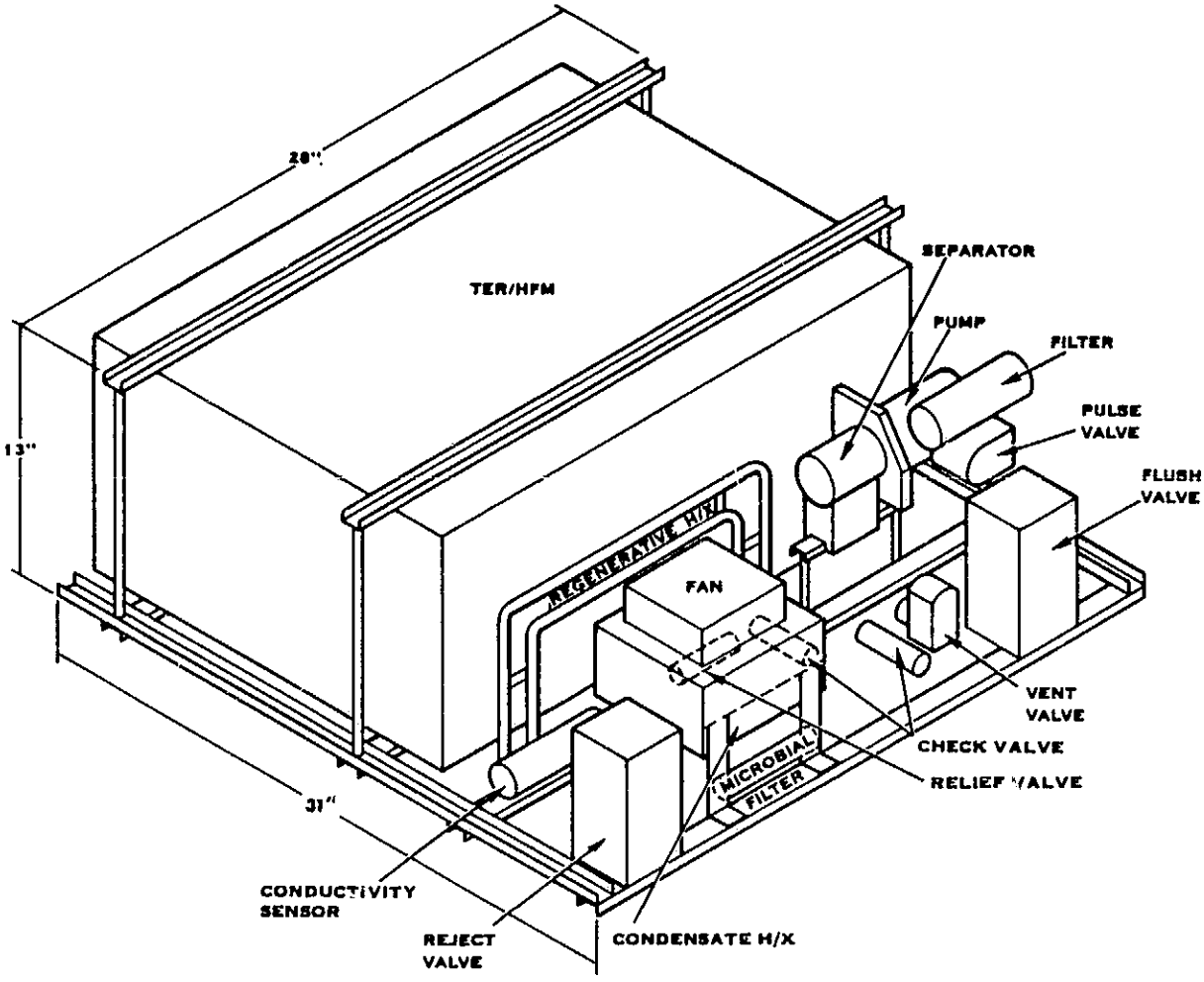

FIGURE 129

TIMES II PACKAGE LAYOUT